A Fuzzy Logic Control System for a Friction Stir Welding Process

By

K.E. Majara

Baccalaureus Technologiae: Engineering: Electrical

Dissertation submitted in full compliance with the requirements for the degree

Magister Technologiae: Engineering: Electrical

in the

Faculty of Engineering, the Built Environment and Information Technology

Nelson Mandela Metropolitan University

Promoters:	Prof. T.I. van Niekerk
	Prof. D. G. Hattingh
Co-promoter:	Mr. I. Clark
Submission Date:	18th January, 2006

Copyright Statement

The copy of this dissertation has been supplied on condition that anyone who consults it is understood to recognise that its copyright rests with the Nelson Mandela Metropolitan University and that no information derived from it, may be published without the author's prior consent, unless correctly referenced.

Declaration

I, Khotso Ernest Majara, hereby declare that:

- At no time during the registration for the degree of Magister Technologiae had I registered for any other university degree.

- The work in this dissertation is my original work and

- All sources used have been acknowledged.

_____ 18th January, 2006

Signature

Acknowledgements

I would like to acknowledge the following for their contributions:

- My promoters, Prof van Niekerk, Prof Hattingh and Mr Clark for their support, guidance and encouragement.

- All the team members in the Manufacturing Technology Research Centre.

- The Central Research Committee of the Nelson Mandela Metropolitan University for financial assistance.

- Grant Kruger, who developed the data acquisition and control for the present FSW machine. Without Grant's system, actual data would be difficult to obtain.

Abstract

FSW is a welding technique invented and patented by The Welding Institute in 1991. This welding technique utilises the benefits of solid-state welding to materials regarded as difficult to weld by fusion processes.

The productivity of the process was not optimised as the real-time dynamics of the material and tool changes were not considered. Furthermore, the process has a plastic weld region where no traditional modelling describing the interaction between the tool and work piece is available.

Fuzzy logic technology is one of the artificial intelligent strategies used to improve the control of the dynamics of industrial processes. Fuzzy control was proposed as a viable solution to improve the productivity of the FSW process.

The simulations indicated that FLC can use feed rate and welding speed to adaptively regulate the feed force and tool temperature respectively, irrespective of varying tool and material change. The simulations presented fuzzy logic technology to be robust enough to regulate FSW process in the absence of accurate mathematical models.

Table of Contents

Abbreviations ……...x

Glossary of Terms..……xi

List of Figures …….....xix

List of Tables …..……xxiv

1 Introduction 1

1.1 Statement of the Problem 3

1.2 Sub-Problems 4

1.3 Hypothesis 4

1.4 Research Delimitations 5

1.5 Assumptions 5

1.6 The Significance of the Research 6

1.7 Research Methodology 9

1.8 Proposed Research Schedule 10

1.9 Budget 11

1.10 Researcher Qualifications 11

1.11 The Organisation of the Dissertation 11

2 Operational Principles of Friction Stir Welding 13

2.1 Friction Stir Weld Region 15

2.2 FSW Process Cycle 16

2.2.1 Surface Seeking Period 17

2.2.2 Plunging Period 18

2.2.3 Dwell Period 18
2.2.4 Welding Period 19
2.2.5 Welding Speed and Feed Rate 20
2.3 Support and Clamping Structure 22
2.4 Welding Tool Properties 24
2.5 Frictional Energy Input (Temperature) 28
2.6 Materials Suitability 33
2.7 FSW Process Monitoring 36
2.8 FSW Setup 36
2.9 Fuzzy Control in Machining Processes 39
2.10 Fuzzy Logic Control in Turning Process 40
2.11 Summary 45
3 Fundamental Concepts of Fuzzy Logic Controllers 47
3.1 Control System Architecture for a FSW Process 49
3.2 Fuzzy Logic Control Structure 50
3.2.1 Normalization 51
3.2.2 Input Fuzzification 51
3.2.3 Membership Functions 52
3.2.4 Rule Bases 57
3.2.5 Fuzzy Inference System and Defuzzification 59
3.2.6 Denormalization 64
3.3 Tuning Fuzzy Logic Controllers 64
3.4 Fuzzy Logic Control of a FSW process 66

3.4.1 FSW Process Parameters 67
3.4.2 Fuzzy Inputs 68
3.4.3 Fuzzy Inference Engine and Defuzzification 68
3.4.4 Fuzzy Adaptation 69
3.5 Summary 71
4 FSW Data Acquisition and Modelling 72
4.1 FSW Process Parameters 74
4.1.1 Feed Rate and Welding Speed 74
4.1.2 Welded Materials 75
4.1.3 Welding Tools 76
4.2 Experimental Design 77
4.3 FSW Plates Setup 80
4.4 Experimental Data Analysis 82
4.4.1 FSW Regression Models for the Steady State 83
4.4.2 Process Dynamic Models 86
4.5 Summary 89
5 FSW Process Rule Base Development 91
5.1 ANFIS Architecture 94
5.2 ANFIS Learning Procedure 97
5.2.1 The Feed-Forward Pass 97
5.2.2 The Backward Pass 98
5.3 Fuzzy Inference System for a FSW Process 99
5.3.1 Fuzzy Control of Feed Force 100

5.3.2 Fuzzy Control of Welding Temperature 102
5.4 Summary 103
6 Simulations of Fuzzy Control for FSW Process 105
6.1 Simulink Model for Feed Force Regulation 105
6.2 Simulations for Feed Force Regulation 109
6.2.1 Feed Force Regulation on 5083 H321 and 2024 T3 Alloys 109
6.2.2 Feed Force Regulation using Different FSW Tools 111
6.2.3 Welding Speed Adjustment in Feed Force Control 113
6.3 Simulink Model for Tool Temperature Regulation 115
6.4 Simulations for Tool Temperature Regulation 118
6.4.1 Tool Temperature Regulation on 5083 H321 Alloy 118
6.5 Testing and Verification 120
6.5.1 Open Loop Feed Force Analysis 121
6.5.2 Open Loop Temperature Analysis 124
6.6 Summary 127
7 Conclusions and Recommendations 128
References 131
Appendix A: Welded Material Properties 138
A1: Aluminium Alloy (5083 H321) 138
A2: Aluminium Alloy (2024 T3) 139
Appendix B: FSW Tool Design.. 140
B1: FSW Tool With Small Profile (Tool 1) 140
B2: FSW Tool With Big Profile (Tool 2) 141

Appendix C: FSW Experimental Data…. ……142

C1: FSW machine data. ……..…..……142

C2: Expanded View of FSW Welds ……..142

C3: FSW Machine Data Graphs ……..…….……147

C4: Summary of FSW Data ……..…..…….....152

Abbreviations

AI	Artificial Intelligence
ANFIS	Adaptive Neuro-Fuzzy Inference System
CNC	Computer Numerical Control
FIE	Fuzzy Inference Engine
FIS	Fuzzy Inference System
FLC	Fuzzy Logic Controller
FSW	Friction Stir Welding
HAZ	Heat Affected Zone
MF	Membership Function
MTRC	Manufacturing Technology Research Centre
NMMU	Nelson Mandela Metropolitan University
RPM	Revolutions Per Minute
TMAZ	Thermo Mechanically Affected Zone
TWI	The Welding Institute

Glossary of Terms

Advancing Side: The side of the FSW tool where the direction of the tool surface, due to the tool rotation, and the translation of the weld material are in the same direction.

Aggregation: The combination of the consequents of each rule in a fuzzy inference system in preparation for the defuzzification process.

ANFIS: Adaptive Neuro-Fuzzy Inference System is a technique used for establishing or tuning zero-order Takagi–Sugeno type FIS systems based on the matched input-output training data.

Antecedent: The initial (or “if”) part of a fuzzy rule.

Consequent: The final (or “then”) part of a fuzzy rule.

Defuzzification: The process of transforming a fuzzy output of a fuzzy inference system into a crisp output.

Down (axial) Force:	The downward force (kN) applied to the FSW tool, to plunge the probe into the work piece and maintain shoulder contact with the surface of the work piece during welding.
Dwell Period:	A time period in the FSW process after fully plunging the tool pin, required to ensure the material to be welded is sufficiently plasticized before the weld traverse begins.
Fuzzy Inference System (FIS):	The overall name for a system that uses fuzzy reasoning to map an input space to an appropriate output space.
Fuzzification:	The conversion of a numerical (crisp) value into degrees of membership for the membership functions defined for the linguistic variable.
Fuzzy Logic (FL):	A superset of conventional (Boolean) logic that recognises more than simple true and false values. With fuzzy logic, members of a fuzzy set have a degree of membership that (typically) ranges from 0 to 100%. The fuzzy sets are used to transform crisp values into linguistic terms.

Fuzzy Inference:	It is the process of formulating an output from the mapping from a given input according to the fuzzy rule base.
Fuzzy Rule Base:	It is a group of IF-THEN rules using linguistic variables for representing the knowledge database of a system
Fuzzy Set:	A set which can contain elements with only a partial degree of membership.
Fuzzy Singleton:	A fuzzy set with a membership function that is unity at one particular point and zero everywhere else.
Heat Affected Zone (HAZ):	The area in a FSW weld located close to the weld centre that has experienced a thermal cycle, which has modified the microstructure and/or the mechanical properties of the material. No plastic deformation occurs in this area.
Intelligent System:	An automated system designed to process information and make decisions using written rules that mimic the way a human would work. Intelligent systems can be used to monitor physical processes in real time and make critical decisions in the absence of human interaction.

Implication:	The process of shaping the fuzzy set in the consequent based on the results of the antecedent side.
Linguistic variable:	A member of a set of linguistic interpretations describing a range of crisp values (a universe of discourse).
Machine Intelligence:	It is made up of various intelligent techniques (fuzzy logic, neural networks etc.) and expert criteria (operator knowledge), with one or more high resolution levels (hierarchical levels), which together manipulate process conditions resulting in a change of the process parameters.
Macrostructure	The general crystalline structure of a metal and the distribution of impurities seen on a polished or etched surface by either the naked eye or under low magnification of less than x10.
Mamdani-Style Inference:	A type of fuzzy inference in which the fuzzy sets from the consequent of each one of the activated rules are combined through the aggregation operator and the resulting area of fuzzy sets is defuzzified to yield the output of the system.

Membership Function:	It is a curve that defines how each point in the input space maps to a membership value (degree of membership) between 0 and 1.
Parent Material:	A material that may have experienced a thermal cycle from the weld, but is not affected by the heat in terms of microstructure or mechanical properties.
Plunge Depth:	The maximum depth the tool shoulder penetrates into the weld panels, measured normal to the weld panel surface.
Process Control:	A system of measurements and actions within a process intended to ensure the output of the process conforms to pertinent specifications.
Process Modelling:	The concise description of the total variation in one quantity by partitioning it into a deterministic component given by a mathematical function of one or more quantities, x_1, x_2, x_3 plus a random component that follows a particular probability distribution.

Residual Stress:	Macroscopic stresses that are set up within a metal as the result of non-uniform plastic deformation. This deformation may be caused by cold working or by drastic gradients of temperature from quenching or welding.
Retreating Side:	The side of the FSW tool where the local direction of the tool surface due to tool rotation and the direction of traverse, are in the opposite direction.
Rotation Speed:	The rate of angular rotation (usually specified in RPM) of the welding tool about its axis.
Singleton Output Function:	An output function that is given by a spike at a single point on the universe of discourse rather than a continuous curve.
Takagi–Sugeno Inference:	A type of fuzzy inference in which the consequent of each rule is a linear combination of the inputs. The output is a weighted linear combination of the consequents.

Tensile Strength:	The maximum stress in uni-axial tension testing which a material will withstand prior to fracture. The ultimate tensile strength is calculated from the maximum load applied during the test divided by the original cross-sectional area.
Thermo Mechanically Affected Zone (TMAZ):	The weld nugget where the material recrystallised due to high temperature distortion.
Tool Pin (Probe):	Part of the welding tool which rotates; it is normally shaped so that it sweeps out in a cylinder shape or a truncated cone. The probe extends from the shoulder so it enters the joint-line.
Tool Shoulder:	Part of the FSW tool which rotates and is normally disk shaped. It also forms the weld cap.
Tool Tilt Angle:	The angle at which the FSW tool is positioned relative to the work piece surface, i.e. zero tilt tools are positioned perpendicular to the work piece surface.

Transverse Force:	The force (kN) required to translate the rotating FSW tool through the work piece material along the joint.
Voids:	FSW welds can contain areas within the weld nugget where improper consolidation of the plasticized material occurred. This leaves cavities in or along the surface of the weld, greatly reducing the mechanical properties of the weld.

List of Figures

Figure 2.1: A basic FSW process setup for making butt joints. 14

Figure 2.2: The four distinct friction stir weld regions [Kallee, 1999]. 15

Figure 2.3: The FSW process, (a) preparing to plunge, (b) plunging 16

pin into the material, (c) force applied on shoulder, and 16

(d) transversing along the weld line [Georgeou, 2004]..... 16

Figure 2.4: The FSW cycle using vertical force (Fz) and tool temperature (T_{PIN}) [Hattingh et al., 2004]..... 17

Figure 2.5: Welding speeds for FSW butt-welds on different materials [Kallee et al., 1998]. 22

Figure 2.6: The clamping arrangement for FSW process [Blignault, 2002]. 23

Figure 2.7: Heat transfer between the welding tool and the welded material [Chao et al., 2003]. 29

Figure 2.8: The FSW tool with a thermocouple. 33

Figure 2.9: FSW of dissimilar aluminium alloys [Lee et al., 2003]. 34

Figure 2.10: FSW research platform at NMMU. 37

Figure 2.11: An Instrumented chuck for FSW process [Hattingh et al., 2004]..... 38

Figure 2.12: Structure of the fuzzy torque control system for a cutting process.. 40

Figure 2.13: A work piece with step changes in depth of cut [Liang et al., 2003]. 44

Figure 2.14: Feed adjustment using a 4-flute tool [Liang et al., 2003]..... 44

Figure 3.1: The overall control architecture for the control of a FSW process. ... 49

Figure 3.2: The triangular membership functions. 53

Figure 3.3: Fuzzy variable evaluation event [Berkan et al., 1997]. 55

Figure 3.4: Membership functions for (a) inputs and (b) outputs. 56

Figure 3.5: Multiple rules activated by two inputs 60

Figure 3.6: Takagi–Sugeno style inference mechanism. 62

Figure 3.7: A Takagi-Sugeno fuzzy model as a piece-wise linear approximation of a nonlinear system. 63

Figure 3.8: Block diagram of the proposed FLC for FSW system. 66

Figure 4.1: The data acquisition and models development. 73

Figure 4.2: FSW process parameters and conditions. 74

Figure 4.3: The FSW tools used [Blignault, 2002]. 76

Figure 4.4: The nominal sizes and basic layout of the FSW welds. 81

Figure 4.5: FSW-welds (for both 2024 and 5083 alloys). 83

Figure 4.6: Feed rate and welding speed vs feed force. 84

Figure 4.7: Feed rate and welding speed vs tool temperature. 85

Figure 4.8: FSW material plate setup for first order modelling. 86

Figure 4.9: Bending 1 (F_X) response at 5083 H321-2024 T3 interface. 87

Figure 4.10: Bending 2 (F_Y) response at 5083 H321-2024 T3 interface. 87

Figure 4.11: Temperature (T) response at 5083 H321-2024 T3 interface 88

Figure 4.12: Compression force (F_Z) response at 5083 H321-2024 T3 interface. 88

Figure 4.13: Tool torque (T_T) response at 5083 H321-2024 T3 interface. 88

Figure 5.1: ANFIS structure [Ship–Peng, 2001]. 95

Figure 5.2: The membership functions for feed force error. 101

Figure 5.3: The membership functions for feed force change. 101

Figure 5.4: The surface response for feed rate adjustment. 102

Figure 5.5: The surface response for welding speed adjustment. 103

Figure 6.1: The FSW model for feed force regulation. 106

Figure 6.2: Normalization block for feed force control. 107

Figure 6.3: Feed rate adjustment block for feed force control. 109

Figure 6.4: Effects of different aluminium alloys on feed force regulation. 110

Figure 6.5: Effects of different tool designs on feed force regulation. 112

Figure 6.6: Feed force regulation using the welding speed. 114

Figure 6.7: The FSW model for tool temperature regulation. 116

Figure 6.8: Normalization block for tool temperature control. 117

Figure 6.9: Feed rate adjustment block for tool temperature regulation. 118

Figure 6.10: Effect of different alloys on the tool temperature regulation. 119

Figure 6.11: Actual and simulated feed force on 2024 T3 aluminium alloy. 121

Figure 6.12: Actual and simulated feed force on 5083 H321 to 2024 T3 aluminium alloys. 122

Figure 6.13: Actual and simulated feed force on 5083 H321 to 2024 T3 to 5083 aluminium alloys. 123

Figure 6.14: Comparing real and simulated tool temperature on 2024 T3 aluminium alloy. 124

Figure 6.15: Comparing real and simulated tool temperature on 5083 H321 to 2024 T3 aluminium alloys. 125

Figure 6.16: Comparing real and simulated tool temperature on 5083 H321 to 2024 T3 to 5083 H321 aluminium alloy. 126

Figure A -1: 5083 H321 aluminium specifications [Malan et al., 1987].....138

Figure A -2: 2024 T3 aluminium specifications [Malan et al., 1987].....139

Figure B -1: FSW tool with small profile [Blignault, 2002]. 140

Figure B -2: FSW tool with big profile [Blignault, 2002].....141

Figure C-1: FSW-weld (2024 alloy and Tool 1).....142

Figure C-2: FSW-weld (2024 alloy and Tool 1).....143

Figure C-3: FSW-weld (2024 alloy and Tool 2).....143

Figure C-4: FSW-weld (2024 alloy and Tool 2).....144

Figure C-5: FSW-weld (5083 alloy and Tool 2).....144

Figure C-6: FSW-weld (5083 alloy and Tool 2).....145

Figure C-7: FSW-weld (5083 alloy and Tool 1).....145

Figure C-8: FSW-weld (5083 alloy and Tool 1).....146

Figure C-9: FSW-weld (5083 – 2024 – 5083 alloy).....146

Figure C-10: Bending1 (F_X) vs time (samples) graphs for welds 1 to 4.....147

Figure C-11: Bending1 (F_X) vs time (samples) graphs for welds 5 to 8.....147

Figure C-12: Bending2 (F_Y) vs time (samples) graphs for welds 1 to 4.....148

Figure C-13: Bending2 (F_Y) vs time (samples) graphs for welds 5 to 8.....148

Figure C-14: Compression (F_Z) vs time (samples) graphs for welds 1 to 4.....149

Figure C-15: Compression (F_Z) vs time (samples) graphs for welds 5 to 8.....149

Figure C-16: Tool Temperature (T) vs time (samples) graphs for welds 1 to 4. 150

Figure C-17: Tool Temperature (T) vs time (samples) graphs for welds 5 to 8. 150

Figure C-18: Tool Torque (T_T) vs time (samples) graphs for welds 1 to 4. 151

Figure C-19: Tool Torque (T_T) vs time (samples) graphs for welds 5 to 8. 151

Figure C-20: Feed rate (F_R) and Welding speed (W_S) vs bending 2 (F_Y). 152

Figure C-21: Feed rate (F_R) and Welding speed (W_S) vs compression (F_Z).....152

Figure C-22: Feed rate (F_R) and Welding speed (W_S) vs tool torque (T_T). 153

List of Tables

Table 1.1: Proposed research schedule. 10

Table 1.2: Estimated costs of the whole project.....11

Table 2.1: Different material and tool factors [Kallee et al., 1998].....21

Table 2.2: Effects of FSW tool dimensions on weld quality [Deqing et al., 2004]. 26

Table 2.3: Data channels provided by the FSW chuck [Hattingh et al., 2004]. ...39

Table 3.1: Rule base for the control of reference. 58

Table 4.2: The independent variables settings for the experimental design. 78

Table 4.3: Fractional experimental matrix for the FSW process. 79

Table 4.4: Constant parameter settings for all welds. 81

Table 4.5: Variable parameter settings for the welds. 82

Table 4.6: Regression models for the FSW process. 85

Table 4.7: The tool temperature range due to tool and material change.....86

Table 4.8: First order models for FSW process. 89

Table C - 1: FSW machine data.....142

Chapter 1

Introduction

The Friction Stir Welding (FSW) is a welding technique invented and patented by The Welding Institute (TWI) in 1991 [Skinner, 2003]. FSW process was established in the Manufacturing Technology Research Centre (MTRC) at Nelson Mandela Metropolitan University (NMMU) in 2003. A non-consumable welding tool is pressed and rotated at the interface of the two materials to be joined together. The frictional force generates adequate heat energy between the welding tool and the welded materials so that the material interface is transformed into its plasticized state [Thomas et al., 2002].

The shoulder of the welding tool compresses the surface of the work-piece and contains the plastic weld region. This shoulder forms the main source of energy when welding thin material. Tool probe design is also a crucial parameter to control the flow of the material to form a satisfactory weld at optimised energy input rates. The FSW tool is moved along the joint, leaving the mixed material interface to be solidly joined by the cooling process [Chao et al., 2003].

The FSW process has several independent parameters such as the plunge depth, welding speed and feed rate. The tool downward force, tool-torque, weld temperature, force against the tool movement and force perpendicular to the direction of tool movement form the group of the process dependent variables.

FSW process brings the benefits of solid-state welding to materials, such as aluminium alloys (2xxx and 5xxx series), regarded as difficult to weld by fusion processes [Thomas et al., 2002]. Generally, the frictional force has non-linear characteristics and varies with the load on a machine [Koren, 1997].

The FSW process enters the plastic weld region where no traditional dynamic modelling describing the interaction between the tool and work piece is available. In addition, the objectives of the proposed control algorithm for FSW include broader manufacturing goals, product quality, production efficiency and flexibility [Yen et al., 1995].

Given the history of non-linearity of machining processes, the multiple input-output parameters and the overall performance objectives, a framework for analysis via fuzzy logic is suggested [Yen et al., 1995].

The tool plunge depth has a direct influence on the amount of the tool downward force and weld temperature. The feed force increases significantly with the increase in the feed rate while the tool toque is significantly influenced by both the feed rate and welding speed [Johnson, 2001].

It is therefore possible to regulate the dependent variables with the aid of the tool plunge depth, feed rate and welding speed. The lack of adaptation to on-line welding process conditions is a crucial barrier to any further improvement in the process productivity in FSW.

1.1 Statement of the Problem

Developing and implementing a dedicated control system for each and every tool change and/or work piece material change is costly and time consuming, and therefore impractical.

1.2 Sub-Problems

To implement a flexible control system for a FSW process, the following problems need to be addressed:

- Study the fundamental concepts of FSW process.
- Study the fundamental concept of fuzzy logic control.
- Study the fundamental concepts of statistics and robust experimental design.
- Develop an experimental setup with varying process conditions and process control parameters, record process response parameters and perform statistical data analysis.
- Use regression analysis and develop a FSW simulation model and implement it in a MatLab simulation environment.
- Develop adaptive fuzzy structures for the control of welding temperature and feed force for varying tool shape and work piece material.

1.3 Hypothesis

Fuzzy logic can be used as a robust control system for varying tool and material changes in a FSW process, whilst ensuring the process parameters are maintained within acceptable limits to ensure optimal and safe operation.

1.4 Research Delimitations

- This research project primarily focussed on the steady state region of the FSW process.
- The accuracy of the data was determined by the sensor limitations of the FSW research platform.
- FSW process conditions were analysed using 6mm, 2024 T3 and 5083 H321 aluminium alloys for the linear butted joints and two welding tools with different profiles.
- This research focussed on the development of a fuzzy logic system for adaptive control of feed rate and spindle speed for feed force and temperature variables respectively. Other process variables were kept within their safety margins.

1.5 Assumptions

- The correlation between the feed rate and rotational speed for feed force and temperature variables will be adequate for control purposes.
- The weld temperature and feed force would be related to the weld characteristics and process safety.

1.6 The Significance of the Research

The increased use of aluminium is of great interest to the automobile industry with the goal of reducing the weight of road vehicles. FSW process was used to weld aluminium alloys, across the 2xxx, 5xxx, 6xxx and 7xxx series, some of which are almost being classified as being unweldable by fusion welding techniques. FSW can also be used to weld dissimilar aluminium alloys [Johnson et al., 2003]. FSW has the following advantages over the fusion welding techniques [Skinner, 2003]:

- It is energy efficient and requires minimal, if any, consumables.
- It produces desirable microstructures in the weld and heat-affected zones.
- It is environmentally friendly (no fumes, noise, or sparks).
- It can successfully join materials that are unweldable by fusion welding methods.

These advantages had led to the FSW process being one of the major advances in welding technology in recent years. The FSW process had been practised mostly by the conservative welding community. Conservative machining parameters are preset and often kept unchanged throughout the entire weld regardless of the real-time welding and tool conditions. This configuration does not enable the FSW machine to adapt to diverse real-time welding and tool conditions [Guerra et al., 2002].

Furthermore, to avoid weld defects, tool breakage and machine overload, welding parameters tend to be selected conservatively based on the most severe conditions expected. This property tends to limit the performance of FSW when the varying process conditions are not considered [Guerra et al., 2002].

Little research had been conducted in modelling the dynamic interaction between tool and work piece and hence the low level control of the FSW process. The lack of FSW models presents the complexity in cases where this process has to be optimally controlled. In the interim, fuzzy logic technology is proposed as a solution to the control of FSW process. This technology is able to use casual models, is robust and quick to implement as compared to other control strategies [Isermann et al., 1998].

The above issues give rise to the development of the control system that utilises on-line feedback information in the FSW process. This feedback information was recognised as a crucial barrier for further increase in productivity, reducing defective parts, improving process safety, product quality and reliability in other end milling processes [Liang et al., 2003].

FSW process involves the characteristics that are difficult to describe mathematically because of the physical processes taking place [Koren, 1997]. The conventional control methods are based on the processes that can be modelled mathematically while fuzzy controllers are based on artificial reasoning techniques that do not need exact system models [Haber et al., 1998].

A fuzzy logic controller (FLC) presents more control functionality than a conventional process controller and is able to include broader performance objectives. The FLC generally holds the potential to increase automation levels. It can be incorporated in multilevel architectures to provide supervisory and fault diagnostic capabilities, control the multi-inputs, multi-outputs process where those parameters have association between them. It can provide the communication interfaces for the managerial procedures [Haber et al., 1998].

This research introduces the application of fuzzy logic technology to the regulation of critical parameters of FSW process. In particular, FLC will be evaluated on its adaptability to the tool and material changes to the FSW process. FLCs were used to successfully control other machining processes, such as the material removal process [Liang et al., 2003].

NMMU has taken a big step in the introduction of FSW technology in South Africa. One of the MTRC's goals is to promote FSW technology in South African industries. By improving the control of the FSW process, the transfer of this technology from academia to local industries will be realised.

1.7 Research Methodology

To develop a control system, the following methods were used:

- Perform an extensive literature survey into the FSW process.
- Perform an extensive literature review into the concepts of fuzzy logic technology.
- Create an experimental design and perform data analysis to develop a statistical model of the FSW process and implement it in MatLab.
- Design an adaptive FLC system to control feed force and temperature in a FSW process to accommodate various process conditions, namely tool and material change.
- Experiment and customize the FLC for the FSW process within the MatLab environment.
- Test and verify the design with the industrial FSW process.

1.8 Proposed Research Schedule

Table 1.1: Proposed research schedule.

Task No:	Task Name	Start	Finish
1	Learn about FSW process	August 2003	November 2003
2	Learn about FLCs	February 2004	May 2004
4	Experimental design methodology	June 2004	August 2004
5	FSW data acquisition and analysis	September 2004	November 2004
6	Develop and implement a FLC for feed force in MatLab	February 2005	March 2005
7	Adaptive fuzzy rules for feed force	March 2005	April 2005
8	Analysis of FLC with and without adaptive rules for feed force.	May 2005	June 2005
9	Develop and implement a FLC for welding temperature in MatLab	July 2005	August 2005
10	Adaptive fuzzy rules for weld temperature	August 2005	September 2005
11	Analysis of FLC with and without adaptive rules for temperature control	October 2005	November 2005
12	Writing Dissertation	February 2005	January 2006

1.9 Budget

Table 1.2: Estimated costs of the whole project.

Operational software	Use what is available
Hardware	Use what is available
Material	R 10 000
Printing Costs	R 1 000
Total Costs	R 11 000

1.10 Researcher Qualifications

N-Dip:	Electrical Engineering	PET	2000
B-Tech:	Electrical Engineering	PET	2002

1.11 The Organisation of the Dissertation

Chapter 2 presents the fundamental concepts of the FSW process and the influence of the independent variables on the dependent ones.

Chapter 3 presents an introduction to the FLCs and discusses their usage for intelligent monitoring and control of machining processes.

Chapter 4 presents the method of executing the trial weld tests in an open loop environment. It also includes the analysis of the results acquired as well as the development of the statistical models for the FSW process.

Chapter 5 describes the procedure for the development of feed rate and welding speed FLCs for the regulation of feed force and welding temperature respectively.

Chapter 6 presents the simulation of the FSW process in MatLab as well as the verification of the FSW models against the actual FSW data.

Chapter 7 provides a conclusion of the research and suggestions for further study.

Chapter 2

Operational Principles of Friction Stir Welding

FSW produces high quality welds that can be fabricated with absence of solidification cracking, porosity, oxidation and other defects typical of traditional fusion welding techniques [Chao et al., 2003]. FSW has the capacity to develop welds of materials and alloys that were difficult to weld using traditional welding methods [Deqing et al., 2004]. It is used to join dissimilar aluminium alloys, having different mechanical properties, without weld zone defects, even under a wide range of welding conditions [Lee et al., 2003].

One particular benefit of FSW is the formation of the weld joint created by the solidification of the plasticized parent materials rather than using a filler material. The filler material normally produces welds with inferior properties to those made up of only the parent material. The FSW process also produces welds with narrower heat-affected zones than those produced by fusion welding techniques [Deqing et al., 2004].

Figure 2.1 illustrates the basic setup typical of the FSW process. The rotating FSW tool pin is plunged into the interface at one end of the material, and halted until there is adequate frictional energy to plasticize the material around the tool shoulder before the tool transverses the material interface. As the tool is moved along the welding joint, it leaves the plasticized material to be cooled, thus solidly bonding the interface [Colegrove et al., 2003].

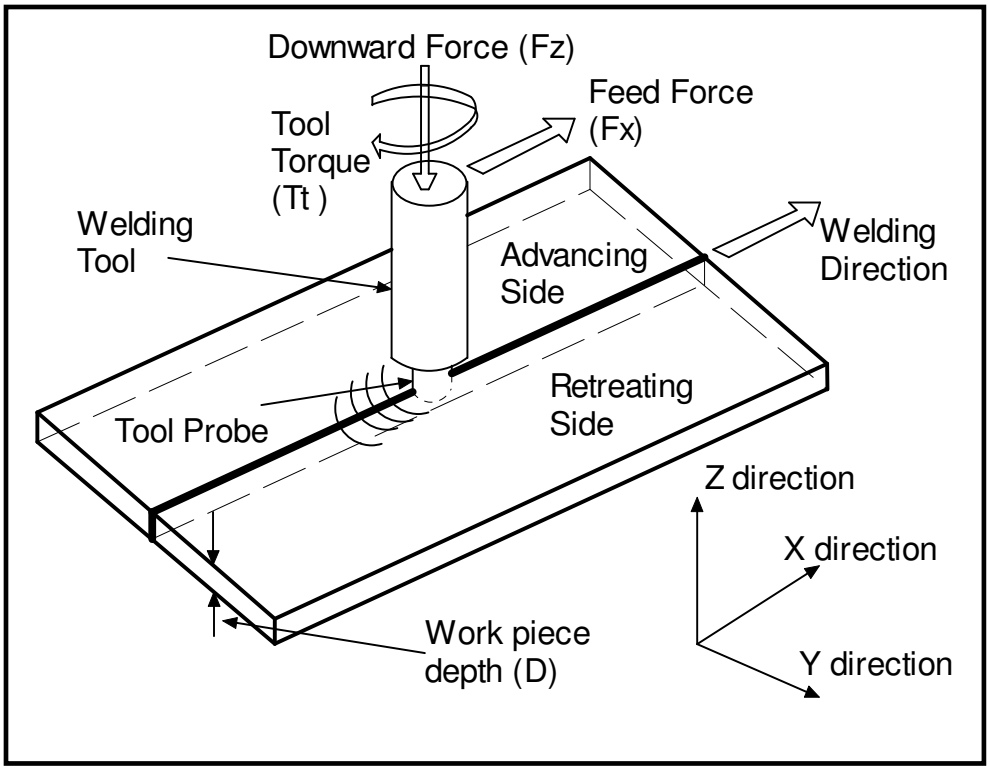

Figure 2.1: A basic FSW process setup for making butt joints.

The tool probe or pin profile tends to control the mixture of the material for a satisfactory weld. The shoulder of the welding tool compresses the surface of the work-piece and contains the plasticized material within the weld region. It also forms the main source of heat during the welding process.

2.1 Friction Stir Weld Region

The different parts of the welded plate are subjected to varying amount of the heat energy during the FSW process. Figure 2.2 illustrates the expanded view of four distinct weld regions, being categorised according to the macrostructure regions [Colegrove et al., 2003].

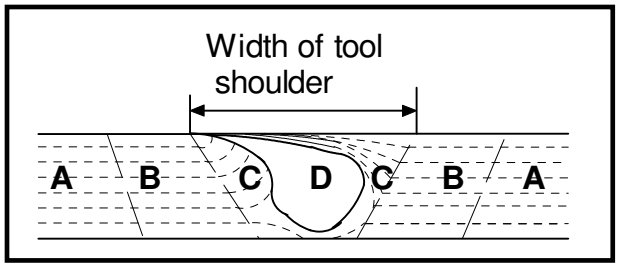

Figure 2.2: The four distinct friction stir weld regions [Kallee, 1999].

Region D marks the dynamically recrystallised region (DRZ) or the nugget of the weld, where the material recrystallised due to the high temperature distortions. There is also the thermo-mechanically affected zone (TMAZ) marked as region C where the high temperature and strain rates are not sufficient to recrystallise much material. The heat-affected zone (HAZ) is marked by region B and the unaffected parent material is marked by region A [Colegrove et al., 2003].

It was established that the area of the stir zone slightly decreased, due to the different cooling rate, when the welding speed is increased [Lee et al., 2003]. Therefore, the welding speed can be used to regulate the tool temperature, which can be related to the dimensions of the weld zone.

2.2 FSW Process Cycle

The quality and properties of the FSW welds are controlled by the welding parameters of the process, such as the pin rotation speed, diameters of the pin and shoulder, pressure and rate of translation of the material around the tool pin [Deqing et al., 2004]. Figure 2.3 illustrates the FSW stages, categorised according to the movements of the welding tool.

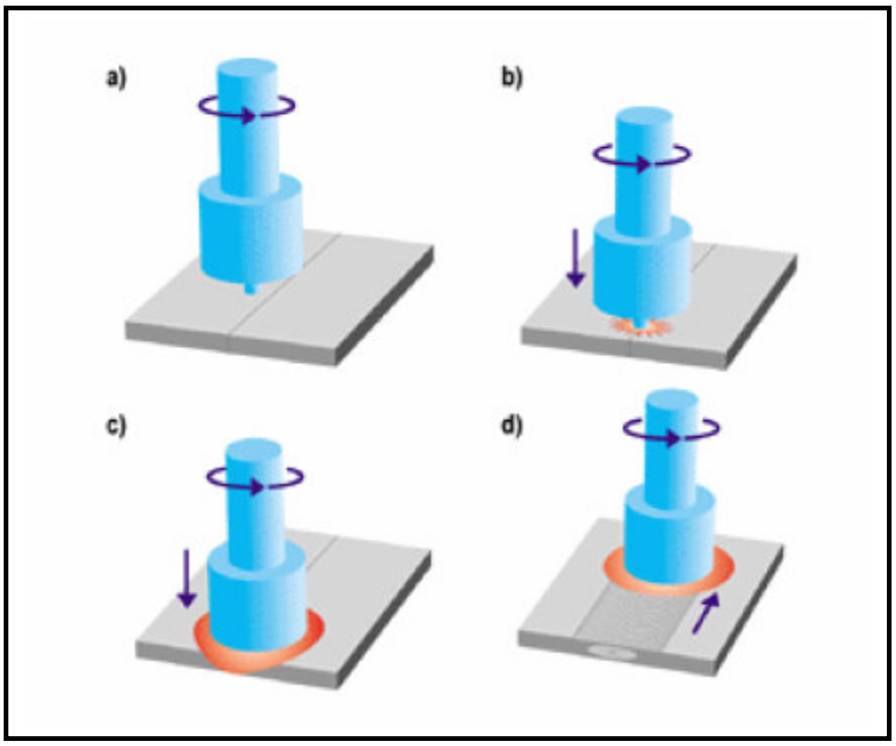

Figure 2.3: The FSW process, (a) preparing to plunge, (b) plunging pin into the material, (c) force applied on shoulder, and (d) transversing along the weld line [Georgeou, 2004].

2.2.1 Surface Seeking Period

Figure 2.4 illustrates the full FSW cycle with the aid of the profiles of the tool downward force (F_z) and Tool pin Temperature (T_{PIN}). The surface seeking period is represented as region A. This is where the tool pin makes an initial contact with the material interface. The FSW machine attempts to detect the surface of the material for a reference position to calibrate itself before the plunging process is commenced. This period is recognised by an initial increase in the value of the downward force (F_Z) [Deqing et al., 2004].

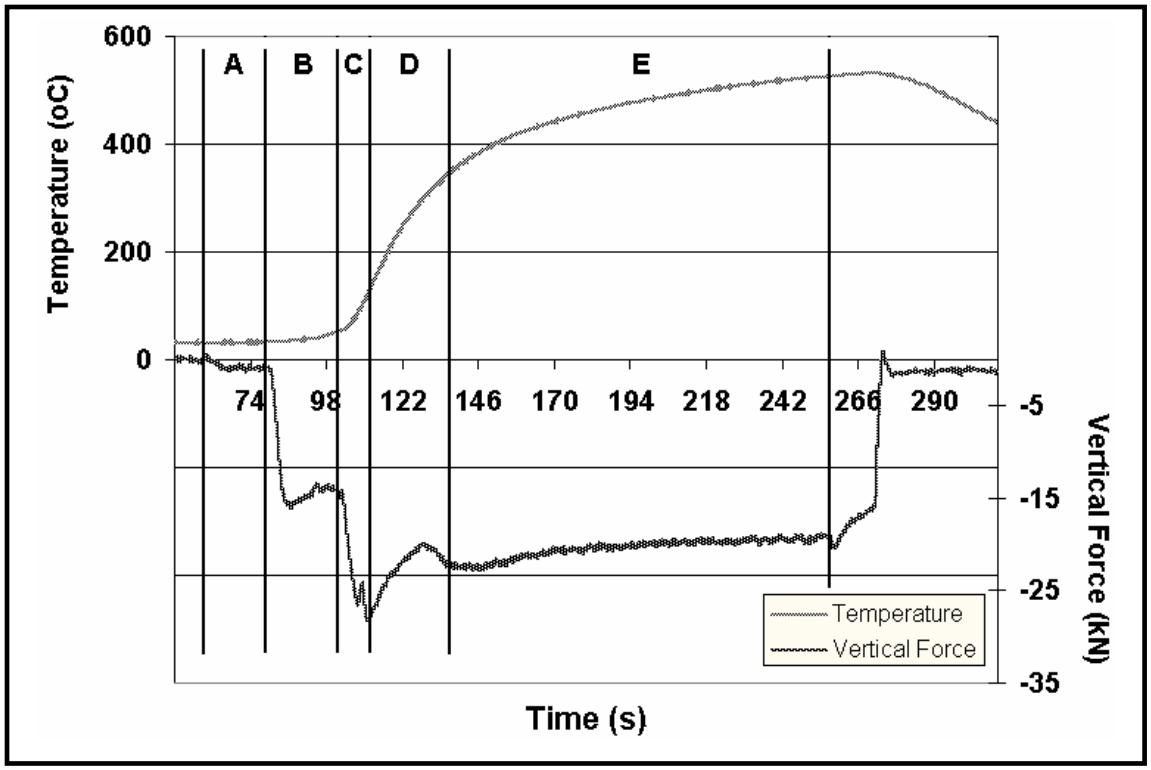

Figure 2.4: The FSW cycle using vertical force (Fz) and tool temperature (T_{PIN}) [Hattingh et al., 2004].

2.2.2 Plunging Period

A rotating FSW tool, with a pin length slightly less than the depth of the welded materials, is plunged into the material joint. The start of the plunging period B is illustrated by the sharp increase of F_Z and this is due to the increased frictional force between the tool pin and material interface. As frictional heating transforms the material into its plasticized state, the vertical force tends to decrease slightly and flatten out [Hattingh et al., 2004].

The tool pin is further plunged into the material interface until the tool shoulder is in close contact with the work surface as illustrated by period C. This period is characterised by a sudden, large increase in F_Z due to the increased contact area between the FSW tool and surface of the welded material [Deqing et al., 2004].

2.2.3 Dwell Period

The dwell period, marked as region D, occurs once the tool had been fully plunged. More heat is generated during the dwell period as all the tool translation energy is fully utilised to heat up the material around it. As the tool pin is rotated, the plasticized material flows around with it, due to the pin threads, thereby distributing the heat energy around the weld zone. This reaction slightly relieves the vertical force exerted on the tool [Hattingh et al., 2004].

2.2.4 Welding Period

Region E marks the welding period when the welding tool traverses along the weld joint. At the start of the welding period, the vertical force is increased slightly as it moves away from the fully plasticized zone. The force (F_X), in the direction of weld, is also increased at the start of this period [Hattingh et al., 2004].

The welding tool is then moved along the joint line and the tool pin provides the stirring action to the material in the two plates to be joined. The plasticized material is confined to the weld zone by the pressure exerted on the metal plates by the tool shoulder. As the tool transverses the weld interface, the weld zone is left to cool down, thereby bonding the two metal pieces together [Chao et al., 2003].

Tarng and Chen had developed a robust fuzzy controller, aimed at adaptively adjusting the feed rate to prevent tool breakage while maintaining a high chip removal rate in end milling operations. Their goal was to obtain an improvement in milling process productivity by use of an automatic regulation of the cutting force [D'Errico, 2001]. The same concept is introduced in FSW process where the feed rate is used to control the feed force.

2.2.5 Welding Speed and Feed Rate

The feed rate and welding speed of the FSW tool have an influence on micro hardness and tensile strength of the FSW welds. The ratio between the tool rotational speed and feed rate has a profound effect on the quality of the welding process and should be in a reasonable range for obtaining good welds [Deqing, et al., 2004].

An empirical rule, as represented by Formula 2.1, had been developed by TWI to determine the typical feed rates for different tool profiles and materials. The formula presents the feed rate in mm per minute, material factor (φ_{FSW}), tool factor (ψ_{FSW}) and material thickness (t) in mm. The formula correlates the feed rates on a selected joint geometry, to the given tool materials and tool design specifications [Kallee et al., 1998].

$$V_{FSW} = \frac{(\varphi_{FSW} \bullet \psi_{FSW})}{t} \qquad (2.1)$$

The probability of producing a good weld depends on the material and tool factors presented by Table 2.1. This empirical rule can be used to determine typical feed rates that cater for the type of material and the tool geometry [Kallee et al., 1998].

Table 2.1: Different material and tool factors [Kallee et al., 1998].

Material	**Material factor (φ_{FSW})**	**Tool factor (ψ_{FSW})**
Lead	3700	1
Aluminium 6xxx	1200	1
Aluminium 5xxx	700	1
Aluminium 7xxx	600	1
Aluminium 8xxx	600	1
Aluminium 2xxx	600	1
Magnesium	400	1
Copper	300	1
Titanium	100	1

An interactive software package had also been developed at TWI to provide technical and economical data for users of FSW process for butt joints. Figure 2.5 shows the recommended rotation welding speed for different materials with various thickness values [Kallee et al., 1998].

This research project is based on two aluminium alloys, 2024 T3 and 5083 H321, with a thickness of 6mm. The welding speeds of up to 200 revolutions per minute (RPM) are recommended for these alloys, as illustrated in Figure 2.5.

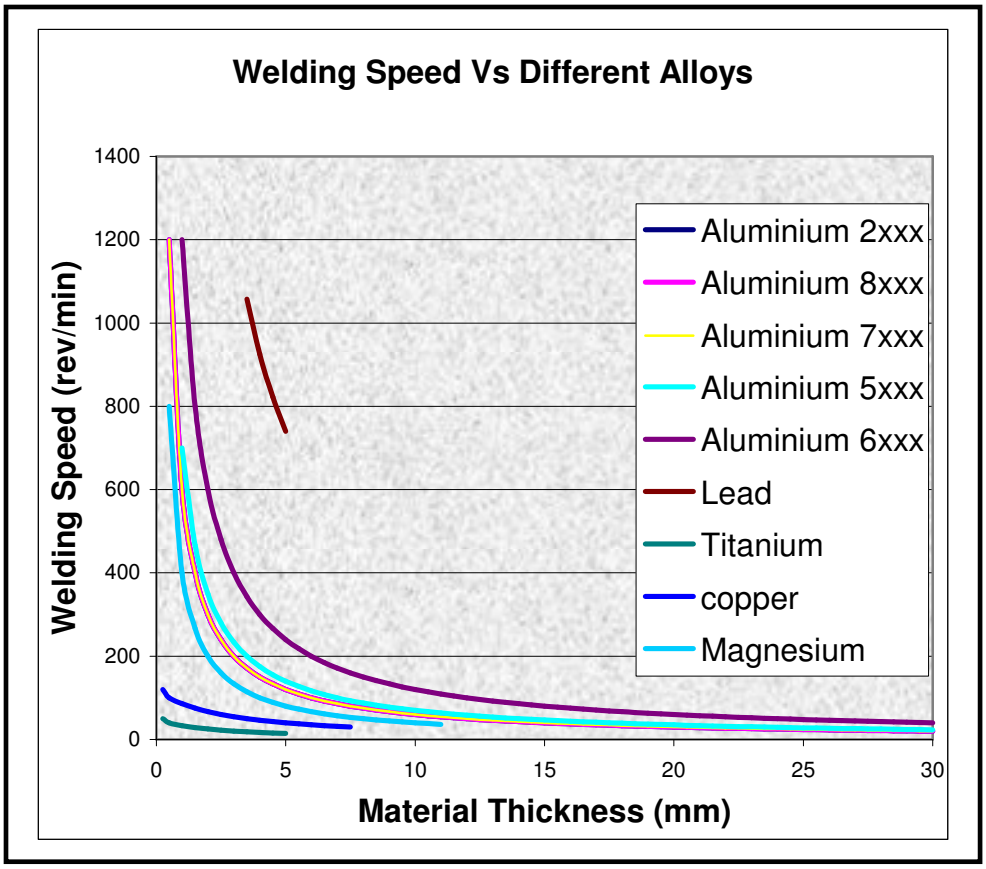

Figure 2.5: Welding speeds for FSW butt-welds on different materials [Kallee et al., 1998].

2.3 Support and Clamping Structure

Figure 2.6 shows the basic structure of the clamping arrangement for holding the specimen during the welding process. This type of setup is typical of a FSW machine designed to perform linear butt joints. The welding tools and backing plates, used to weld aluminium alloys, are normally made up of carbon-steel [Deqing et al., 2004].

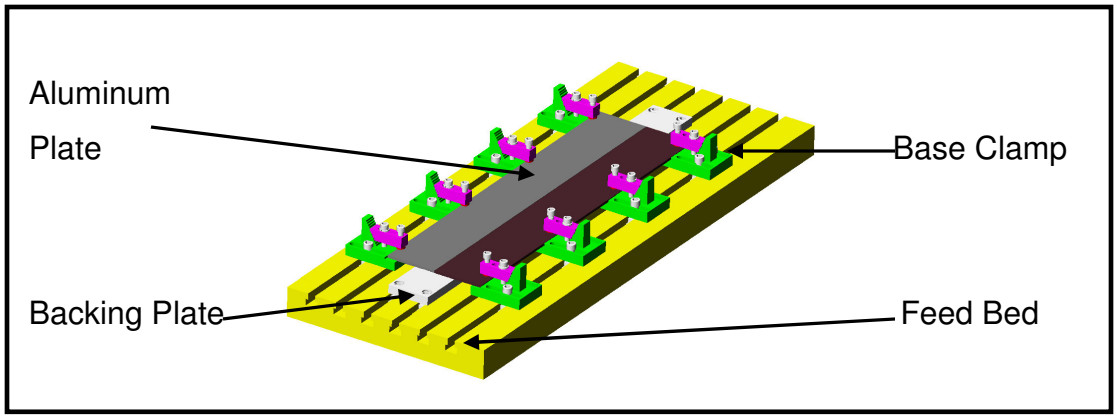

Figure 2.6: The clamping arrangement for FSW process [Blignault, 2002].

The work-piece is normally laid horizontally onto a steel backing plate and the welding direction is made to be perpendicular to the rolled direction of the aluminium plates [Shigematsu et al., 2003]. The pin length of the welding tool is determined by the thickness of the welded plates. The tool pin is designed to be slightly shorter than the thickness, to avoid contact with the backing plate surface and bringing debris into the weld [Chao et al., 2003].

The base clamps are used to rigidly hold the work-piece along its sides; thereby preventing the lateral movement of the work-piece during the welding process. They are also used to prevent the plasticized material from extruding through the interface to the underside of the joint [Deqing et al., 2004].

2.4 Welding Tool Properties

As both the welding tool pin and shoulder contribute to the generation of energy input to the weld, one of the main issues is how their combinations affect the quality of the produced weld. Deqing had conducted experiments to determine the relationship between the dimensions of the welding tool and the quality of the produced weld [Deqing et al., 2004].

The design procedure and materials required for the manufacturing of the welding tool are critical to the successful material flow and consolidation around the keyhole, and consequently the weld integrity [Thomas, 2002]. The pin diameter is made to be smaller than the diameter of the tool shoulder, about one-third of the shoulder's diameter for the production of good quality welds [Deqing et al., 2004].

The welding tool shoulder is considered to be the primary source for the heat generation during the welding process. It prevents material expulsion and also assists in the material movement around the tool. The tool pin stirs the material around the tool and also acts as a secondary source of heat energy [Colegrove et al., 2003].

When thin metal plates are welded, the main source of heat is due to the friction between the welding tool shoulder and the contact surface of the material. The friction between the rotating tool pin and the welded material supplies more heat as the work piece thickness is increased [Colegrove et al., 2003].

A study of FSW process by Deqing on 3mm thick L2Y2 aluminium was conducted to determine the effects of tools of different dimensions on the production of sound welds. The different tools, with pin diameters varying from 2.7 to 3.8mm and shoulder diameters ranging from 6 to 18mm, were used in FSW process where aluminium plates were welded. The various rotational speeds, ranging from 850 to 1860 RPM, and welding rates, ranging from 30 to 160 mm/min, were used. Table 2.2 presents the results of the experimentation [Deqing et al., 2004].

The welds were evaluated by considering their properties such as the microstructures, micro-hardness and tensile strength. The results of these experiments show that the dimensions of the welding tool had a profound effect on the production of sound welds. Therefore, the design of the welding tool is critical to the success of FSW process, which is important to control heat gain and loss of the process, and the quality of the welds [Deqing et al., 2004].

Table 2.2: Effects of FSW tool dimensions on weld quality [Deqing et al., 2004].

Tool No:	Welding Head Diameters (mm)		Pressure (MPa)	Rotational Speed (RPM)	Travel Rate (mm/min)	Weld Quality
	Pin	Shoulder				
1	2.7	6	9.3	1860	45–70	Fair
2	2.7	8	5.0	1860	45–72	Good
				1560	30–45	
3	2.7	10	3.9	1860	72–128	Fair
				1560	59–128	Good
				850	30–90	Fair
4	3.0	6	9.9	1860	45–72	Fair
				1560	42–110	
5	3.0	9	4.0	1860	53–128	Best
				1560	42–110	
				850	30–90	
6	3.3	7	7.0	1860	45–90	Fair
				1560	30–60	
7	3.3	10	3.5	1860	72–136	Good
				1560	45–128	
				850	30–72	
8	3.3	13	2.4	1560	110–158	Fair
				850	72–128	
9	3.6	8	6.5	1860	90–136	Fair
				1560	72–110	
10	3.6	11	3.2	1560	90–158	Fair
				850	45–90	Good
11	3.9	8	5.8	1860	90–158	Fair
				1560	59–128	
12	3.9	12	2.9	1560	110–136	Fair
				850	59–90	

It was discovered that welding heads with small shoulder diameters could not make sound welds at the lowest rotational speed; even when the tool is exposed to high pressure, due to insufficient heat generation. The same tools made successful welds at higher rotational speeds and very low travel rates with relatively high pressure [Deqing et al., 2004].

The welding heads with large shoulder diameters were unable to make welds at the highest rotational speeds, even under the lowest pressure due to excessive heat generation by the welding head. The reduction of rotational speed and the increase in the travel rate accomplished welds with surfaces that were usually depressed, uneven and full of voids and barbs. The different types of welding tools affected the production of welds according to [Deqing et al., 2004]:

- The black regions, at the top and bottom of the welds, were slightly larger than the shoulder diameters for all the welds.
- The feed rate of the welding tool affects the micro hardness of the weld. The micro-hardness of the weld decreases as the travel rate increases.
- The hardness strength of the FSW welds has shown a strong dependency on the pin travel rate. The hardness strength of the weld first increases, reaches a maximum and then decreases with increasing travel rate of the welding tool pin.

Considering Table 2.2, it was observed that the welding tools, having their pin diameters being one-third of the shoulder diameters, produced most of the good welds. The best welds with smooth surfaces pore-free structure were obtained by using head 5 at all the rotational speeds with a broader range of travel speeds [Deqing et al., 2004].

2.5 Frictional Energy Input (Temperature)

The frictional energy, generated at the interface between the welding tool and the work-piece, is the process parameter that determines the success of the FSW process. The heat influences the shape and microstructure of the weld, as well as the residual stress and distortion of the work-piece. The heat must be high enough so that the tool pin can stir the material, but not too high to melt the material interface or shorten the lifespan of the welding tool [Chao et al., 2003].

Heat input, in welding, is always difficult to determine accurately, due to losses of radiation, convection and conduction from the weld. In FSW, the same problem of heat measurement is experienced, and enough energy must be transferred to the process to account for heat loss through the tool and base plate [Johnson et al., 2003].

The heat transfer and temperature distribution in both the welding tool and the work piece need to be understood so as to relate their importance to the success of the FSW process. A heat analysis of the FSW process was conducted to determine the input heat flux. This heat flux is generated by the friction between the welding tool and the welded material. Figure 2.7 illustrates the experimental setup used to execute the experiments [Chao et al., 2003].

Formula 2.2 presents the model to illustrate the energy balance of the welding tool. The heat flow, in the welding tool and machine heat, involves the heat flux (Q_3) to the welding tool from the friction between the tool and the surface of the welded material. The heat, lost by the surface of the tool to the environment through convection, is represented by q_1. The transfer of heat to the machine head is presented by Q_4 [Chao et al., 2003].

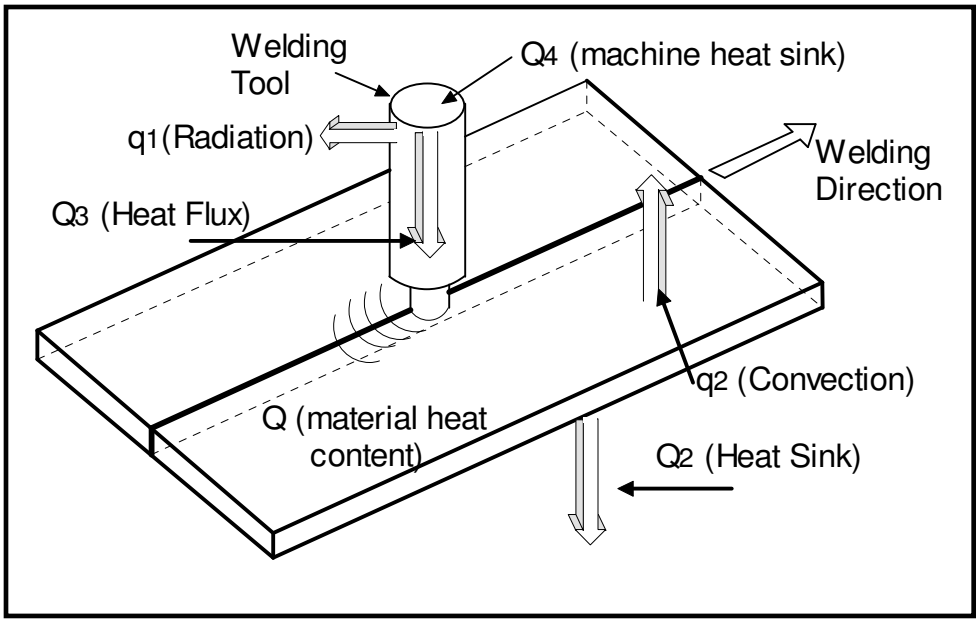

Figure 2.7: Heat transfer between the welding tool and the welded material [Chao et al., 2003].

$$Q_3 = Q_4 + q_1 \qquad (2.2)$$

The heat loss through convection is significant only when the welding temperature exceeds 500^0 C and it is rare to exceed this temperature level in the aluminium joining process. It is for this reason that q_1 was considered as negligible during the aluminium welding process [Chao et al., 2003].

It was also difficult to estimate Q_3, as it is likely to be a function of dynamic frictional coefficient, tool downward force and tool temperature. An inverse engineering approach was used to determine the heat flux quantities [Chao et al., 2003].

Formula 2.3 presents the model to illustrate the heat transfer from the frictional heating to the material being welded. Q_1 represents the heat flux generated between the tool and the material. Since the machine head is very large relative to the tool, it serves as a heat sink.

$$Q_1 = Q_2 + q_2 + Q \tag{2.3}$$

The machine head is modelled as a large body with constant ambient temperature and Q_2 represents the heat conducted away from the bottom of the work piece. Q represents the increase in the heat content of the work piece while q_2 represents heat conducted away from the surface of the welded material [Chao et al., 2003].

This experimentation indicated that slightly less than 5% of the total heat generated from friction at the interface of the tool and the work piece flows to the tool and 95% of the heat flows to the work piece. Several factors could be attributed to these results.

Aluminium has higher thermal conductivity than steel, which normally makes up the tool for the FSW process. Therefore, the heat would flow faster to the work piece than it flows to the welding tool. The work piece is very large as compared to the welding tool and therefore serves as a heat sink [Chao et al., 2003].

The results of this experimentation indicated that although only 5% of the heat was transferred to the tool, the peak temperature in the tool is about the same as the corresponding peak temperature in the work piece. Therefore, the amount of heat produced by the FSW process on the welding region can reasonable be acquired by measuring the welding tool temperature [Chao et al., 2003].

Formula 2.4 relates the total energy input once the parameters of the FSW process had been chosen. The total energy (E) is related to the Frictional coefficient (μ) between the welding head and the work piece, downward force (P) on the tool shoulder, tool rotation speed (R), and diameters of the shoulder (θ) and pin (ϕ) of the welding tool.

$$E = \pi\mu PR\left(\frac{\theta^2 + \theta\phi + \phi^2}{45(\theta + \phi)}\right) \quad (2.4)$$

The heat generation in FSW process is directly proportional to the friction coefficient and friction area between the welding head and work piece surfaces, rotation speed of the welding head pin and the pressure applied to the welding tool head [Deqing et al., 2004].

A thermocouple to measure the FSW tool temperature is normally inserted inside the welding tool as shown in Figure 2.8. The accuracy of temperature measurement in FSW is affected by electrical noise, rubbing of the thermocouple against the tool, imprecise thermocouple positioning, steep thermal gradients and thermal lag [Colegrove et al., 2003]. Therefore, the FLC is considered as the suitable option to control temperature in a FSW process as it can tolerate imprecise data.

Experiments indicated that the maximum temperature created by the FSW process range from 80 to 90% of the melting temperature of the material being welded. The welding defects and large distortions, commonly associated with fusion welding, are minimised in the case of FSW due to the low welding temperature.

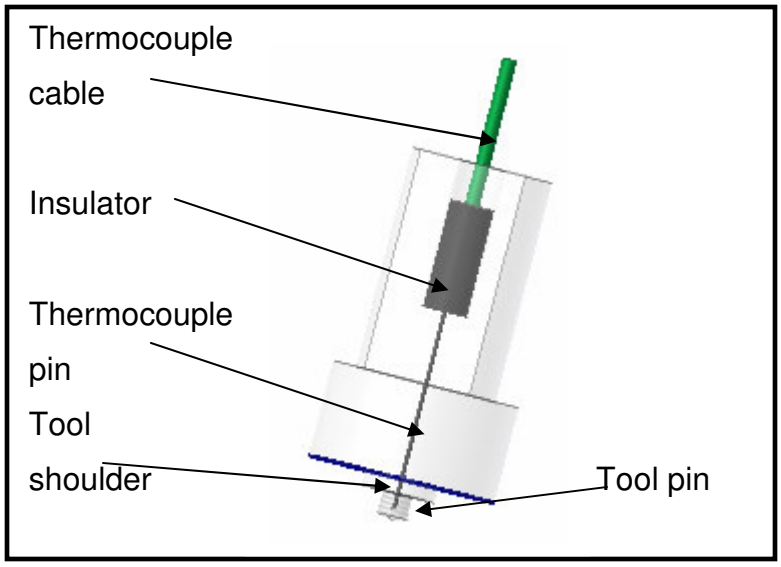

Figure 2.8: The FSW tool with a thermocouple.

The heat efficiency of FSW is relatively high: about 95% due to 5% of heat conducted away by the welding tool. The traditional fusion welding process has heat efficiency of between 60 to 80% [Chao et al., 2003].

2.6 Materials Suitability

It was discovered that the FSW process enables the welding of different aluminium alloys, copper, magnesium and other low-melting metallic materials [Chao et al., 2003]. In one of these experiments, the aluminium alloys, A356 and 6061 were successfully welded.

One alloy was positioned on one side of the weld line while the other one was fixed on the opposite side. Figure 2.9 illustrates the setup used to join the two aluminium alloys [Lee et al., 2003].

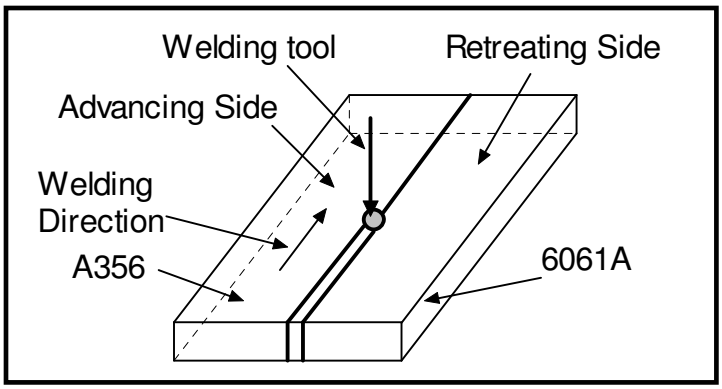

Figure 2.9: FSW of dissimilar aluminium alloys [Lee et al., 2003].

The feed rate was varied between 87 and 267 mm/min, while the welding speed and tool inclination angle were fixed at 1600 RPM and 3^0 respectively. The mechanical and microstructure properties of the weld joints were mainly dominated by properties of the material at the retreating side [Lee et al., 2003].

The area of stir zone was slightly decreased with an increase in the feed rate due the extended welding time, which provides more frictional input energy per unit length. The weld zone was composed of increased plastic deformation at low feed rates. The area of the stir zone showed almost to be the same regardless of the fixed side of the material. The area of the stir slightly decreased as feed rate was increased due to the different welding time and the cooling rate [Lee et al., 2003].

The Hardness of the stir zone had higher values when the 6061 alloy was located on the retreating side, as the retreating side material dominated the microstructure of the stir zone. The transverse tensile strength of the joints showed a similar value with that of A256 base metal regardless of welding conditions. The longitudinal tensile strength was high when 6061 alloy was located on the retreating side [Lee et al., 2003].

The results of this experiment indicate that welds with sound surface quality were produced. The FSW process is therefore an applicable welding method for joining dissimilar formed Al alloys even under different feed rates. It was also discovered that the alloy, on the retreating side, has great dominance as far as the properties of the weld zone are concerned [Lee et al., 2003].

Therefore, the production of the welds can be improved by using different feed rates on different materials. The chemical compositions of the welded materials will affect the magnitude of the produced feed force. When different materials are welded, the feed force can be used as an indication to the magnitude of the feed rate to be used.

2.7 FSW Process Monitoring

The measurement of forces and torques, during the FSW process, was used as a valuable aid to understanding and developing this process. Monitoring some of the forces enables on-line quality control assessment to be made during the production process [Johnson, 2001].

The theme of this research is to incorporate the control mechanism to enable the controller to adapt to tool and material change during the steady state region. The feed rate and tool rotational speed are used to control the feed force and the tool temperature respectively, while plunge depth is kept constant. However, the ratio between the tool rotational speed and its travel rate should be in a reasonable range to obtain high performance welds [Deqing et al., 2004].

2.8 FSW Setup

Figure 2.10 illustrates the FSW research platform used for research activities at NMMU. A conventional Nicolas Correa F3U-E CM milling machine forms the basis of the adapted milling machine for FSW process. The welding machine has a table size of 100 by 700 mm. The 5.5kW and 1.5kW 3-phase squirrel cage induction motors are used for the spindle and bed feed respectively [Kruger, 2003].

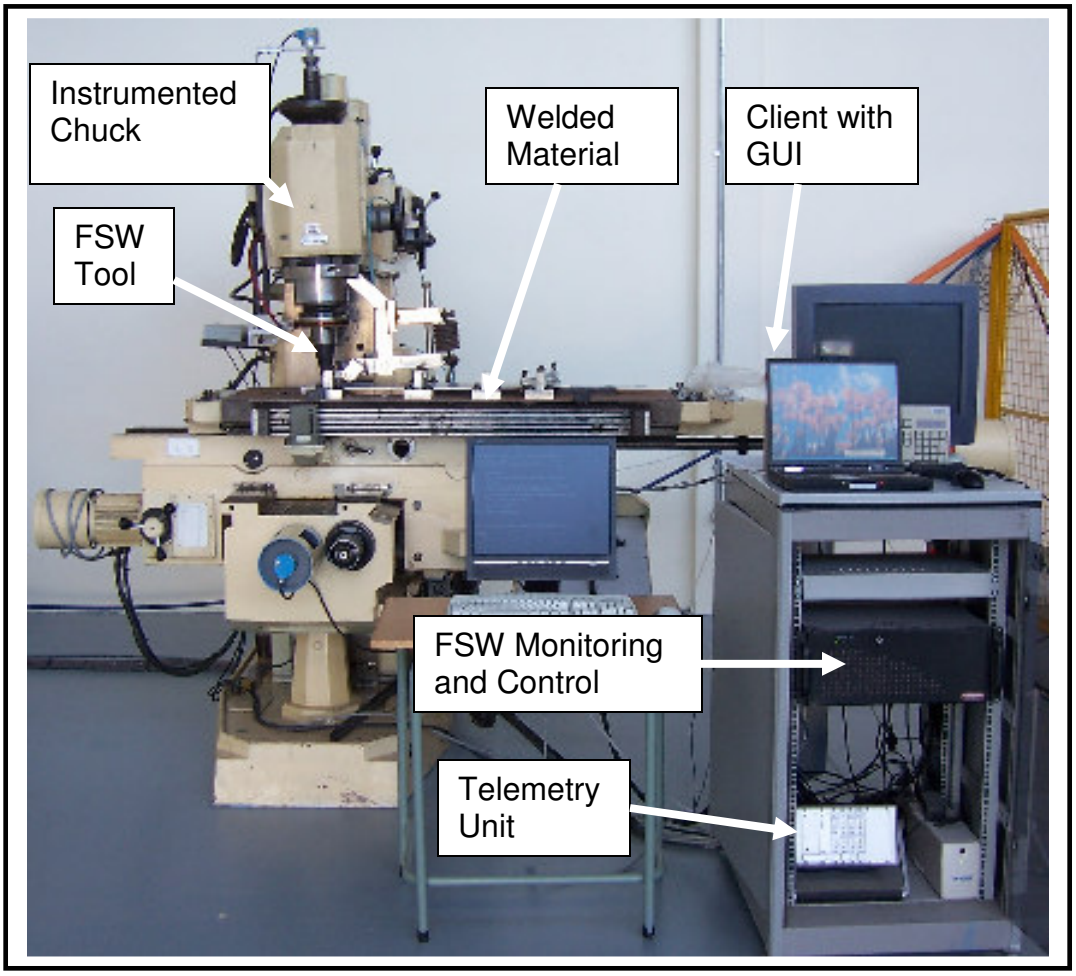

Figure 2.10: FSW research platform at NMMU.

Siemens Micromaster 440 Inverters provide the interfaces between each motor and the computer. The computer controlled electromagnetic clutches and brakes are used to control the bed feed movement. The welding head is able to move in the up-down direction, while the table can be moved in the forward-backward and sideways directions. One of the machine's limiting factors is that the machine can only move one axis at a time [Kruger, 2003].

A FSW instrumented chuck was used to acquire the sensory information from the tool platform, and provide feedback to implement a multi-variable control scheme for the weld process. Such an instrumented chuck, as illustrated in Figure 2.11, was assembled at NMMU to provide on-line measurement of the main parameters that characterise the FSW process [Hattingh et al., 2004].

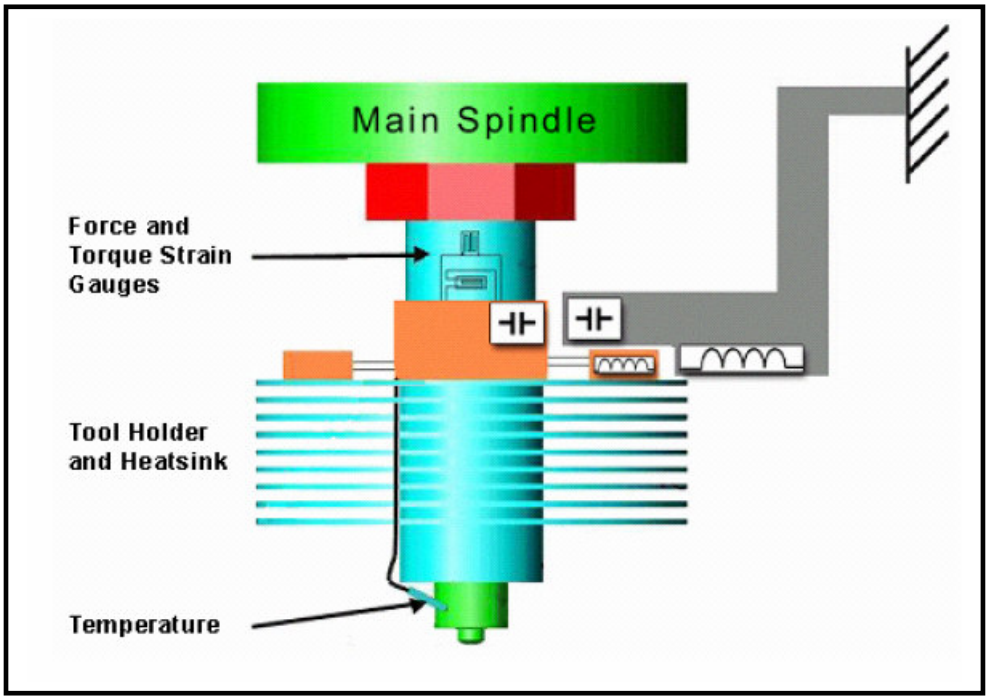

Figure 2.11: An Instrumented chuck for FSW process [Hattingh et al., 2004].

This sensing system, as illustrated in Table 2.3, had been developed to perform the on-line measurement of FSW variables such as tool torque, tool temperature, and downwards force applied by the tool shoulder to the material, as well as a horizontal force vector measured through 360^0 as the tool rotates [Hattingh et al., 2004].

Table 2.3: Data channels provided by the FSW chuck [Hattingh et al., 2004].

Channel	Description	Sampling Frequency
F_V	Horizontal force as a rotating factor	125Hz
F_Z	Vertical force	10Hz
T_{PIN}	Tool pin temperature	1Hz
T_{GAUGE}	Chuck electronics temperature	1Hz
T_T	Tool torque	10Hz

2.9 Fuzzy Control in Machining Processes

The recent decades were characterised by the generalised application of modern technology to improve controlled systems' behaviour and by the development of new control strategies. Fuzzy logic technology, as one of the artificial intelligent (AI) strategies, is widely used because of its practical impact on dynamic plant control [Haber et al., 1998].

FSW can be classified within the category of the end milling processes that are too complex to be thoroughly described by using mathematical models. The complexity of the end milling processes is due to non-linearities, parameter interactions as well as the machine tools and machine tools drives' dynamics. There are also many parameters to be determined and many assumptions are required to integrate and decrease the number of parameters [Liang et al., 2002].

2.10 Fuzzy Logic Control in Turning Process

A FLC was used in an experiment where the spindle speed and the feed rate controlled the spindle power in a typical turning process. The spindle power was maintained at the reference level using either feed rate only or a combination of feed rate and spindle speed, in order to evaluate the performance of these control strategies [Liang et al., 2002]. Figure 2.12 illustrates the block diagram of this system to control the tool torque (T).

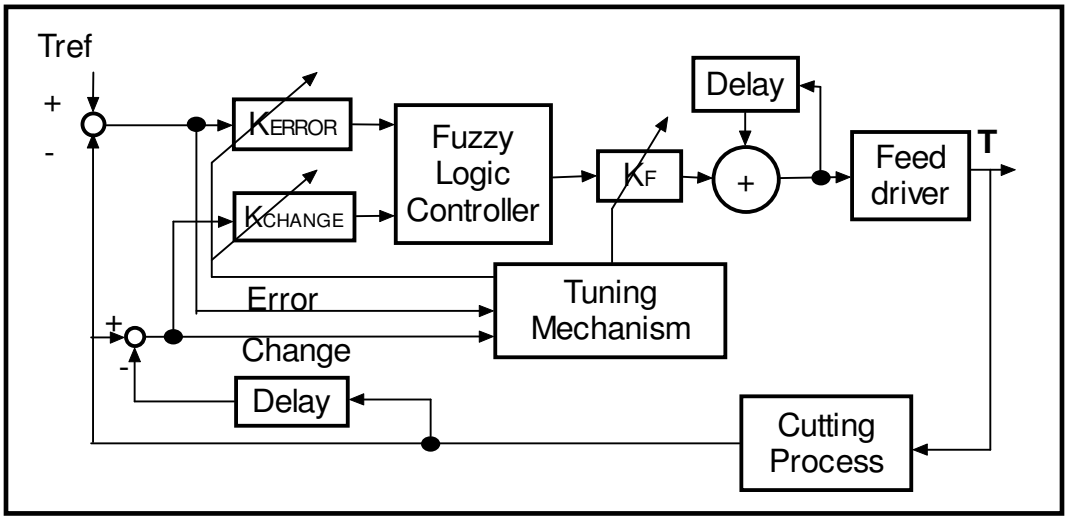

Figure 2.12: Structure of the fuzzy torque control system for a cutting process.

The control system used two inputs, torque error and torque change. The output of the system was the command for feed rate adjustment. The main elements of the fuzzy control system included a FLC and a tuning module. FLC generated primary command for feed rate adjustment to maintain a good steady-state and transient response [Liang et al., 2003].

The output scaling factor was further fine tuned by a tuning module to adapt to the dynamic machining conditions. In addition to modifying the output scaling factor, the tuning module was also used to adaptively adjust the input scaling factors in response to the dynamics of changing machining processes [Liang et al., 2003].

Equations 2.5 and 2.6 were used to obtain the torque error and rate of change of torque respectively. Equations 2.7 and 2.8 were used to transform the error and rate of change of error respectively. The triangular and spike membership functions (MFs) were used to transform the inputs and outputs respectively. The nine fuzzy sets were used at the inputs and outputs in the range of [-1, 1]. The input scaling factors, K_{ET} and K_{CT}, for the torque error and torque change, are derived from Equations 2.9 and 2.10 [Liang et al., 2003].

$$ET_{(i)} = T_{REF} - T_{(i)} \tag{2.5}$$

$$CT_{(i)} = ET_{(i)} - ET_{(i-1)} \tag{2.6}$$

$$et_{(i)} = ET_{(i)} K_{ET} \tag{2.7}$$

$$ct_{(i)} = CT_{(i)} K_{CT} \tag{2.8}$$

$$K_{ET} = \begin{cases} 1/(T_{Max} - T_{Ref}) & \text{if } T_{Ref} \geq T_{(i)} \\ 1/(T_{Ref} - T_{Min}) & \text{if } T_{Ref} \leq T_{(i)} \end{cases} \tag{2.9}$$

$$K_{CT} = \{1/(T_{MAX} - T_{MIN}) \tag{2.10}$$

The quality of the process was measured using the performance index value as illustrated by Equation 2.11 for both the error and rate of change of error. This index value was used to control actions by adjusting the input and output scaling factors [Liang et al., 2003].

$$\mathrm{PI}_{\mathrm{ET}}(i) = \sqrt{\frac{\sum_{j=i-n+1}^{i} (ET(i))^2}{n}} \tag{2.11}$$

The input tuning factors were applied to adaptively strengthen or weaken control actions in response to the on-line signals. It is natural to tune the scaling factor based on a control performance indicator. In this study, the tuning factor for torque error was specified according to performance index as presented by Equation 2.12.

$$\mathrm{K}_{\mathrm{t,ET}}(i) = \left(\frac{PI_{ET}(i-d)}{\varepsilon_{ET}} \right)^{\alpha_{ET}} \tag{2.12}$$

The constant (ε_{ET}) represented the bandwidth of the tolerance zone, *d* time delay, and α_{ET} a constant in the range of [0, 1]. The constant, ε_{ET}, was set to 0.1 in these experiments. The tuning factor for torque change can be derived similarly. It is noted that sometimes the $K_{t,ET}(i)$ could be very large moving the $et(i)$ value well beyond the fuzzy domain of [-1, 1], and it was therefore restricted within the fuzzy domain [Liang et al., 2003].

The adjustments of feed and spindle were performed not only on the amount of deviation from the control target but also on the trend of the deviation. The second tuning factor $K_{F2}(i)$ is introduced to accommodate this consideration. Equation 2.13 presents the algorithm used to calculate the tuning parameter, $K_{F2}(i)$ [Liang et al., 2003].

$$
\begin{aligned}
&\text{if } \left|\frac{\mathrm{CE}_{(t)}}{CE_{(t-1)}}\right| \geq 1 \\
&\quad \textit{if } sign\,CT_{(i)} \neq CT_{(i-1)} \quad \textit{set } k_f(i) \simeq 1 \\
&\quad \textit{else if } \left|ET_{(i)}\right| \leq \left|ET_{(i-1)}\right| \quad \textit{set } k_f(i) \simeq \left|\frac{CT_{(i)}}{CT_{(i-1)}}\right|^{\beta} \\
&\quad \textit{else if } \left|ET_{(i)}\right| \geq \left|ET_{(i-1)}\right| \quad \textit{set } k_f(i) \simeq \left|\frac{CT_{(i-1)}}{CT_{(i)}}\right|^{\beta} \\
&\textit{else} \quad \textit{set } k_f(i) \simeq 1
\end{aligned}
\tag{2.13}
$$

This control system was used to machine a steel work piece with step changes in depth of cut as illustrated in Figure 2.13. The tests were conducted for a length of 150mm, using three types of end mill tools: 4-flute 14.3mm, 3-flute 25.4mm and 4-flute 25.4mm diameter cutters [Liang et al., 2003].

Figure 2.14 illustrates the results of one of these experiments used to maintain constant torque at different depths of cut. The three tools were for examining the system's adaptability to tool changes. It was established that the system adapted quite well for each one of the three tools. The system responded very well and the torque was well regulated around the reference level in all the three cases.

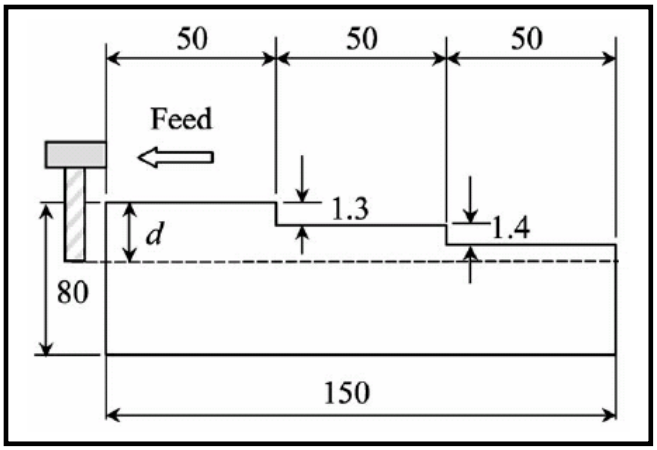

Figure 2.13: A work piece with step changes in depth of cut [Liang et al., 2003].

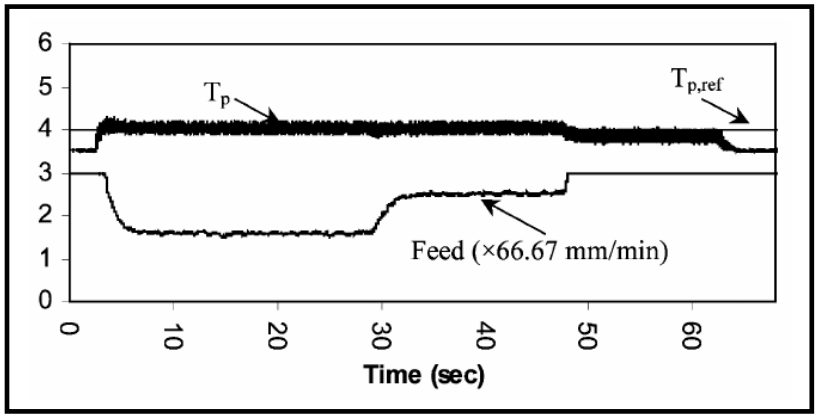

Figure 2.14: Feed adjustment using a 4-flute tool [Liang et al., 2003].

Liang presented a fuzzy control system for CNC machining processes. Both end milling and turning tests were carried out on industrial machines. The test results show that the system adapts reasonably well to a variations in depth of cut, work piece material change, tool changes, and process changes. It was also demonstrated that it is possible to implement a single control system, for different machining processes, in a real manufacturing environment [Liang et al., 2003].

2.11 Summary

FSW process enables the solid-state welding of different alloys that had been difficult to weld using the traditional welding methods [Deqing et al., 2004]. FSW produces welds with properties as good as that of the parent material due to the absence of filler material. The process produces welds with less defects and narrower heat affected zones than the traditional welding methods [Chao et al., 2003].

Although FSW is a versatile process, little research had been conducted as far as modelling the dynamics of the process. A robust controller that does not require accurate mathematical modelling is needed to optimally control this process.

Fuzzy logic technology had been used to control other end milling processes that are difficult to model. Liang used FLC to successfully regulate the milling process irrespective of the tool and material changes. FLC was used without accurate mathematical models of the process under consideration.

FLC is considered as a suitable option to control the FSW process. Fuzzy logic theory is based on the artificial reasoning techniques that do not need exact mathematical models. It enables the controller to view the complicated process as just a black box with a number of inputs and outputs [Haber et al., 1998].

The frictional energy input is the most important parameter of the FSW process that determines the success of the process [Chao et al., 2003]. It was also established that this energy input is the result of the frictional energy between the FSW tool and welded material [Colegrove et al., 2003]. Therefore, the adjustment of the tool rotational speed and transverse rate result in the regulation of the energy input and other dependent parameters of the process.

Chapter 3

Fundamental Concepts of Fuzzy Logic Controllers

The use of computer numerical control (CNC) machining centres has expanded rapidly through the years. A great advantage of the CNC machining centre is that it reduces the skill requirements of machine operators. However, a common drawback of CNC end milling is that its operating parameters such as spindle speed or feed rate are prescribed conservatively either by a part programmer or by a relatively static database in order to preserve the tool. As a result, many CNC systems run under inefficient operating conditions [Yang et al., 2002].

The variations in the characteristics of milling processes and process non-linearities, are the bottlenecks in the development of the formal mathematical models. Fuzzy logic technology provides an alternative to the formal model development. This simplified viewpoint presents a process as a black box with its input and output variables [Haber et al., 1998].

FLC theory, compared to other mathematical theories, is perhaps the most adaptable theory in practical applications. The main reason is that a fuzzy set has the property of relativity, variability and inexactness in the definition of its elements [Bryan et al., 1997].

Instead of defining an entity in calculus, assuming that its model is not exactly known, a fuzzy set can be used to define the same entity by allowing possible deviation and exactness in its role [Bryan et al., 1997]. Fuzzy logic may be used as a mathematical model to mimic human logic in engineering solutions.

Fuzzy logic is implemented in a natural language and much limited in its operation, and cannot match the scope of human thinking. However, it can derive a solution for a given case from a set of rules that were defined for similar cases [Von Altrock, 1995].

Natural language is perhaps the most powerful form of conveying information that humans possess for any given problem or situation that requires solving or reasoning. It is for the following reasons that Fuzzy logic is implemented in natural language [Berkan et al., 1997]:

- Natural language allows fuzzy logic to be implemented in solving many engineering problems as well as other practical applications.
- Since fuzzy logic can handle some form of uncertainty and imprecision which are inherent in natural language, it can be used as a mathematical foundation of our natural language.
- Many engineering rules can be formulated based on the observations and responses of the process. The experiences of the expert can also be incorporated into the fuzzy logic rules.

3.1 Control System Architecture for a FSW Process

FSW is a complex process difficult to predict and model due to the characteristics of friction [Koren, 1997]. Figure 3.1 illustrates the proposed architecture for the control of the FSW process.

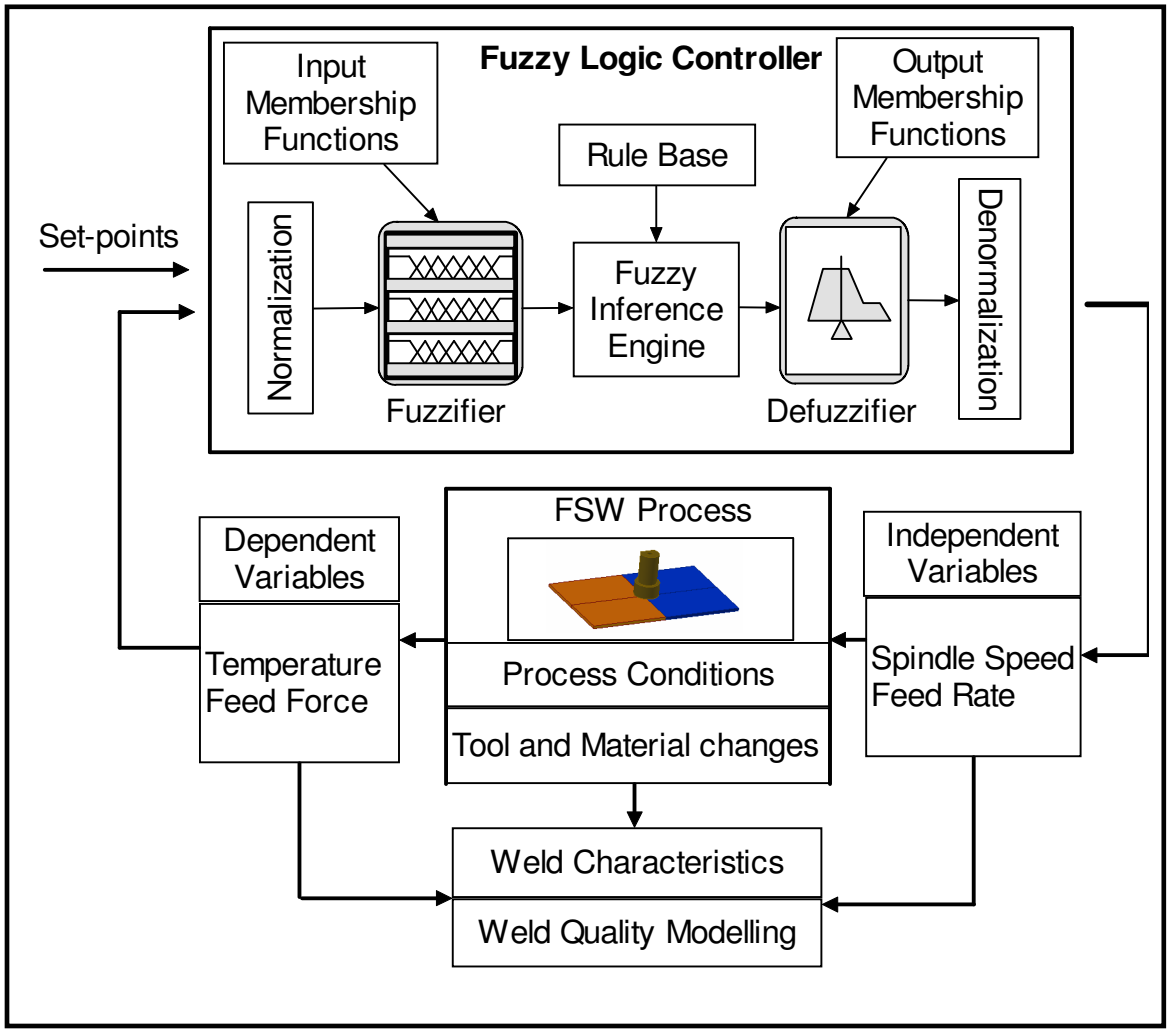

Figure 3.1: The overall control architecture for the control of a FSW process.

The FSW process inputs, in the fuzzy model, can be subdivided into action variables, namely feed rate and spindle speed, and also process conditions such as the tool type and material properties. The system outputs are feed force and tool temperature, which are related to the constraints given by the power of the spindle and feed motors.

3.2 Fuzzy Logic Control Structure

The control system architecture for a FSW process, as illustrated in Figure 3.1, has a FLC as an intelligent part of the control arrangement. The FLC consists of a fuzzifier, a Fuzzy Inference Engine (FIE), input and output MFs, a rule-base and a defuzzifier [Dweiri et al., 2003].

The rule base contains a number of fuzzy IF-THEN rules, which form a database to define a matched implication between an input and output of each rule. A FIE performs the inference operations on the activated rules at each computational cycle to form an aggregated output [Dweiri et al., 2003].

3.2.1 Normalization

The goal of this input data processing is to ensure that data is in an appropriate level for data transformation. Data is transformed from numerical to probabilistic format for the FLC operations. The MFs concept enables the FLCs to process mixed data, in both the numerical and symbolic (linguistic) forms [Berkan et al., 1997].

Another important property of the normalization stage is that when an input data set is partially ambiguous or unacceptable, a FLC may still produce reasonable results. This property, often called robustness against missing data, requires unique treatment during the input data processing [Berkan et al., 1997].

3.2.2 Input Fuzzification

A FLC algorithm is based on possibility computations only. Therefore, the units of the input data to the inference computations must be in probabilistic format. In practical life, however, data is not in the form of possibilities. The transformation, from the practical units to the possibility units, is referred to as evaluating fuzzy variables. Such a transformation is made possible with the aid of inputs MFs [Berkan, 1997].

3.2.3 Membership Functions

The MFs are made up of the Fuzzy sets in fuzzy logic theory. These sets have two important properties. The first property is that the elements (i.e. the singletons) of a fuzzy set are, in one analogy, “aware” of each other by their relative distribution of the degree of membership. Therefore, all elements carry twofold information, their degree of inclusion to the set and their relative standing among others [Berkan et al., 1997].

The second property is the error phenomenon. When approaching a crisp set boundary defined by the characteristics function, the possibility of erroneous inclusion of an element to the set due to the measurement uncertainties increases exponentially. In an infinitely small interval around the exact boundary, the possibility of erroneous inclusion approaches 1, meaning an absolute indecision. However, the possibility error in the degree of inclusion is spread over the entire set somewhat uniformly in fuzzy sets. Thus, there is no localized point of absolute indecision in fuzzy sets [Koivo, 2004].

For example, a sensor input value is assigned to the linguistic values, defined by MFs, resulting into the fuzzified values of the original input signal. Figure 3.2 illustrates the triangular MFs, made up of fuzzy sets of “negative”, “zero” and “positive” [Koivo, 2004].

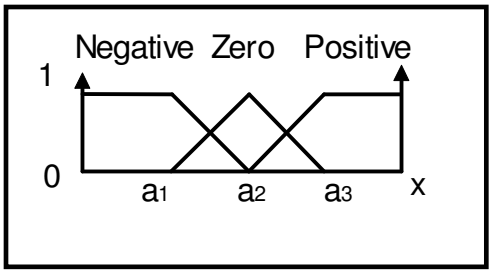

Figure 3.2: The triangular membership functions.

The membership value of an input depends on its relative distance from the point of unity membership of each MF. The membership value is reduced by moving from the centre of the fuzzy set. The rate of reduction in membership strength is determined by the shape of the MF. The triangular MFs are the mostly commonly used as they have high computational efficiency.

The triangular membership sets, as illustrated in Figure 3.2, can be expressed mathematically by Equations 3.1 through to 3.3. The parameters, a_1, a_2 and a_3, determine the positions of the MFs, and affect the shape of the MFs. The MFs normally overlap each other such that an input has at least one membership value of more than 50% belonging to one of the overlapped functions.

$$\mu_A\text{Negative}(x) = \begin{cases} 1 & x \le a_1 \\ \dfrac{(x - a_2)}{(a_1 - a_2)} & a_1 \langle\ x \le a_2 \\ 0 & \text{otherwise} \end{cases} \qquad (3.1)$$

$$\mu_A \text{Zero}(x) = \begin{cases} \dfrac{(x-a_1)}{(a_2-a_1)} & a_1 < x \le a_2 \\ \dfrac{(x-a_2)}{(a_2-a_3)} & a_2 < x \le a_3 \\ 0 & \text{otherwise} \end{cases} \tag{3.2}$$

$$\mu_A \text{Positive}(x) = \begin{cases} \dfrac{(x-a_2)}{(a_3-a_2)} & a_2 < x \le a_3 \\ 1 & a_3 < x \\ 0 & \text{otherwise} \end{cases} \tag{3.3}$$

Each crisp input is evaluated against every MF within the variable's universe of discourse and stored as a fuzzy variable. When evaluating an antecedent fuzzy variable for a given input data, all the MFs are evaluated.

The result of the evaluation is a vector (or a set) of MFs with each element indicating the possibility produced by this input data entry. Each input, which can be either a single point or a distribution of points, is applied to the data transformation process via MFs. Figure 3.3 illustrates this evaluation process.

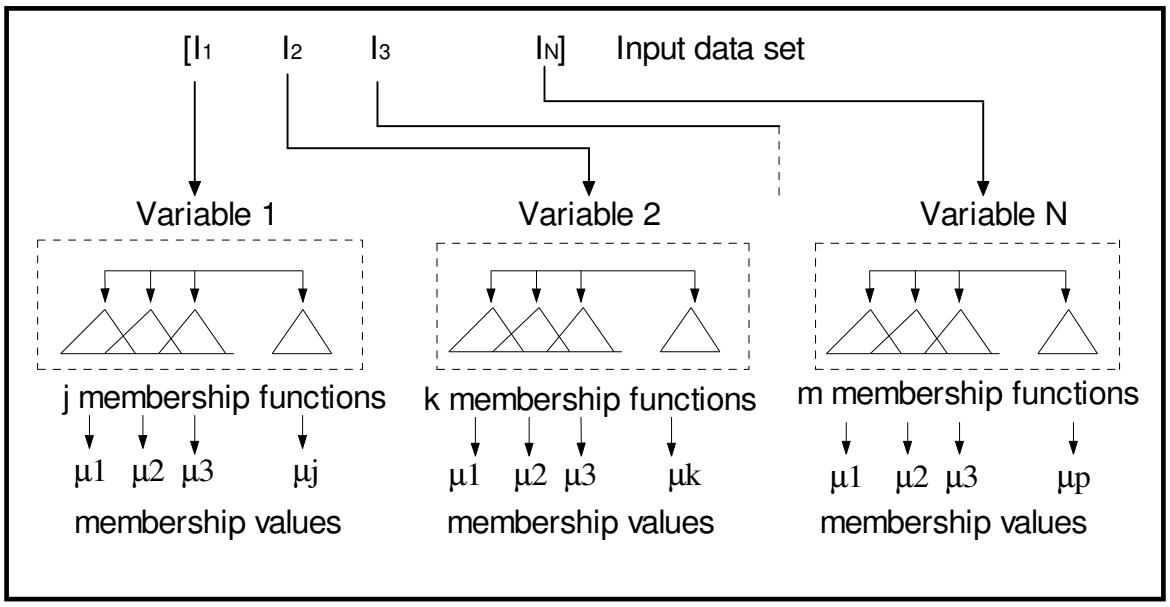

Figure 3.3: Fuzzy variable evaluation event [Berkan et al., 1997].

The geometrical shape of the MF is the characterisation of uncertainty in the corresponding fuzzy variable. Therefore, a high level of detail (i.e. high resolution) in shape design must be considered as a conceptual error (i.e. uncertainty must not be defined in detail). One exception of the rule is the probabilistic design in which uncertainty is purely represented by probability distribution in the presence of reliable data [Berkan et al., 1997].

There are a number of challenges encountered during the design of the input MFs for each fuzzy input and output MFs for each fuzzy output according to the given data pairs. According to [Von Altrock, 1995], some of these encountered difficulties include the need to:

- Find the appropriate number of MFs (also referred to as the number of mapping categories of granularity) and their locations in the discourse of the universe. This requirement affects the mapping between the input–output relationships.
- Determine the shapes of the MFs which normally have some impact on the overall solution.
- Determine the universe of discourse that represents the extension of validity of the fuzzy inference rules on each variable domain.

Seven MFs can be used to represent the inputs and outputs of a typical process to cater for enough rule coverage and these functions are illustrated in Figure 3.4. These fuzzy sets are negative large (NL), negative medium (NM), negative small (NS), zero (ZR), positive small (PS), positive medium (PM) and positive large (PL) for both the inputs and outputs.

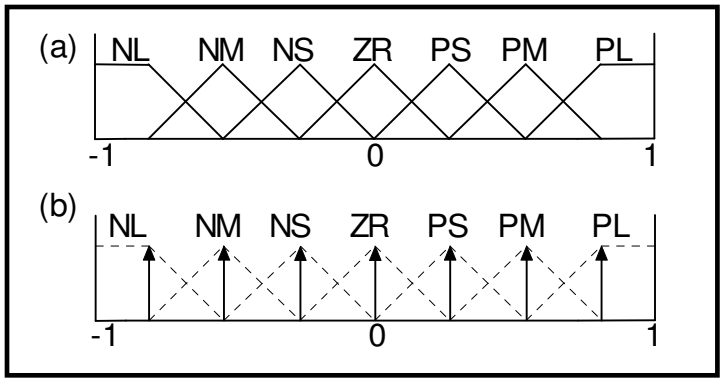

Figure 3.4: Membership functions for (a) inputs and (b) outputs.

The triangular MFs are commonly used at the input stage of the FLC as they simplify the mathematical operations, and are widely adopted in the literature. Another important factor is that the number of the MFs and their locations on the universe of discourse affect the basic fuzzy algorithm relatively more severely than the effects caused by the shape variations among the MFs [Berkan et al., 1997].

The output MFs are simply the singleton with their heights truncated by the weight due to the implication process. These output MFs are normally used when a Takagi–Sugeno inference process is used at the output stage. The spike MFs are preferred as they have high computational efficiency. The defuzzification result is simply the weighted average of the locations of a few involved spikes rather than finding the centre of an area, as in the case of a Mamdani-style inference process [Liang et al., 2003].

3.2.4 Rule Bases

The fuzzy rule base is one of the crucial components of the FLC structure and is presented in Table 3.1. It is a collection of control rules that defines the system behaviour and replaces the typical mathematical process modelling. The fuzzy rules, which use the fuzzy inputs to determine the system actions, are obtained from skilled operators, experiments and prior knowledge of the process to be controlled [Liang et al., 2002].

Table 3.1: Rule base for the control of reference.

Input error								
Output		**NL**	**NM**	**NS**	**ZR**	**PS**	**PM**	**PL**
	NL	PL	PL	PM	PS	ZR	NS	NM
Rate of	**NM**	PL	PL	PM	PS	ZR	NS	NM
Change	**NS**	PL	PM	PS	ZR	ZR	NS	NM
Of error	**ZR**	PM	PS	ZR	ZR	ZR	NS	NM
	PS	PL	PM	PS	ZR	NS	NM	NL
	PM	PL	PM	PM	NS	NM	NL	NL
	PL	PL	PM	PL	NM	NL	NL	NL

The number of dependent process variables to be controlled in a particular experimentation will determined the number of rule bases. Each rule base contains a knowledge database used to control particular independent variables.

This arrangement is required, as in the case where each independent variable affects the dependent variables differently. In a typical FSW process, the spindle speed and the feed rate rule bases can be formulated to control the welding temperature and feed force, respectively.

3.2.5 Fuzzy Inference System and Defuzzification

Each one of the rules can be written as an IF-THEN statement that describes the consequential action to antecedent requirements of such a rule. The combination of the input error and rate of change of the error can represent an antecedent part of a fuzzy rule. For example, if the measured value is less than its target value and the currently measured value is lower than its previously sampled one, then a small increase in a control variable is required [Berkan et al., 1997]. This may be translated into the following fuzzy rule:

IF Error is NS and Error_Change is NS then Output is PS (3.4)

Each pair of error and rate of change of error generally activates several fuzzy rules at one instance. Figure 3.5 illustrates the multiple, activated rules. All the four activated rules contribute to the strength of the control action, which is determined by the aggregation section of the FLC.

A fuzzy inference system (FIS) executes the following steps at each operational cycle on the fuzzy IF-THEN rules [Dweiri et al., 2003].

- Compare the inputs variables with the MFs on the premise part to obtain the membership values of each linguistic label.
- Combine, through a specific T-norm operator, the membership values on the premise part to get the firing strength for each rule.
- Generate the qualified consequences to produce a crisp output.

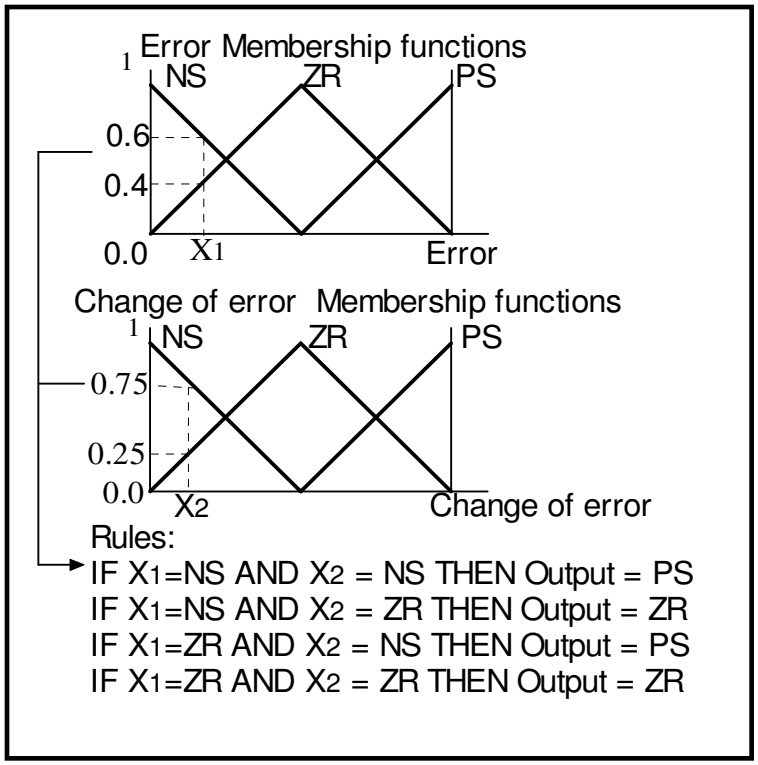

Figure 3.5: Multiple rules activated by two inputs.

Several types of the fuzzy inference systems (FIS) were proposed in the literature. FIS systems can be classified into three types, depending on the types of the fuzzy reasoning and fuzzy IF-THEN rules employed:

- Tsukamto fuzzy model: The output of this model is the average of each rule's crisp output induced by the rule's firing strength and the output of the MF. The output of this scheme must be monotonically non-decreasing [Dweiri et al., 2003].

- Mamdani fuzzy model: The overall fuzzy output of this model is derived by applying the OR operation to the triggered rules. Various schemes such as centre of area, bisector of area, mean of maximum and centre of gravity, are used to derive the final crisp output [Dweiri et al., 2003].

- Takagi–Sugeno fuzzy model: The output of each rule is a linear combination of the input variables plus a constant term. The final output is the weighted average of each rule's output [Dweiri et al., 2003].

The Takagi–Sugeno inference model has the following advantages [Liang et al., 2003].

- It guarantees the continuity of the output surface.
- It is well suited for mathematical analysis.
- It works well with optimisation and adaptive techniques.

When a Takagi–Sugeno inference process is used, the output of the FLC is simply the weighted average of the spike locations. The weight of each singleton MF is derived from the respective spike height being truncated following the implication rule. Figure 3.6 illustrates the Takagi–Sugeno inference system, where one pair of inputs has activated four rules. The fuzzy rules, generated by a typical Takagi–Sugeno inference mechanism, are listed in Equations 3.5 through to 3.8.

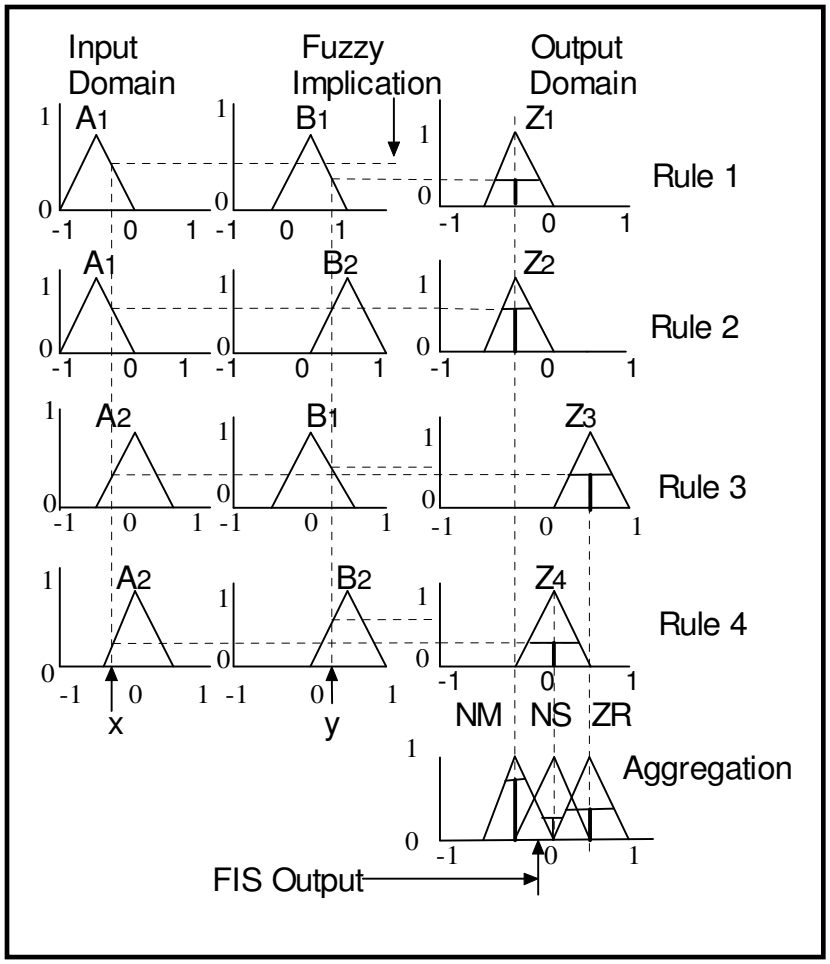

Figure 3.6: Takagi–Sugeno style inference mechanism.

Rule 1: if x is A_1 and y is B_1 then $z_1 = a_1x + b_1y + r_1$ (3.5)

Rule 2: if x is A_1 and y is B_2 then $z_2 = a_1x + b_2y + r_2$ (3.6)

Rule 3: if x is A_2 and y is B_1 then $z_3 = a_2x + b_1y + r_3$ (3.7)

Rule 4: if x is A_2 and y is B_2 then $z_4 = a_2x + b_2y + r_4$ (3.8)

The Takagi–Sugeno model can be regarded as a smooth piece-wise linear approximation of a non-linear function. Figure 3.7 illustrates a typical Takagi-Sugeno system with three rules covering a subset of the operating domain that can be approximated by a local linear model and the corresponding rules are listed as follows:

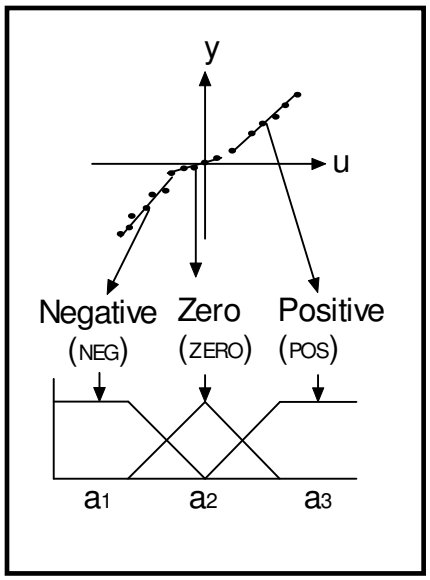

Figure 3.7: A Takagi-Sugeno fuzzy model as a piece-wise linear approximation of a nonlinear system.

Rule 1: if *u* is NEG then $y_1 = a_1u + b_1$ (3.9)

Rule 2: if *u* is ZERO then $y_2 = a_2u + b_2$ (3.10)

Rule 3: if *u* is POS then $y_3 = a_3u + b_3$ (3.11)

Output $$y = \frac{\left(\mu_{NEG}(u)\,y_1 + \mu_{ZERO}(u)\,y_2 + \mu_{POS}(u)\,y_3\right)}{\left(\mu_{NEG}(u) + \mu_{ZERO}(u) + \mu_{POS}(u)\right)} \quad (3.12)$$

The aggregated output of the FLC is further processed by the denormalization unit output of the system control architecture. The crisp output control is required since the output is used to drive the system devices, such as the spindle and bed feed motor drives, in the case of FSW process.

3.2.6 Denormalization

The output data processing is used the transform the output data of the FLC system from the probabilistic form into their numerical equivalences. The transformation is required as the process hardware can only be operated in the numerical data format [Berkan et al., 1997].

3.3 Tuning Fuzzy Logic Controllers

If the transfer function of the process is known, the optimisation techniques can be used to obtain the optimal parameters of the fuzzy controller. However, if the transfer function is unknown, there are other alternatives that can be considered [Haber et al., 1998]. The following techniques can be used to create a FLC with adaptation capabilities [Liang et al., 2002].

- Membership function tuning.
- Linguistic rule tuning.
- Input and output scaling factors (gain coefficient) tuning.

The first two techniques usually require additional algorithms such as neural network and genetic algorithms; whereas the input and output factor tuning technique is simple to implement [Liang et al., 2002]. The last technique is considered as one of the most effective techniques used to optimise the performance of FLC and has high computational efficiency.

Prozcyk and Mamdani analysed the behaviour of the controlled process while adjusting the scaling factors. An increase in the magnitude of the input scaling factor (for error and change in error), makes the performance measurement more sensitive around the set point and less sensitive during the rise time. A low value for the output scaling factor causes a slow rise time, but increases the region of fastest convergence [Haber et al., 1998].

Hence, it is possible to obtain a damped response by regulating the scaling factor in real time. Unlike conventional controllers, which are designed for certain process conditions, the controller herein proposed could be applied to a wide range of process conditions [Haber et al., 1998].

3.4 Fuzzy Logic Control of a FSW process

Figure 3.8 illustrates the proposed FLC system for the FSW process. This control system has two inputs and two outputs. The two inputs are the error and rate of change of the error. The two outputs are the adjusted feed rate and spindle speed. The main components of the system include a FLC for generating the recommended feed rate and spindle speed adjustments. A tuning module is used to fine tune the output scaling factors to adapt to the dynamic welding conditions.

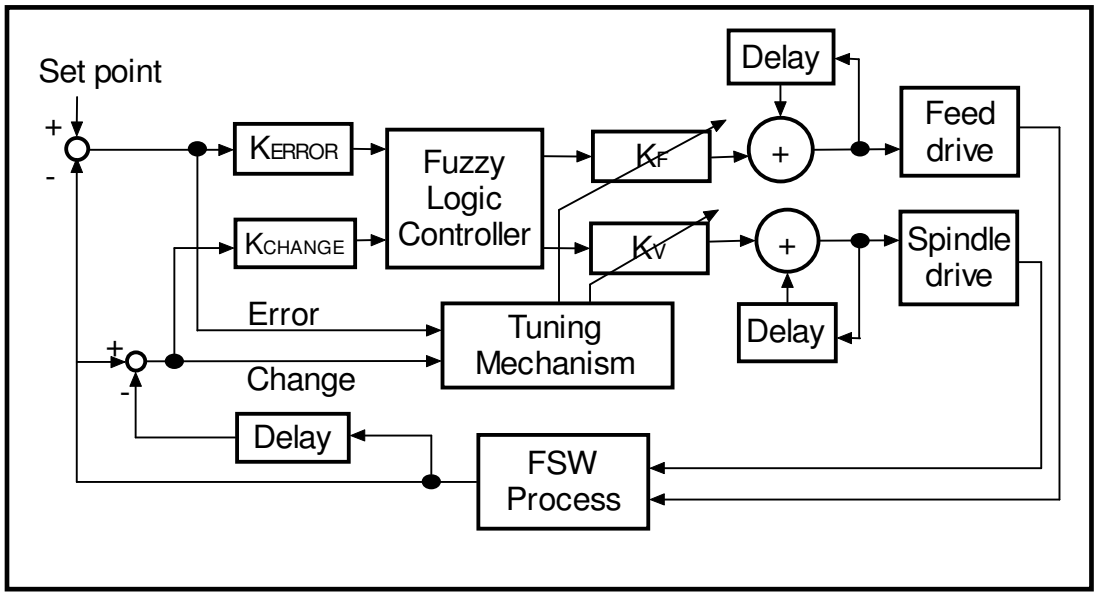

Figure 3.8: Block diagram of the proposed FLC for FSW system.

3.4.1 FSW Process Parameters

The feed force can be used as an important parameter to consider for improved productivity in a FSW process. It was established that the feed rate has a major effect on the amount of feed force produced during the FSW process. Therefore, the produced feed force can be used as a good indication to the level of productivity in the FSW process [Johnson, 2001].

The feed force, to a large extend, also affected the amount of frictional heat produced. It had been established that the strength of the metal, at the interface between the rotating tool and the work piece, falls to below the shear stress as the temperature increases. The plasticized material is then extruded from the leading side to the trailing side of the tool as the tool is steadily moved along the joint line [Thomas et al., 2003].

The frictional energy is the process parameter that determines the success of the FSW process. The heat influences the shape and microstructure of the weld, as well as the residual stress and distortion of the work-piece. The heat must be high enough so that the tool pin can stir the material, but not too high to melt the material interface or shorten the lifespan of the welding tool [Chao et al., 2003].

3.4.2 Fuzzy Inputs

If the feed force is the process variable under consideration, then the two inputs, feed force error and rate of change of feed force, are calculated at each sampling instant. Equations 3.13 and 3.14 present the error and rate of change of error respectively. Equations 3.15 and 3.16 presents the input scaling factors that are used to normalize the two inputs.

$$F_{Error(t)} = F_{Reference} - F_{Measured(i)} \tag{3.13}$$

$$F_{Change(t)} = F_{Measured(i)} - F_{Measured(i-1)} \tag{3.14}$$

$$KF_{Error(t)} = (F_{Error(i)} - F_{Mid}) / (1/2 * F_{Range}) \tag{3.15}$$

$$KF_{Change(t)} = (F_{Change(i)} - F_{Mid}) / (1/2 * F_{Range}) \tag{3.16}$$

3.4.3 Fuzzy Inference Engine and Defuzzification

The Takagi–Sugeno inference system guarantees the continuity of the output surface, suited for mathematical analysis and works well with optimisation and adaptive techniques. When this inference process is used, the output of the FLC is simply the weighted average of the singleton MFs.

The rule consequences, instead of being formed by fuzzy sets, are linear parametric equations defined by the inputs of the system. The rules generated by a typical Takagi–Sugeno inference mechanism for error (e) and rate of change of error (c), are illustrated in Equations 3.17 and 3.18 respectively.

$$\text{if e is NL and c is NL then Out}_i = W_i(e * NL + c * NL + r_i) \quad (3.17)$$

$$\text{if e is NM and c is NM then Out}_j = W_j(e * NM + c * NM + r_j) \quad (3.18)$$

The output of the Takagi–Sugeno fuzzy model is a linear combination of the input variables plus a constant term. The final output is the weight average of each rule's output. The establishment of this fuzzy model is based on the Adaptive Neuro-Fuzzy Inference System (ANFIS). The major advantage of this method is that it is not necessary to have any prior knowledge of rule consequent parameters [The MathWorks, 2004].

3.4.4 Fuzzy Adaptation

Conservative machining parameters are preset and often kept unchanged throughout the entire weld regardless of the real-time welding and tool conditions. This methodology does not allow the machine to adapt to diverse real-time welding and tool conditions, and is limited to rigid execution of Numerical Control (NC) – style properties [Guerra et al., 2002].

The parameter compensation, in fuzzy logic controlled systems, had been attempted through several approaches. The recent approaches such as gain adaptation, gain scheduling and parameter tuning were adopted successfully in several FLC systems [Nagarajan, et al., 2001].

It was a challenging problem to compensate for the unknown parameters in real-time control applications. The FLC can be made to be adaptive with the aid of techniques such as MF tuning, input and output scaling factor tuning, as well as linguistic rule tuning [Liang et al., 2002].

The control actions are influenced by the machining processes and the environments in which they operate. The tuning is done based on the idea that the controlled variables can be adjusted in response to not only the amount of deviation from the control target, but also to the trend of the deviation [Liang et al., 2002]. The following algorithm uses the error (e) and rate of change (c) to tune the performance of the FLC.

$$
\begin{aligned}
&\text{if } \left|\frac{\mathrm{CE}_{(t)}}{CE_{(t-1)}}\right| \geq 1 \\
&\quad \textit{if } sign\,CT_{(i)} \neq CT_{(i-1)} \qquad set\, k_f(i) \simeq 1 \\
&\quad \textit{else if } \left|ET_{(i)}\right| \leq \left|ET_{(i-1)}\right| \quad set\, k_f(i) \simeq \left|\frac{CT_{(i)}}{CT_{(i-1)}}\right|^{\beta} \\
&\quad \textit{else if } \left|ET_{(i)}\right| \geq \left|ET_{(i-1)}\right| \quad set\, k_f(i) \simeq \left|\frac{CT_{(i-1)}}{CT_{(i)}}\right|^{\beta} \\
&\quad \textit{else} \quad set\, k_f(i) \simeq 1 \\
&\textit{Where} \quad \beta = 0.125
\end{aligned}
\tag{3.19}
$$

3.5 Summary

Fuzzy logic technology offers an alternative to formal model development as it provides a simplified view of the process to be controlled. The robustness of the FLC enables the control of the processes irrespective of the absence of accurate mathematical models that define those processes, as in the case of a FSW process.

The Takagi-Sugeno inference was chosen as the suitable FIS for the control of a FSW process as it has high computational efficiency and is well suited for optimisation and adaptive techniques. The output of the proposed fuzzy control system was tuned with the aid of output scaling factors to make the controller adaptive.

There is a lack of mathematical models for the regulation of a FSW process. The rule base of the FLC replaced the mathematical modelling of the FSW process. The FSW experimental design is used to acquire the casual relationships between the process inputs and outputs in order to customize the rule base of the fuzzy controller.

Chapter 4

FSW Data Acquisition and Modelling

FSW is a process that reflects non-linear characteristics including the dynamics of the machine tool and machine tool drives. In order to successfully develop a control system, one needs to have mathematical models to describe such a process for simulation purposes. The control models can be generated through reverse engineering approaches, as in the case of a FSW process, where there is a lack of such quantitative models [Deqing et al., 2004].

The objective of this step is to acquire the characteristics of the FSW process with the aid of the experimental design approach. The goal of the experimental approach is to investigate the mathematical effect of one factor independently from others, as well as the interaction between those variables on the process output [Zeelie, 1997].

Statistical models have to be derived in spite of the variability in the experimental results. The collection of relevant experimental data, mean value of the results, a qualitative estimate of the variability of the results, and techniques to access the validity of our models form a sequence of events to be followed in order to reach the correct conclusions [Zeelie, 2003].

The characteristics of the FSW process are acquired with the aid of the experimental design as illustrated in figure 4.1. The regression models are used to customise the FLC rule base. The regression models and FLC are implemented in MatLab for simulation purposes.

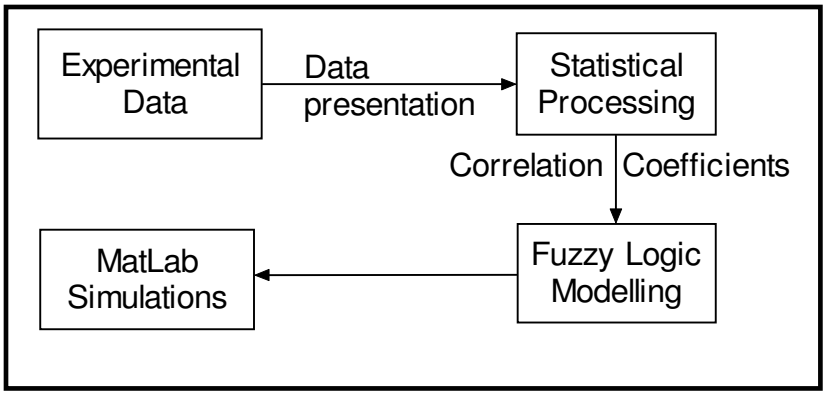

Figure 4.1: The data acquisition and models development.

The developed models are then used to generate the input-output data patterns for the formulation of a Takagi–Sugeno FLC. This system is characterised by the linear functions that forms part of the output MFs. The FLC is customised by tuning the MFs parameters, based upon the desired relationship between the matched input–output data sets [The MathWorks, 2004].

4.1 FSW Process Parameters

4.1.1 Feed Rate and Welding Speed

The tool feed rate and welding speed form the main parameters of the FSW process. The feed rate affects the micro hardness of the weld and decreases as the feed rate is increased. The hardness strength of the welds has a strong dependency on the tool welding speed. The hardness strength of the weld increases first, reaches a maximum and then decreases with an increase in welding speed [Deqing et al., 2004]. Figure 4.2 illustrates the experimental domains for the welding parameters, welding conditions and process variables.

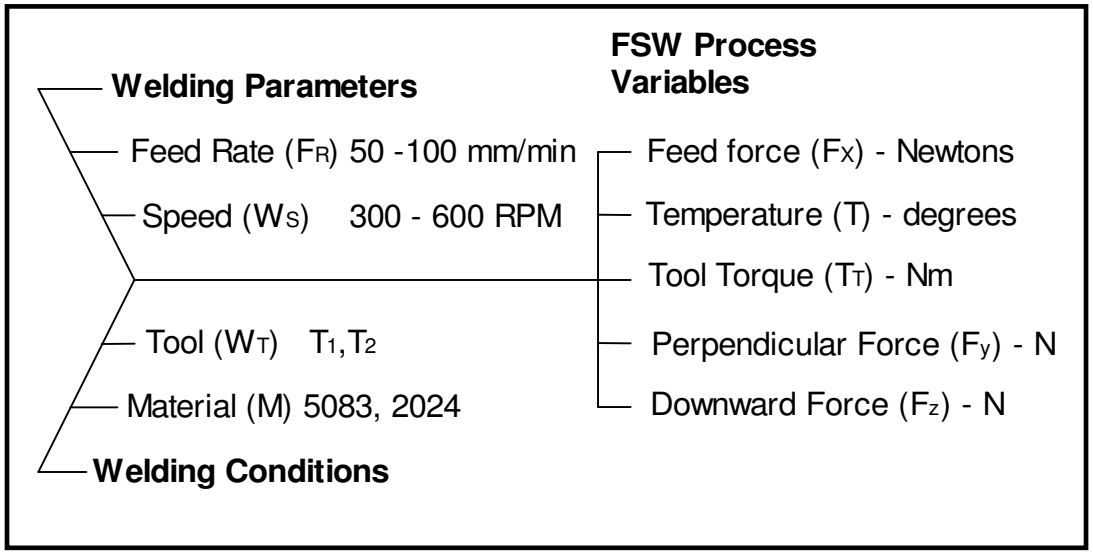

Figure 4.2: FSW process parameters and conditions.

4.1.2 Welded Materials

Several research groups had proved that the FSW process is a welding procedure versatile enough to successfully weld most aluminium alloys, copper, magnesium and other low-melting metallic materials [Chao et al., 2003]. Table 4.1 presents the chemical composition of the aluminium alloys used.

Table 4.1: Chemical compositions of aluminium alloys used [Georgeou, 2004].

2024 – T3					
Comp.	%Wt.	Comp.	%Wt	Comp.	%Wt
Al	93.5	Fe	Max 0.5	Si	Max 0.5
Cr.	Max 0.1	Mg	1.2-1.8	Ti	Max 0.15
Cu	3.8-4.9	Mn	0.3-0.9	Zn	Max 0.25
5083 – H321					
Comp.	%Wt.	Comp.	%Wt	Comp.	%Wt
Al	94.8	Fe	Max 0.4	Si	Max 0.4
Cr.	0.05 -0.25	Mg	4 - 4.9	Ti	Max 0.15
Cu	Max 0.1	Mn	0.4-1	Zn	Max 0.25

The idea of this research is to create a controller adaptive enough to enable the welding of these two alloys. These alloys have different properties such as the microstructure of the material that will influence the hardness of the stir zone [Lee et al., 2003]. The proposed controller will be used to adaptively maintain a particular set point irrespective of the material being welded.

It is also important to notice that stirring through the solid plate gave virtually identical force and torque levels as those measured when welding two plates together. This fact is very important to consider when one is planning to run the experiments while reducing the experimental costs [Johnson, 2001].

4.1.3 Welding Tools

The Design of the FSW tool is important to the success of the welding process since the frictional force dictates the amount of produced energy input. The pin causes some additional heating and extensive plastic flow in the work piece material on either side of the butt joint as the tool rotates [Colligan, 1999].

Figure 4.3 illustrates the two types of tools used to weld the 5083 H321 and 2024 T3 aluminium alloys in this study. The pin is usually equipped with a screw thread. This thread assists in ensuring that the plastically deformed work piece material is fully delivered around the pin, resulting in a void-free weld. These tools have different draft angles and different tool profiles are used to influence the amount of material flow around the FSW tool [Colligan, 1999].

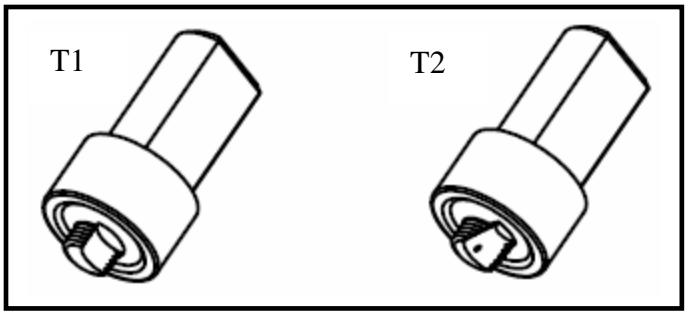

Figure 4.3: The FSW tools used [Blignault, 2002].

The length of the tool pin is made to be shorter than the depth of the welded material. To achieve full closure of the root, it is necessary for the pin to pass very close to the back-plate, since only a limited amount of plastic deformation occurs below the pin, and then only very close to the pin surface [Colligan, 1999].

The tool shoulder provides additional frictional force between the FSW tool and the material surface. The shoulder also holds the plasticized material within the weld nugget. This compressed plasticized material is rotated around the tool and enables uniform distribution of heat around the tool [Guerra et al., 2003].

Since the design of the welding tool has an influence on the amount of heat produced during the welding process, a generic controller can be used to maintain a particular process variable irrespective of the process variations caused by the different tools [Deqing et al., 2004].

4.2 Experimental Design

The experimental design, a well developed subject area within the field of statisticians, has the power of developing the system models together with the advantages of saving time, effort and money. These statistical methods of analysis enable clear data presentation, extraction of much information in a given set of experiments, and derivation of correct conclusions in spite of variability in the experimental results [Zeelie, 2003].

Table 4.2 presents the independent FSW variables to be considered in this research. These variables are used in the two-level factorial design where each variable is coded into the two states, being 1 for high value, -1 for low value and 0 as the mid point.

Table 4.2: The independent variables settings for the experimental design.

	Factor Settings		
	-1	0	+1
Speed (W_S)	300	450	600
Feed rate (F_R)	50	75	100
Material (M)	5083	N/A	2024
FSW Tool (W_T)	T_1	N/A	T_2

Table 4.3 presents the fractional factorial design which requires eight experiments for four variables. The number of experiments increases sharply with the increase in number of factors to be investigated in a full factorial design. It is also possible to treat high order interactions as just estimates, being considered as insignificant when compared to estimates of the low order interactions. Extra variables can be introduced to the arrangement; and thus reduce the number of experimental runs required for a particular number of variables [Zeelie, 2003].

Table 4.3: Fractional experimental matrix for the FSW process.

FSW Experimental Design Matrix								
Run Order	**1**	**W_S**	**F_R**	**M**	**W_T**	**W_SF_R**	**W_SM**	**F_RM**
8	1	-1	-1	-1	-1	1	1	1
5	1	1	-1	-1	1	-1	-1	1
6	1	-1	1	-1	1	-1	1	-1
4	1	-1	-1	1	1	1	-1	-1
7	1	1	1	-1	-1	1	-1	-1
2	1	1	-1	1	-1	-1	1	-1
1	1	-1	1	1	-1	-1	-1	1
3	1	1	1	1	1	1	1	1

Each experimental weld cycle, in a fractional factorial design, is used in combination with the other results to compute: an average response, all main effects and all multi-level interactions depending on the number of factors under consideration. It is worth noting that each individual experimental weld cycle is equally important to the overall result [Zeelie, 2003].

The experiment results may always be subjected to non-random, time-dependent errors. It may not be practical to eliminate all non-random errors at all times. Therefore, the experiments were conducted in a random order, as presented in Table 4.3, to change the nature of time-dependent (systematic) to time-independent (random) errors. This technique helps to distribute the systematic errors randomly over the whole range [Zeelie, 2003].

4.3 FSW Plates Setup

Figure 4.4 illustrates basic layout of the welds made by the FSW process where the data is presented, with the exit hole as the reference position. The coordinate system includes the following information:

- x is positive in the direction of the tool traverse. y is positive normal to the tool movement and parallel to the weld panel surface.
- z is positive normal to the weld panel surface, zero at the original weld panel surface and positive into the weld panel.
- (x,y,0) is the position on the weld panels which is in the centre of the picture and v(x,y,z) is the relative position from which the picture is viewed.

For example. a picture of a weld transverse macro-section taken at x = -20mm would have p(-20,0,0) and v(-1,0,0), and would define the view as looking along the weld axis towards the tool exit position.

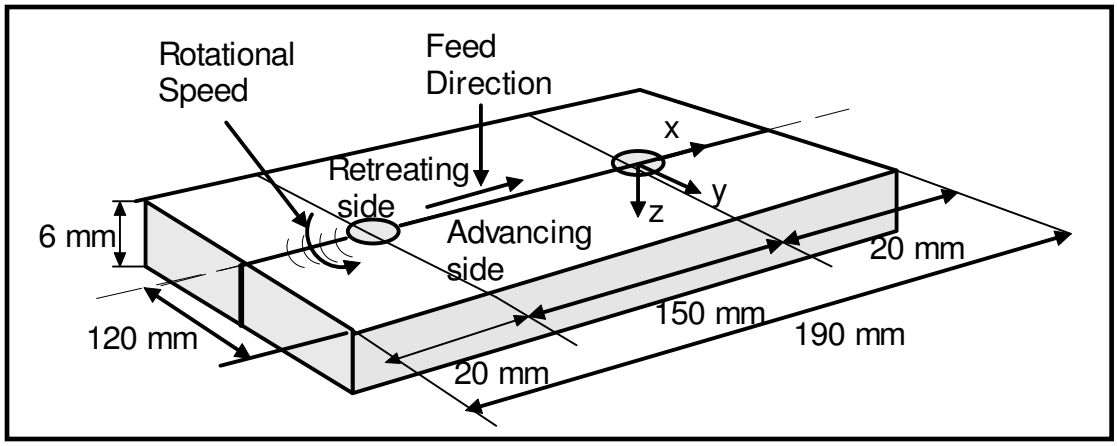

Figure 4.4: The nominal sizes and basic layout of the FSW welds.

Table 4.4 presents the various constants used for executing all the welds. The material, tool profile, feed rate and welding speed are the process parameters that are being considered for this research, while the rest of the system parameters are kept constant. Both tools had the same shoulder and pin dimensions but different tool profiles.

Table 4.4: Constant parameter settings for all welds.

Weld parameter	**Settings**
Tool Tilt Angle	2.5 degrees
Tool Probe Length	5.7 mm
Plunge and Extract Feed Rates	10 mm/min 10 mm/min
Plunge and Extract Tool Speed	600 RPM 300 RPM
Plunge Depth	0.1 mm
Dwell Period	8 seconds

Table 4.5 presents the variable parameters settings used for all welds. The variable process parameters were adjusted according to the four factors, two-level, fractional factorial design. It was established that three-level or higher order interactions often offer little contribution to the overall performance of most processes, and therefore they can be considered as a noise factor [Zeelie, 2003].

Table 4.5: Variable parameter settings for the welds.

parameter	**Variable Parameter Settings**							
Weld	**1**	**2**	**3**	**4**	**5**	**6**	**7**	**8**
$\mathbf{W_T}$	T1	T1	T2	T2	T2	T2	T1	T1
M	2024	2024	2024	2024	5083	5083	5083	5083
$\mathbf{F_R}$	100	50	100	50	50	100	100	50
$\mathbf{W_S}$	300	600	600	300	600	300	600	300

4.4 Experimental Data Analysis

Figure 4.5 presents all the produced welds for an experimental design. When these welds are visually inspected, they all have good weld surfaces. Enlarged views of these welds are attached in Appendix C.

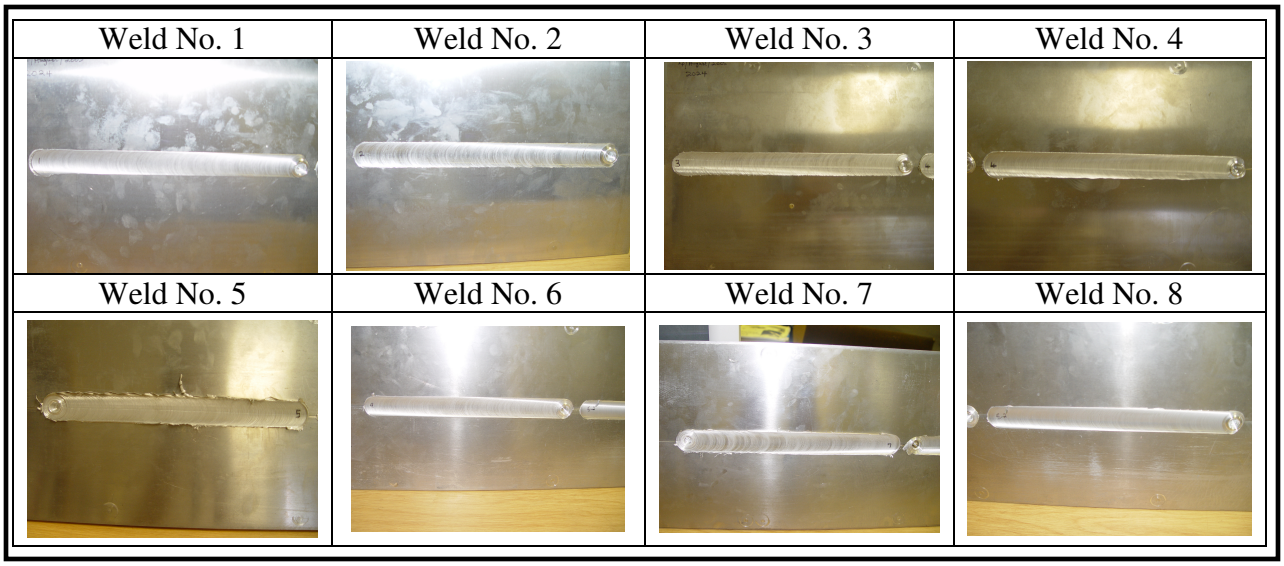

Figure 4.5: FSW-welds (for both 2024 and 5083 alloys).

The idea of this project is to provide close loop control of the FSW process but not to investigate the whole spectrum of parameters within which the process can be operated. The welding parameters were purposely selected within the range where there is a production of relatively sound welds and to establish the domain of operation where the FLC can be used.

4.4.1 FSW Regression Models for the Steady State

Figure 4.6 illustrates the relationship between the feed rate, welding speed, tool designs, material welded and the bending force. The plot indicates that, within a range of about 3000 – 5000N and various combinations of the FSW tools and aluminium alloys, varied feed rates and welding speeds can be used to maintain the feed force when welding.

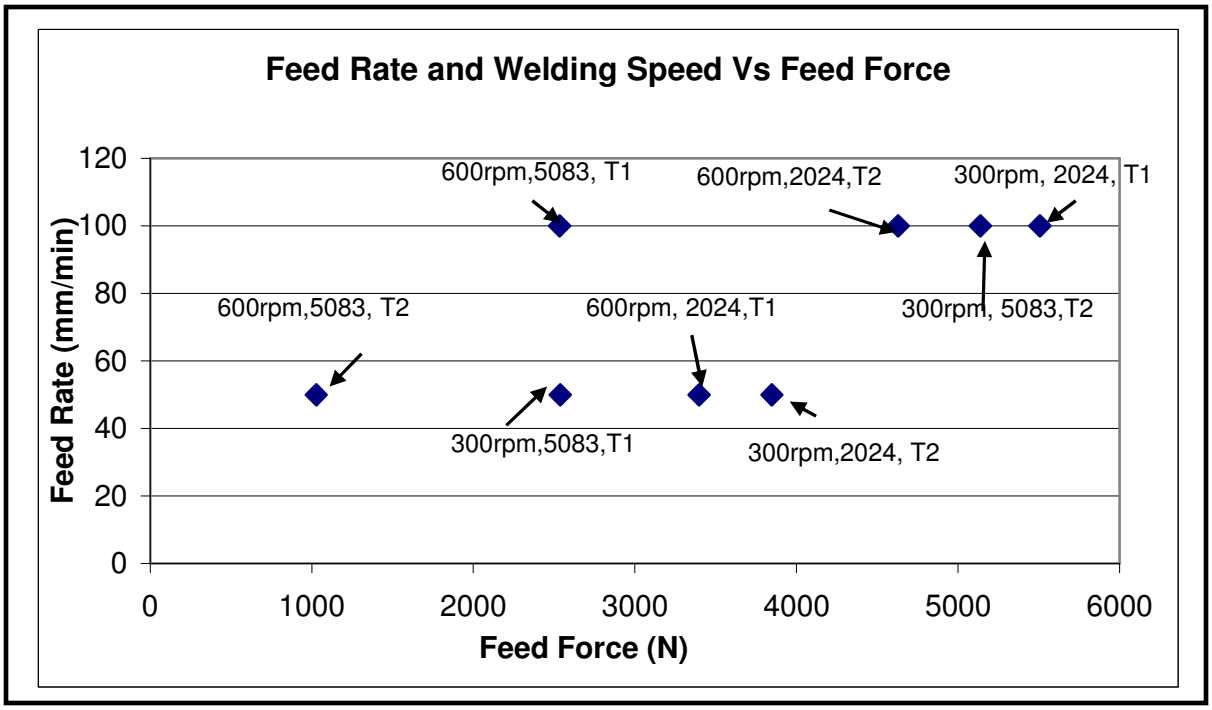

Figure 4.6: Feed rate and welding speed vs feed force.

Figure 4.7 illustrates the relationship between the independent variables and tool temperature. Table 4.6 presents the regression models generated from the data acquired from the FSW machine.

The feed rate (F_R) has to be increased and welding speed (W_S) reduced in order to increase the feed force (F_X). If the tool temperature (T) has to be increased, then the feed rate (F_R) and the welding speed (W_S) should be increased. All the independent variables are normalized within the range of [-1 and +1] before they are applied to the regression formulae.

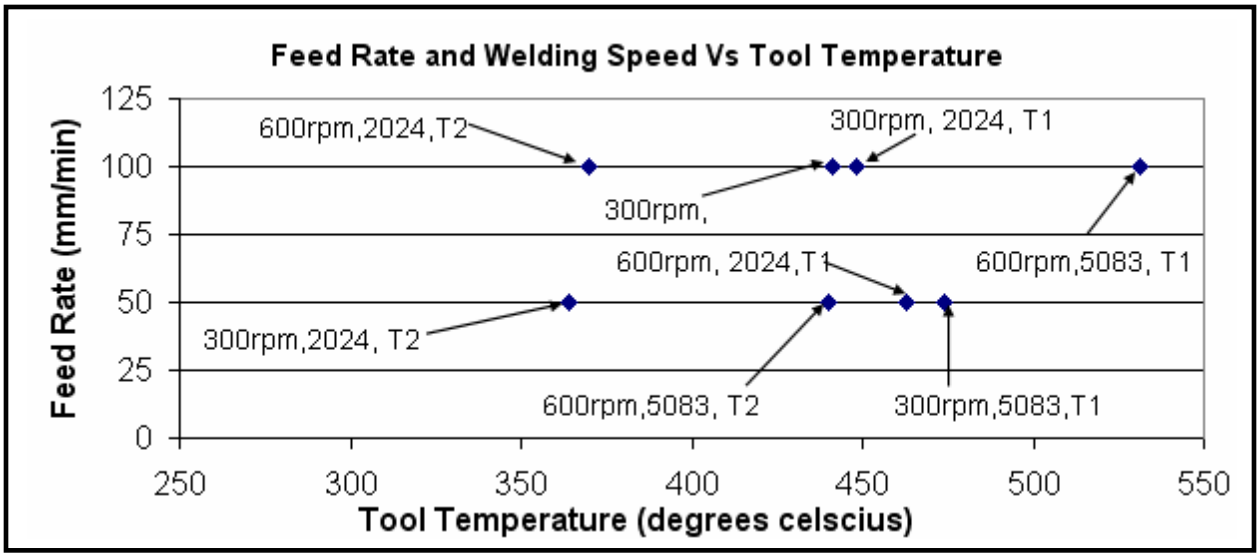

Figure 4.7: Feed rate and welding speed vs tool temperature.

Table 4.6: Regression models for the FSW process.

Regression models for data from FSW machine	Units
$T = 439.75 + 9.5.W_S + 8.F_R - 28.25.M - 37.75W_T - 4.5.W_S.F_R - 10.W_SM - 6.75F_RM$	(^{0}C)
$T_T = 52.26 - 13.51.W_S + 3.8.F_R - 4.28.M - 2.95.W_T - 0.76.W_S.F_R - 1.12.W_SM + 0.56F_RM$	(Nm)
$F_X = 3595 - 696.5.W_S + 868.25.F_R + 775.75.M + 72.5.W_T - 185.25.W_S.F_R + 344.75.W_SM - 145.5.F_RM$	(N)
$F_Z = 9.33 - 0.96.W_S + 1.1F_R - 0.27.M - 0.96.W_T + 0.38.W_S.F_R - 0.03.W_SM - 0.06.F_RM$	(kN)
$F_Y = 3619 - 592.13.W_S + 773.88.F_R + 647.88.M - 2.13.W_T - 304.88.W_S.F_R + 236.13.W_SM - 150.88F_RM$	(N)

Table 4.6 illustrates that the feed rate and welding speed have a small contribution to the tool temperature. The FSW tools and aluminium alloys have a major contribution to the tool temperature. Table 4.7 presents the tool temperature ranges, due to the different combination of welding tools and welded materials.

Table 4.7: The tool temperature range due to tool and material change.

Tool Number	Aluminium Alloy	Temperature Range (degrees C)
1	5083 H321	470 to 535
1	2024 T3	445 to 455
2	5083 H321	390 to 460
2	2024 T3	370 to 380

4.4.2 Process Dynamic Models

The characteristics of the FSW process had categorised the FSW process as a first order system. Figure 4.8 illustrates the setup used to determine the dynamics response of the FSW process. The step input, in the form of a 5083 H321 to 2024 T3 material transition, was used to establish the first order response of the FSW process.

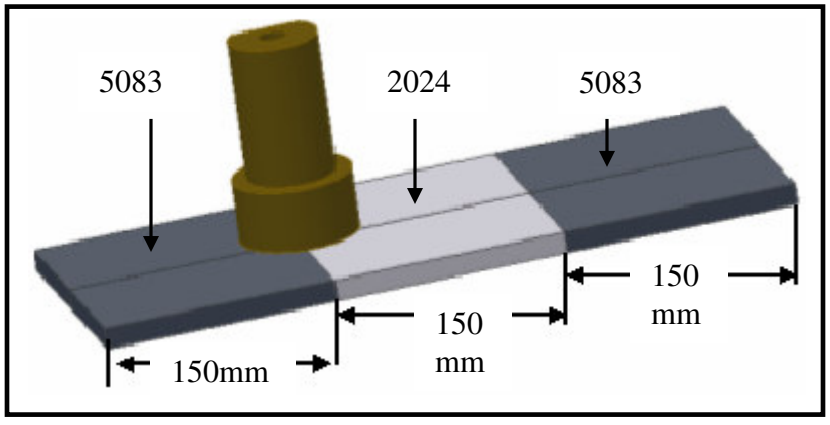

Figure 4.8: FSW material plate setup for first order modelling.

Figures 4.9 through to 4.13 illustrate the various responses of the FSW variables in the time domain. The captured responses indicate that the FSW process can be approximated as a first order response of the system when the FSW tool transverses the weld joint over the plates interface, made up of 5083 H321 and 2024 T3 aluminium alloys.

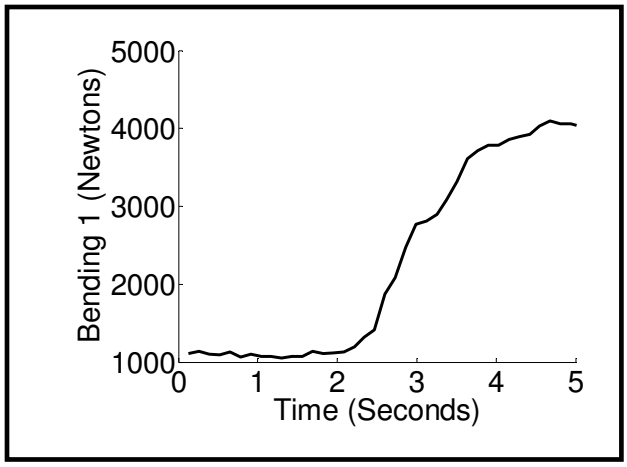

Figure 4.9: Bending 1 (F_X) response at 5083 H321-2024 T3 interface.

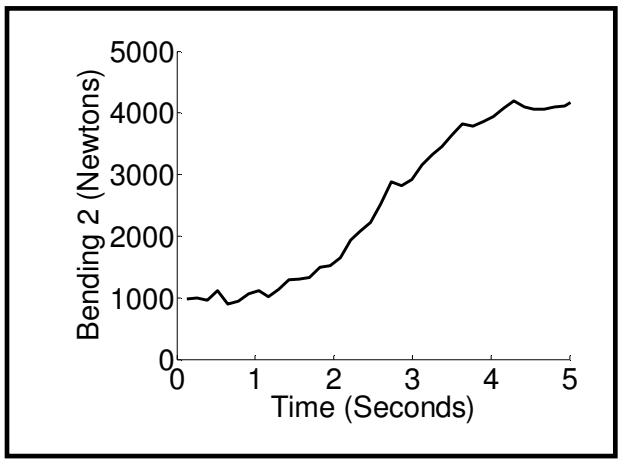

Figure 4.10: Bending 2 (F_Y) response at 5083 H321-2024 T3 interface.

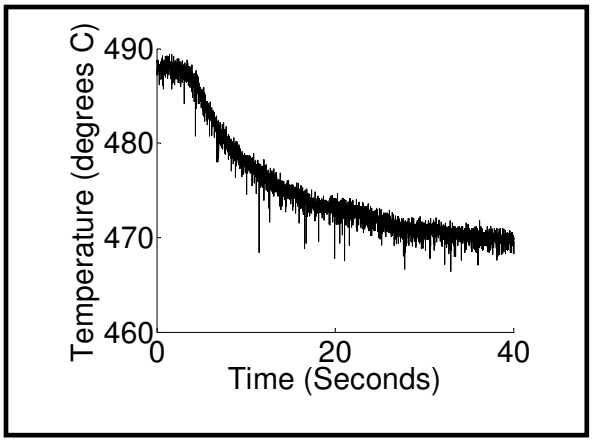

Figure 4.11: Temperature (T) response at 5083 H321-2024 T3 interface.

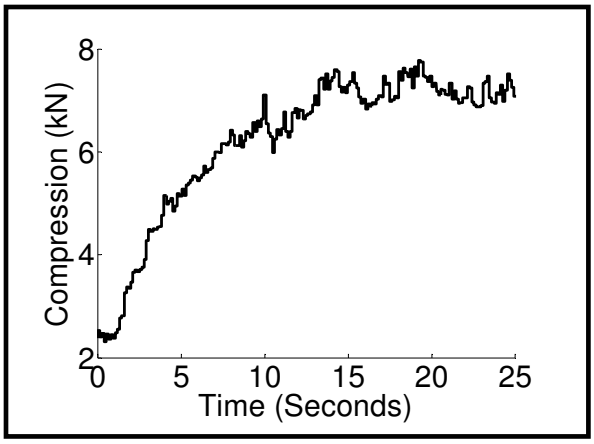

Figure 4.12: Compression force (F_Z) response at 5083 H321-2024 T3 interface.

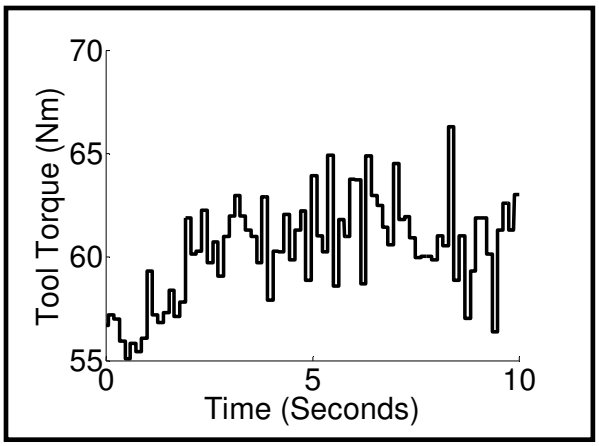

Figure 4.13: Tool torque (T_T) response at 5083 H321-2024 T3 interface.

The responses of these FSW variables resemble the characteristics of a first order system. Therefore, these responses enable the FSW to be generally categorised as a first order system. The collected data had been sampled at a frequency of 1kHz. The process lags are then used to formulate the first order models and are presented in Table 4.8. These models, in s-transform format, are then used in MatLab to simulate the first order response of the FSW process.

Table 4.8: First order models for FSW process.

Process variable	**F_X**	**F_Y**	**T**	**T_T**	**F_Z**
Time (seconds)	1s	1.5s	10s	3s	4s
Laplace Transform	$\frac{1}{s+1}$	$\frac{0.667}{s+0.667}$	$\frac{0.1}{s+0.1}$	$\frac{0.333}{s+0.333}$	$\frac{0.25}{s+0.25}$

4.5 Summary

The ANOVA analysis was used to generate casual models of the FSW process. The analysis was used to relate the effect of the independent variables to the amount of produced dependent variables in different material and tool conditions.

The feed rate had a major effect on the amount of bending in the feeding direction and bending in the direction perpendicular to the movement of the welding tool. The feed force had been used in typical end milling processes in order to enhance the productivity of those processes.

The step input, in the form of material change, was used to investigate the dynamics of the FSW process. The process trends enable the FSW process to be approximated as a first order system, as illustrated in Figures 4.8 through to 4.12. These first order dynamics, in the form of Laplace transforms had been incorporated into the model of the FSW process.

Chapter 5

FSW Process Rule Base Development

The fuzzy rule base is one of the crucial components of the FLC structure as it contains a collection of control rules that define the system behaviour and replace the mathematical modelling of the system. The feedback information can be processed, with the aid of a fuzzy rule base, for further increases in productivity, reducing defective parts, improving process safety and reliability in the FSW process.

Johnson established that the feed force, in the FSW process, is an important parameter to consider for the improvement in the productivity of the process. It has also been established that the feed rate has a major effect on the amount of feed force produced during the FSW process. Therefore, the amount of feed force produced in the FSW process can be used as a good indication of the level of productivity in the FSW process [Johnson, 2001].

FLC presents very interesting tracking features and is able to respond to different dynamic conditions. Also, the fuzzy control computation is very inexpensive, and this regulator could be used for the control of machine tools without significantly increasing the cost of the tool drives.

Another advantage of this method is that it does not require a fixed sampling time. Therefore, fuzzy control is relevant to the control of non-linear processes. Nevertheless, the main problem with fuzzy logic is that there is no systematic procedure for the design of a fuzzy controller [Aguilar et al., 2003].

ANFIS was first developed by Jang and Sun, to take advantage of the best attributes from neural networks and fuzzy systems. ANFIS is a fuzzy inference system (FIS) that uses neural network algorithms to adapt itself in order to achieve better results. The direct advantage that it has over neural networks is that it can also accept linguistic information and adapt itself using numerical data [The MathWorks, 2004].

ANFIS was implemented within the MatLab environment, to establish and tune the first–order Takagi–Sugeno fuzzy models for systems with unknown models. The adaptation process is based upon the desired relationship between the matched input–output data sets [The MathWorks, 2004].

The ANFIS system constructs a FIS with tuned output MF parameters using its learning methods and the input-output data patterns. This provision enables the fuzzy system to adapt to the process data. The major advantage of this method is that it is not necessary to have any prior knowledge of rule consequent parameters [The MathWorks, 2004].

ANFIS is based on the learning principles of neural networks. The use of neural networks, in control applications, has recently experienced rapid growth. The basic objective of a control process is to acquire an input signal and generate a desired output to a process under consideration. As neural control methods found their way into practice, they have opened the door to a wide spectrum of complex control applications [Ship–Peng, 2001].

As the complexity of control applications increase, the greater the need to deal with these difficulties, which requires more intelligent control systems. At present, neural networks represent an important paradigm for classifying patterns, and generating signals to control their environment. According to [Ship-Peng, 2001], the advantages of neural networks are:

- They can be trained using training sets. The connection weights of the neural network can be adapted in order to approximate, according to some predefined criterion, the input-output patterns provided in the training set. After training, the neural network can be used to predict a new output pattern, based on the input pattern only. The learning algorithm allows the adjustment of the connection weights.
- They can approximate non-linear functions. Multi-layer neural networks are special architectures for which powerful learning algorithms exist. Once the connection weights are trained, the neural network can approximate the input-output mapping provided by the training set.

- They can be trained in noisy environments. They possess robust learning algorithms that guarantee convergence in the presence of uncertainties.
- They can easily be implemented on parallel hardware for fast computation.

Fuzzy logic and neural networks are natural complementary tools in building intelligent systems and form the neuro-fuzzy systems. While neural networks are low-level computational structures that perform well when dealing with raw data, fuzzy logic deals with reasoning on a higher level, using linguistic information acquired from domain experts. However, fuzzy systems lack the ability to learn and cannot adjust themselves to a new environment. An ANFIS system had been used previously by other researchers in end milling processes to train FIS systems.

5.1 ANFIS Architecture

Figure 5.1 illustrates the structure of an ANFIS system. The architecture is made up of the fuzzy, product, normalized, defuzzify and total output layers. The fuzzy layer is made up four nodes (A_1, A_2, B_1, B_2), that are made up of four MFs for the two crisp inputs (X and Y). Equation 5.1, with respect to one of the crisp inputs, presents the relationship between the input and output MFs. The output MFs are denoted by O_1,i and $O_{1,}$,j [Lin et al., 2001].

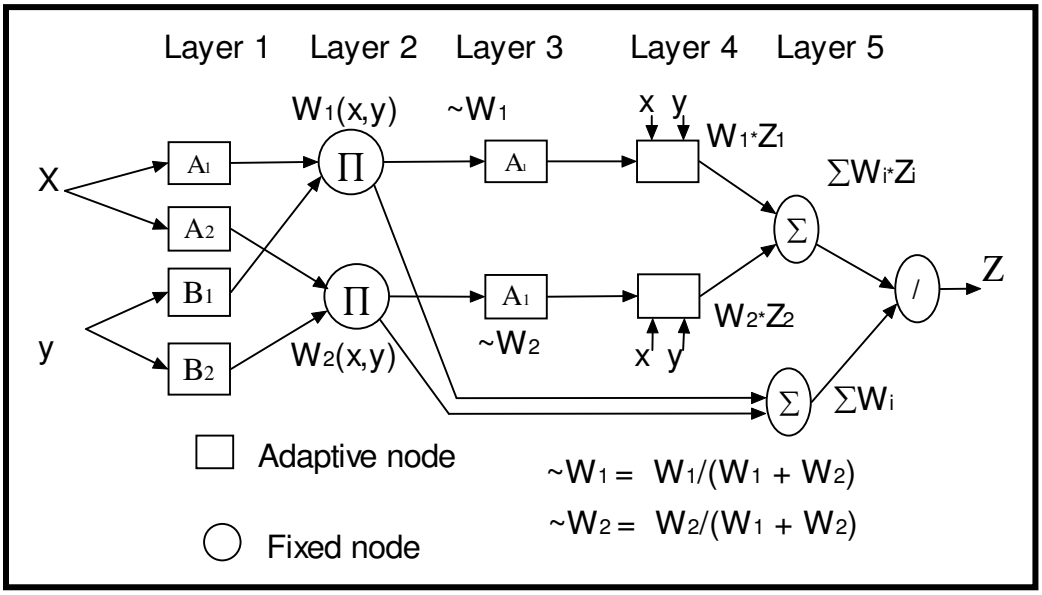

Figure 5.1: ANFIS structure [Ship–Peng, 2001].

$$O_{1,i} = \mu_{Ai}(x), \qquad i = 1,2,... \tag{5.1}$$

The product layer consists of two nodes ($\prod$), and the W_1 and W_2 are the weight functions of the next layer. The output of this layer is the product of the input signal, which is defined by Equation 5.2, and is denoted by $O_{1,j}$ [Lin et al., 2001].

The normalised layer has its nodes labelled (N). The function of this layer is to normalise the weight function in the process according to Equation 5.3. The output of this layer is denoted by $O_{2,j}$ [Lin et al., 2001].

$$O_{1,j} = \mu_{Aj}(x), \qquad j = 1,2 \tag{5.2}$$

$$O_{2,i} = \mu_{Ai}(x) + \mu_{Ai}(y), \qquad i = 1,2 \tag{5.3}$$

The fourth layer is the de-fuzzy layer, whose nodes are adaptive. The input-output relationship of this layer is defined by Equation 5.4. Equation 5.5 presents the linear parameters of the node and are represented by p_i, q_i and r. Equation 5.6 presents the last layer with one node, which is represented by $\sum$. The output of this layer is the total of the input signals, which represent the results of the actual output of the fuzzy controller [Ship–Peng, 2001].

$$O_{3,i} = \text{--}W_i = \frac{W_1}{(W_1 + W_2)} \qquad i = 1,2 \qquad (5.4)$$

$$O_{4,i} = \text{--}W_i f_i = \text{--}W_i (p_i x + q_i y + r) \qquad i = 1,2 \qquad (5.5)$$

$$O_{5,i} = \text{--}W_i f_i = \text{--}W_i \sum (p_i x + q_i x + r) \qquad i = 1,2 \qquad (5.6)$$

The ANFIS system is used to train the first-order Takagi–Sugeno fuzzy models. This FIS system was introduced by Takagi–Sugeno. It was demonstrated to function as an effective model for systems that can be represented by their input-output relationship [The MathWorks, 2004].

The rule consequences, instead of being formed by the fuzzy sets, are linear parametric equations defined by the inputs of the systems [Ship–Peng, 2001]. The Takagi–Sugeno FIS system is computationally efficient, works well with linear techniques such as PID control, and can be used effectively with optimisation and adaptive techniques. It has guaranteed continuity of the output surfaces and is well-suited for mathematical analysis [The MathWorks, 2004].

5.2 ANFIS Learning Procedure

ANFIS uses a hybrid, supervised learning algorithm based on a gradient descent and least-squares estimator. Each training period is made up of one forward pass and one backward pass in the ANFIS training algorithm. The ANFIS system uses one of two types of learning methods; the back-propagation or a combination of back-propagation and gradient-descent optimisation.

The antecedent parameters and consequent parameters are optimised during the ANFIS training algorithm as suggested by Jang. A neural network maps the input MFs and a training set of input-output patterns to form the output linear MFs and their associated equations [The MathWorks, 2004].

5.2.1 The Feed-Forward Pass

The outputs of the first hidden layer are first computed by using the network inputs. Using these values as inputs to the next hidden layer, the outputs of the current layer are obtained. These computations are propagated until the final output of the network is obtained [Babuška et al., 2003].

During this process, all the weights of the neurons remain constant and only the outputs of the neurons are changed due to their inputs. The objective of a forward pass process is to allow the input nodes to receive the input pattern for the computation of their outputs. At the end of this phase, the output neurons will hold the activation values that predict the output of the network.

5.2.2 The Backward Pass

The backward pass executes the second phase of ANFIS learning. The antecedent parameters are tuned at this phase while the consequent parameters are kept fixed. A back-propagation method updates all the parameters of the MFs using the steepest descent method.

The output of the network is compared to the desired output. The difference of these two values, the error, is then used to adjust the weights of the nodes, first in the output layer, then in the layer before, etc., in order to decrease the error. The error is reduced by the gradient-descent optimisation method [Babuška et al., 2003].

The back-propagation method uses the desired outputs corresponding to the input pattern and updates the weights of every neuron according to the error signal. The error signal is identified as the difference between the output of the feed-forward stage and the desired output [The MathWorks, 2004].

The next epoch is executed if the resultant error of the previous epoch is not within the specified margin. As more epochs are executed, the training error decreases throughout the learning process. Therefore, the more the initial MFs resemble the optimal ones, the easier it will for the model parameter training to converge [The MathWorks, 2004].

5.3 Fuzzy Inference System for a FSW Process

This dissertation presents a FLC for the regulation of the feed force and tool temperature in the FSW process. A FLC uses the feed rate and welding speed to adaptively control the feed force and tool temperature respectively, within the tool and material changes.

Fuzzy logic technology has a collection of MFs available to consider. The selection of the MF to be used is very important as it will affect the numerical to probabilistic data transformation. The geometrical shape of the MF is the characterisation of uncertainty in the corresponding fuzzy variable [Berkan et al., 1997].

Three types of the MFs were used to transform the process inputs into their equivalent probabilistic format. Equations 5.7 through to 5.9 present the Gaussian, Sigmoid and Z-shaped functions respectively.

$$f(x;\sigma,c) = e^{\frac{-(x-c)^2}{2\sigma}} \tag{5.7}$$

$$f(x;\sigma,c) = \frac{1}{1 + e^{-a(x-c)}} \tag{5.8}$$

$$f(x;\sigma,c) = \begin{cases} 1, & x \le a \\ 1-2\left(\dfrac{x-a}{b-a}\right)^2 & a \le x \le \dfrac{a+b}{2} \\ 2\left(\dfrac{b-x}{b-a}\right)^2 & \dfrac{a+b}{2} \le x \le a \\ 0, & x \le b \end{cases} \tag{5.9}$$

5.3.1 Fuzzy Control of Feed Force

The feed rate fuzzy controller was used to control the amount of the feed force produced when welding. The feed rate directly influences the amount of feed force used. This controller utilised the error and the rate of change of feed force to regulate the feed force produced. Figures 5.2 and 5.3 illustrate the functions used to fuzzify an error and rate of change of error respectively.

The range of the functions was extended beyond the range [-1,+1] such that the state of the process at such points can still be defined by the fuzzy reasoning. The fuzzy inputs are processed using gauss MFs for simulations purposes. The triangular MFs have high computational efficiency as compared to gauss MFs [Liang et al., 2003] on the other hand; the performance of triangular MFs is only satisfactory only when the fuzzy inputs are not more than two.

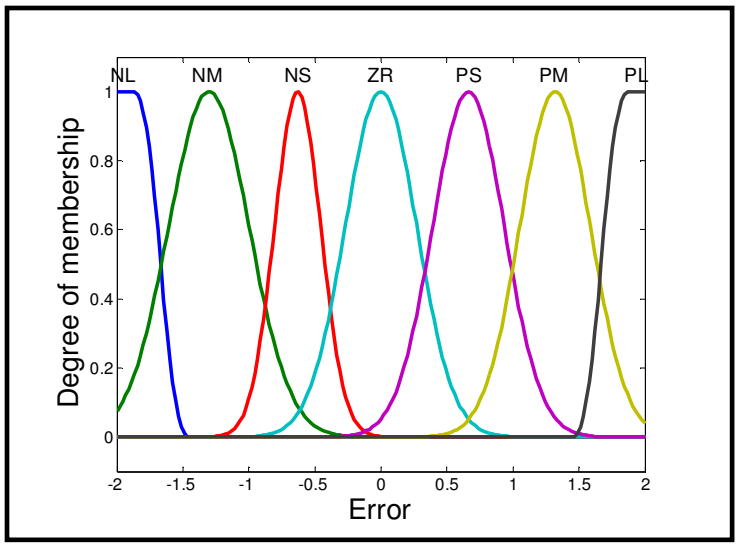

Figure 5.2: The membership functions for feed force error.

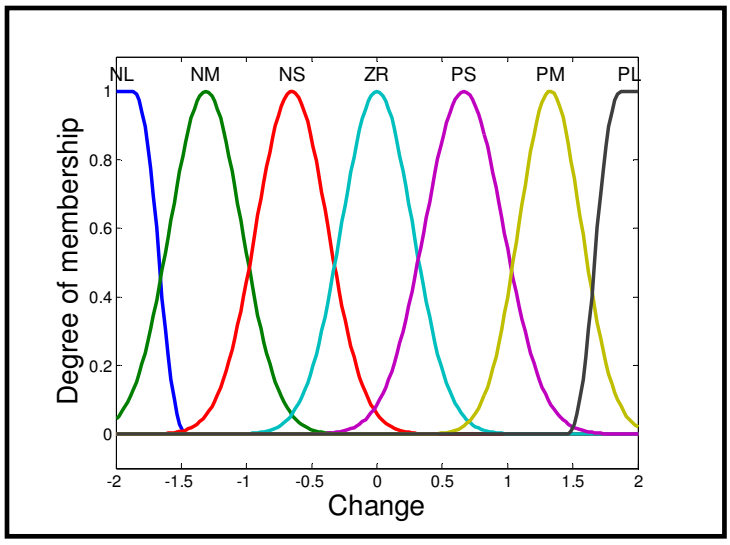

Figure 5.3: The membership functions for feed force change.

The amount of rate of change of the feed force also affects the amount of adjustment of the feed rate. If the current feed force error is zero and the rate of change of error is negative, then the feed rate adjustment is positive. Figure 5.4 illustrated the relationship between the feed force error, feed force change and feed rate adjustment.

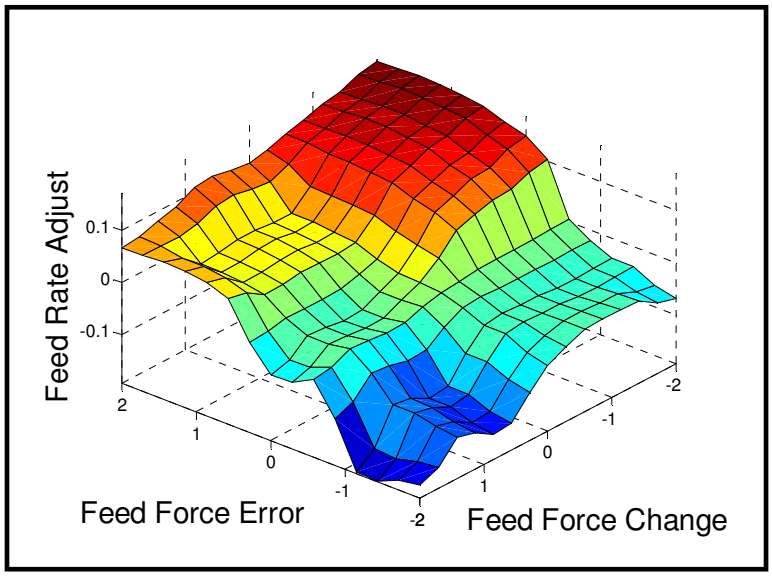

Figure 5.4: The surface response for feed rate adjustment.

5.3.2 Fuzzy Control of Welding Temperature

The frictional energy, generated at the interface between the welding tool and the work-piece, is the most important process parameter that determines the success of the FSW process. The heat influences the shape and microstructure of the weld, as well as the residual stress and distortion of the work-piece [Chao et al., 2003].

All the fuzzy inputs are normalized to the same scale before they are applied to the inputs stage of FLC. Figures 5.2 and 5.3 are also used to fuzzify the temperature error and rate of change of temperature respectively for the adjustment of the welding speed.

The welding speed has a direct influence on the magnitude of the tool temperature. If the current temperature error is positive, then the welding speed adjustment is positive. Figure 5.5 illustrates the relationship between the temperature error, temperature change and Welding speed adjustment.

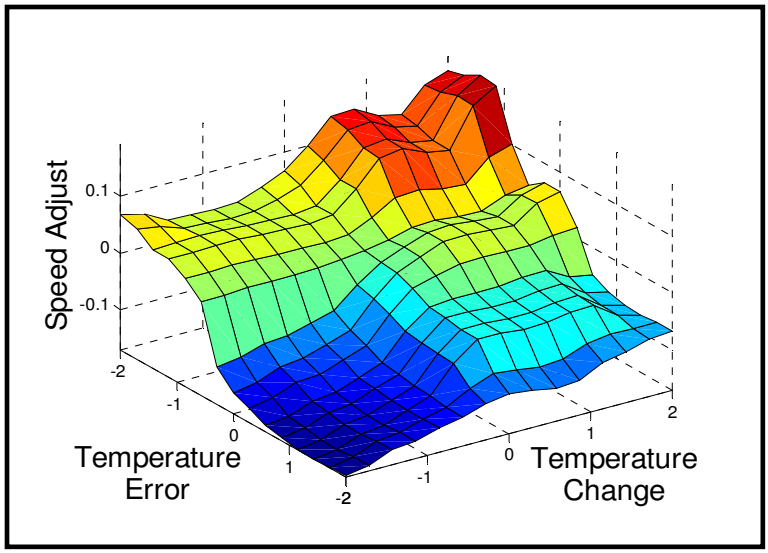

Figure 5.5: The surface response for welding speed adjustment.

5.4 Summary

The fuzzy rule base is one of the crucial components of the FLC structure as it contains a collection of control rules that defines the system behaviour and replaces the mathematical modelling of the system. FLC presents very interesting tracking features that are able to respond to different dynamic conditions. The main problem with fuzzy logic is that there is no systematic procedure for the design of a fuzzy controller.

ANFIS methodology was used to tune the parameters of the fuzzy system. ANFIS takes advantage of the best attributes from neural networks and fuzzy systems. It uses neural network algorithms to establish and train the first–order Takagi–Sugeno FIS system.

The feed rate fuzzy controller was used to regulate feed force in the FSW process as the feed rate had a major impact on the feed force. The welding speed fuzzy controller was generated in order to regulate the welding temperature.

Chapter 6

Simulations of Fuzzy Control for FSW Process

A generic FLC controller is proposed as a viable solution to control the FSW process in such a way that it can maintain a particular set point irrespective of material and tool changes. Such a controller can be used in industrial applications to maximise the performance of those manufacturing processes. It can be very beneficial to save time in designing a controller for each tool and material change.

6.1 Simulink Model for Feed Force Regulation

The steady state and first order models of the FSW process were developed and implemented in Simulink. Tables 4.6 and 4.8 represent the FSW mathematical models for the steady state and first order response. The FLC controller was designed and used to control the FSW process in a simulated environment. Figure 6.1 illustrates the feed force control model implemented and simulated in Simulink.

The FSW model enables the selection of the value of the set point within the domain of experimentation, the welded material, and the tool to be used. The simulated data is exported to the MatLab workspace. The process variables such as error, feed rate and welding speed are easily accessible.

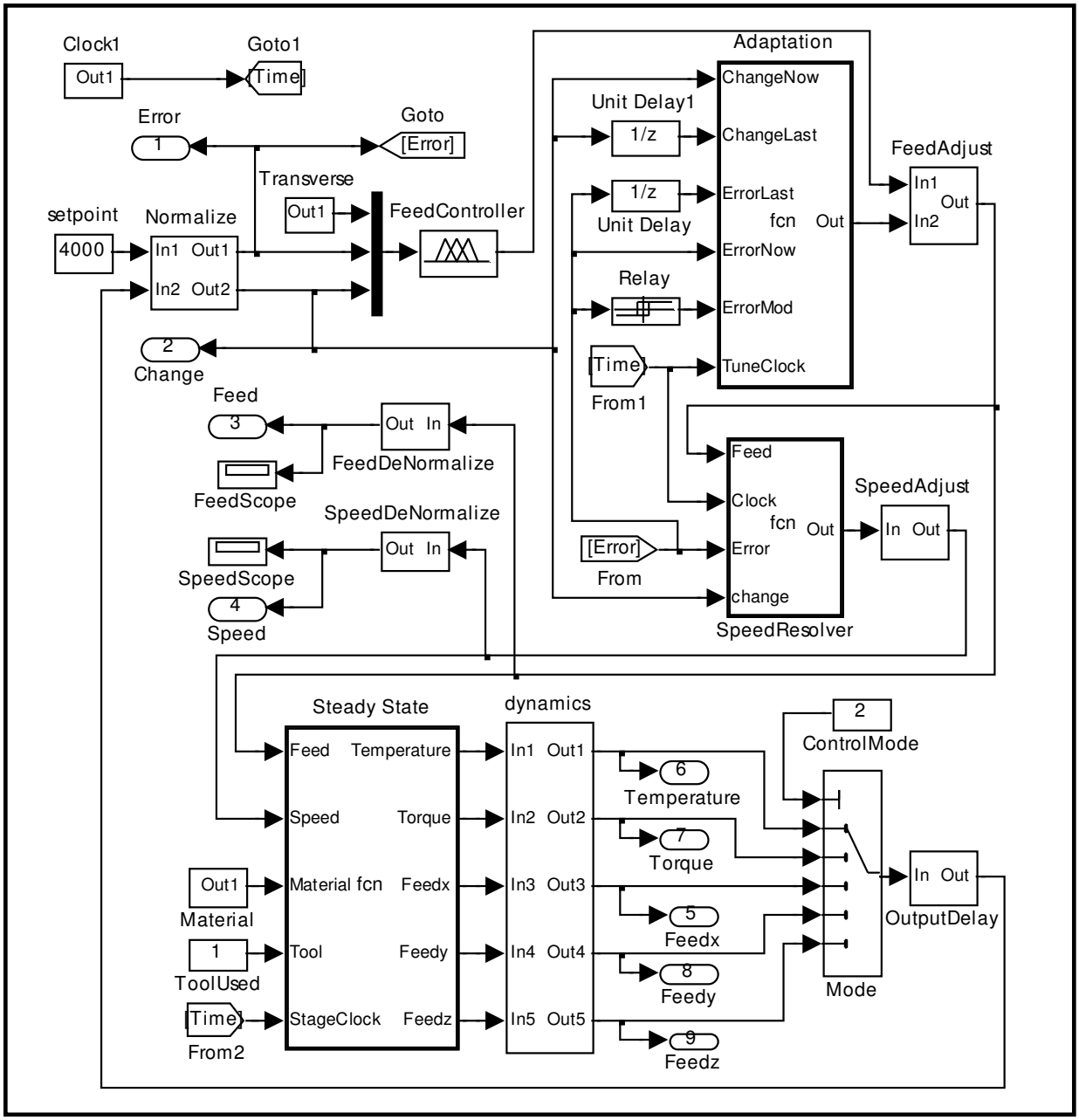

Figure 6.1: The FSW model for feed force regulation.

The normalization stage is used to transform the input data into an appropriate level for the data transformation from numerical to probabilistic format. This stage enables the data transformation even when the data is ambiguous.

Figure 6.2 illustrates the transformation block for the feed force error and rate of change. The constants 3267 and 2406 represent the experimental domain of the produced feed force and 1.4 represents the sensitivity of the controller around the zero error zone.

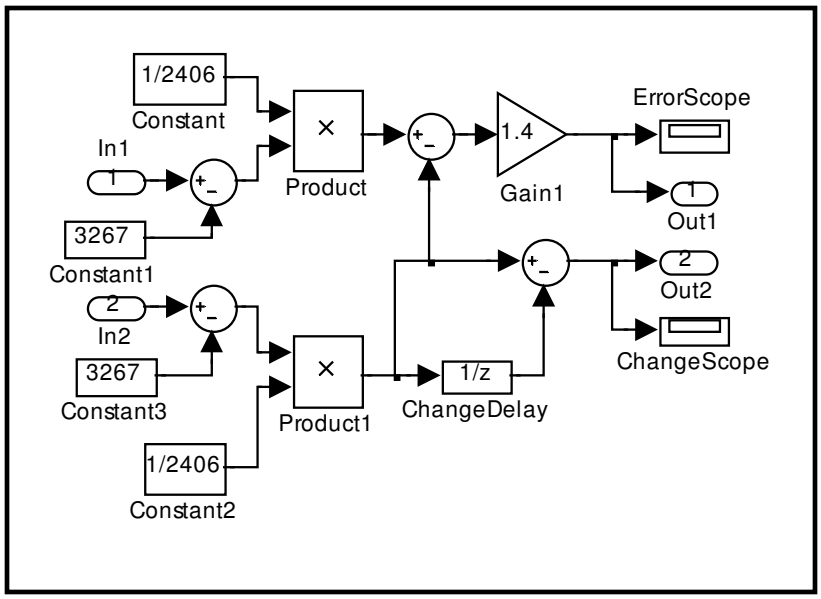

Figure 6.2: Normalization block for feed force control.

Johnson established that feed rate directly affects the magnitude of produced feed force [Johnson, 2001]. The feed force regression model in Table 4.6 generated from the experimental design highlighted the possibility of adjusting feed rate to regulate the feed force. Hence the FLC for feed rate adjustment was developed as outlined in section 5.3.1. This FLC is used to regulate the feed force as illustrated in Figure 6.1.

The adaptation mechanism was also incorporated in Figure 6.1 to enable the adaptability of the FLC to the material and tool changes. Equation 3.9 presents this adaptation algorithm that utilises the error and rate of change of error to adjust the feed rate. The model also “resolves” the welding speed to a certain value depending on the welding tool and material.

Fuzzy technology presents very interesting tracking features and its ability to respond to different feed force dynamics. The controller can be designed in such a way that, instead of having a controller with a particular output for a specified input, a controller can readjust its output according to the current system response.

This technology can incorporate multiple inputs and outputs. It has another advantage of not requiring fixed sampling frequency. Figure 6.3 illustrates the block used to provide the adjustments to the amount of feed rate in the regulation of feed force.

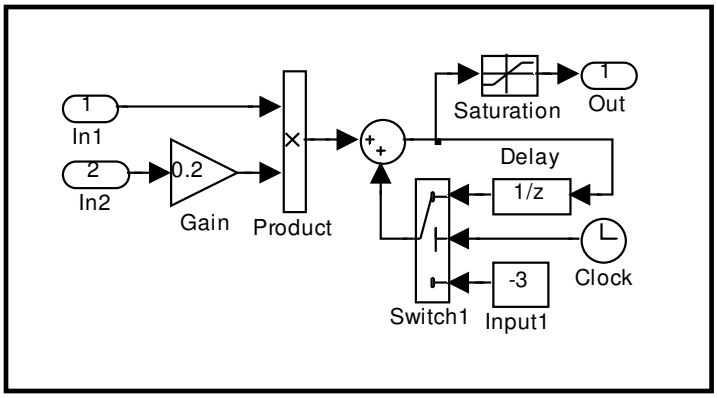

Figure 6.3: Feed rate adjustment block for feed force control.

6.2 Simulations for Feed Force Regulation

6.2.1 Feed Force Regulation on 5083 H321 and 2024 T3 Alloys

Figure 6.4 illustrates the simulated performance of the FLC system, at the set point of 4000N, using FSW tool1 when welding different aluminium alloys at the same weld cycle. The aluminium alloys are placed next to each other such that they are welded together. The aim of this section is to evaluate the performance of the FLC when welding different alloys.

The simulation results indicate good performance of the fuzzy control of a FSW process when welding the different alloys. The feed rate was adjusted quickly and smoothly in response to the variations in the material properties. The feed force was well regulated around the reference level in all the three cases.

Each alloy produces a different feed force, at the same feed rate and welding speed, due to the different material properties. The feed rate was increased to around 98% of its maximum value when welding 5083 H321 alloy and reduced to around 63% of its maximum value when welding 2021 T3 alloy.

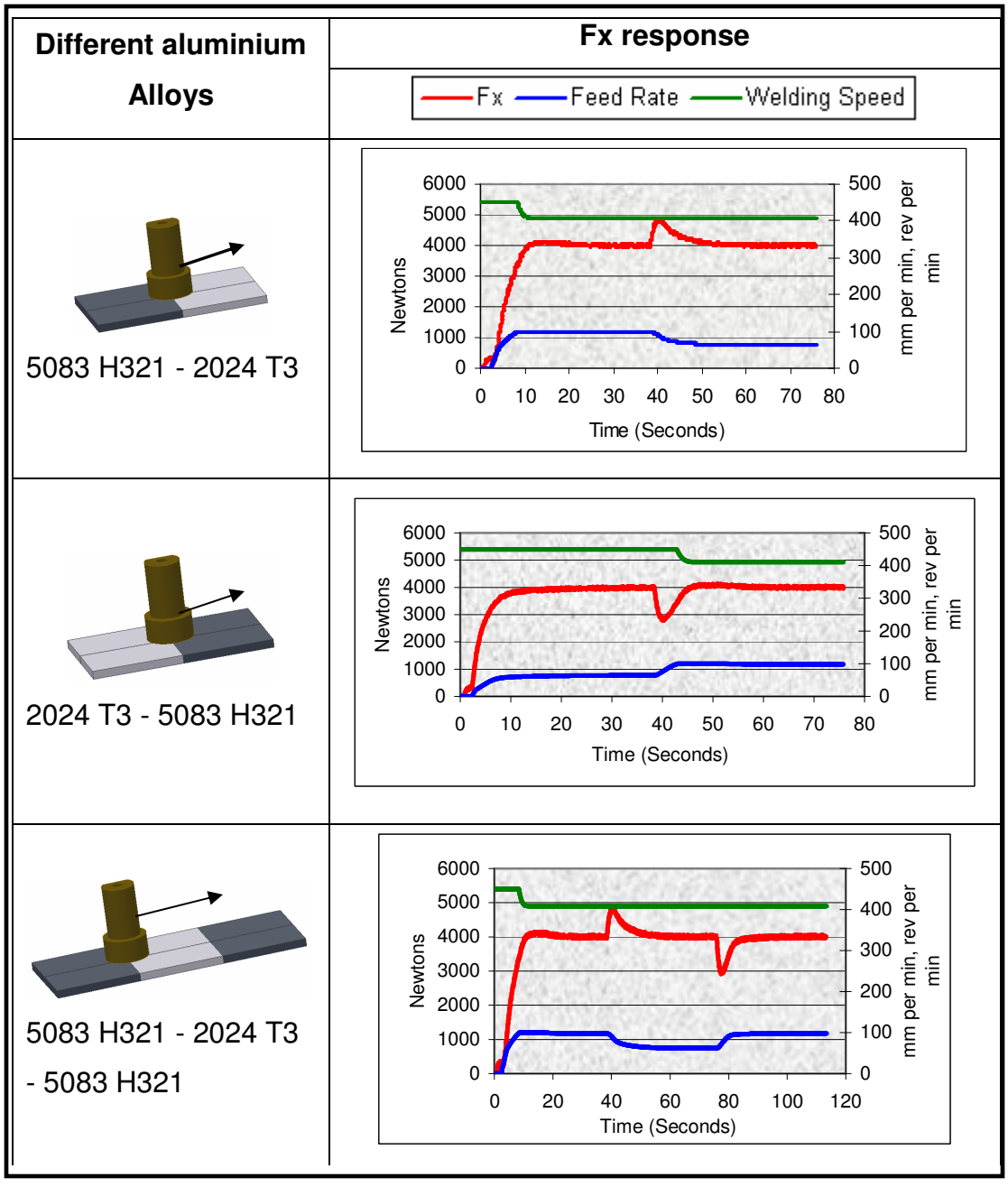

Figure 6.4: Effects of different aluminium alloys on feed force regulation.

When the welding tool is moved from the 5083 H321 alloy into the 2024 T3 alloy, the feed force is increased. Similarly, Johnson had found that the greater forces were produced when welding 2000 series alloys than when welding the 5000 series aluminium alloys [Johnson, 2001]. The fuzzy control methodology was used to regulate the feed force irrespective of the FSW material used even though these materials have different properties.

6.2.2 Feed Force Regulation using Different FSW Tools

Figure 6.5 illustrates the simulated response of the process for the set point of 4000N using two FSW tools, one without a draft angle while the other one with a draft angle of 30^0. The purpose of using these two tools was to examine the adaptability of fuzzy control, rather than the welding efficiency, when tools with different properties are used.

The simulation results, as illustrated in Figure 6.5, indicated good performance of the fuzzy control of FSW process using the two different tools. The feed rate was well adjusted in response to the variations in the tool designs. Therefore, the feed force was well regulated around the reference level throughout the weld length.

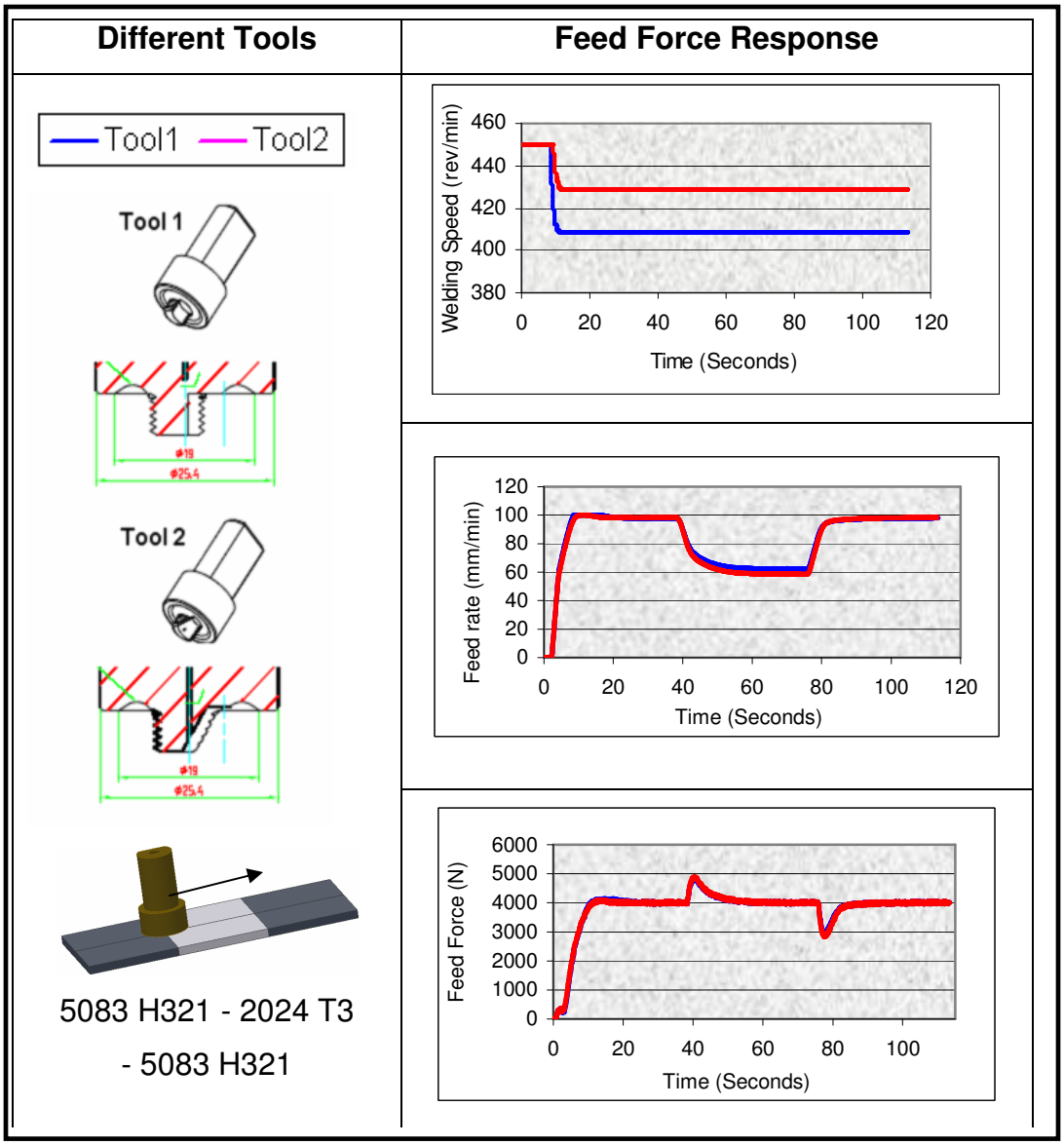

Figure 6.5: Effects of different tool designs on feed force regulation.

The feed rate was adjusted to 100% value of its maximum value when welding 5083 H321 alloy. It was reduced to 63% when welding 2021 T3 alloy with tool 1. When tool 2 was used, the feed rate was adjusted to 100% when welding 5083 H321 alloy, and reduced to 60% on 2021 T3 alloy.

Therefore the simulations illustrated that fuzzy control technology is a viable solution to regulate the FSW process irrespective of the welding tool used when welding different aluminium alloys.

6.2.3 Welding Speed Adjustment in Feed Force Control

The feed rate had been identified as the main parameter to consider in the regulation of the feed force in the FSW process. The welding speed has an effect on the feed force; however, to a lesser extent when compared to the feed rate [Johnson, 2001]. Figure 6.5 illustrates that the welding speed was also used to regulate the feed force.

The welding speed is readjusted in each case such that the feed rate is maximised, using either one of the tools, while maintaining good feed force regulation. The productivity of the welding process can therefore be maximised, irrespective of the tool design, by welding at the maximum feed rate while ensuring that the set point is not exceeded.

Figure 6.6 illustrates the two simulated cases for feed force regulation when using tool1 at different set points. The welding speed is kept constant in one case and readjusted in the second case. The dual-parameter adjustment has a good application in the case where the experimental domain extends a range where the controller must provide a match between the feed rate and welding speed.

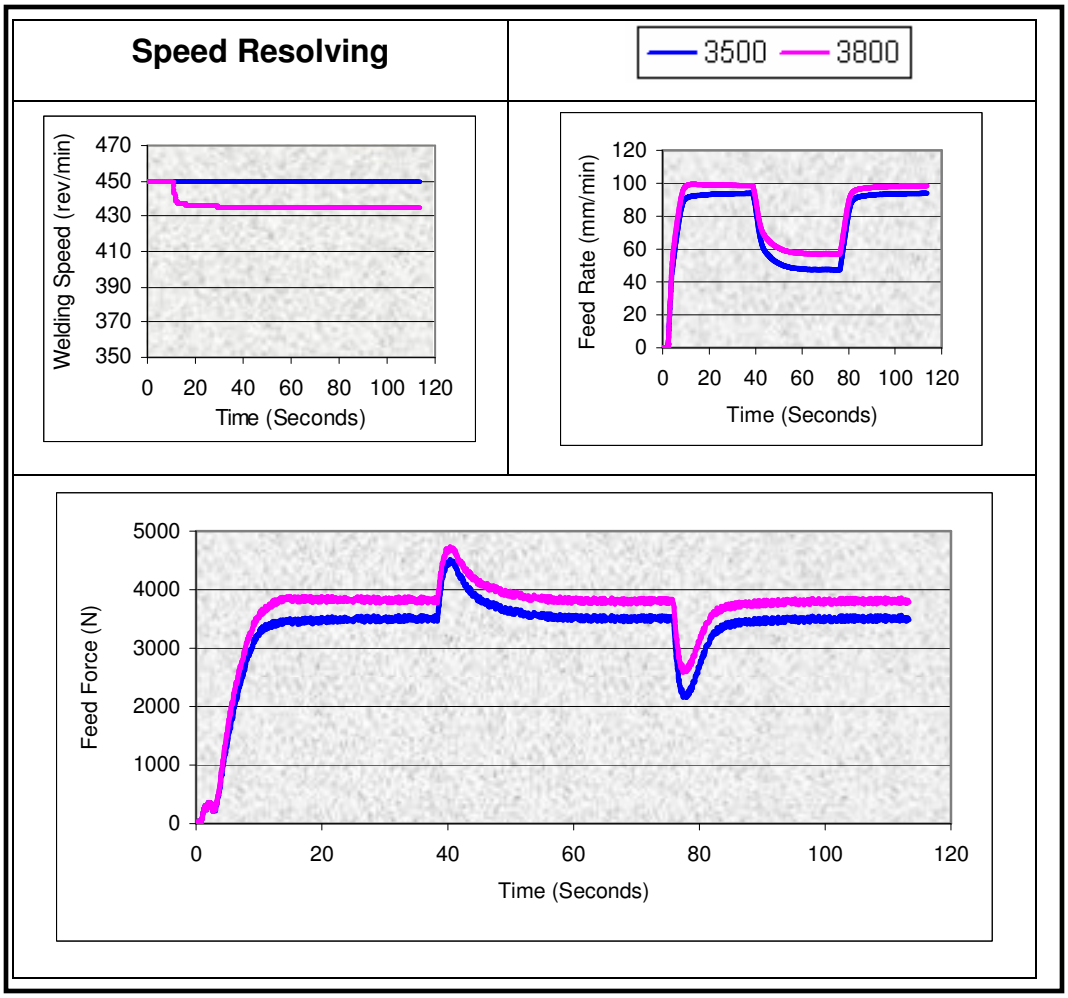

Figure 6.6: Feed force regulation using the welding speed.

When the set point of the feed force is 3800N, the welding speed is reduced to achieve this set point, as the feed rate had already reached its 100% mark of the experimental domain. The welding speed adjustment doesn't compromise the required good productivity, which is enabled with the attained maximum feed rate, while ensuring that the set point is maintained at the required level.

6.3 Simulink Model for Tool Temperature Regulation

The welding speed controller, to regulate the tool temperature was designed and implemented in MatLab. Figure 6.7 illustrates the simulation model for the regulation of welding temperature. The model utilises the tool temperature error and rate of change of error of temperature as the fuzzy inputs to the model. The simulation model regulates the tool temperature with the aid of the welding speed.

The model also includes the normalisation stage, used to transform the temperature error and rate of change of error into an appropriate level before the numerical to probabilistic data transformation is executed. This stage enables the data transformation even when the data is unacceptable.

The welding speed directly affects the magnitude of the produced welding temperature and this fact is supported by the literature review in section 2.5. The welding temperature regression model in Table 4.6 generated from the experimental design highlighted the possibility of adjusting welding speed to regulate the welding temperature. Figure 6.7 includes this FLC developed in section 5.3.2 to regulate the welding temperature.

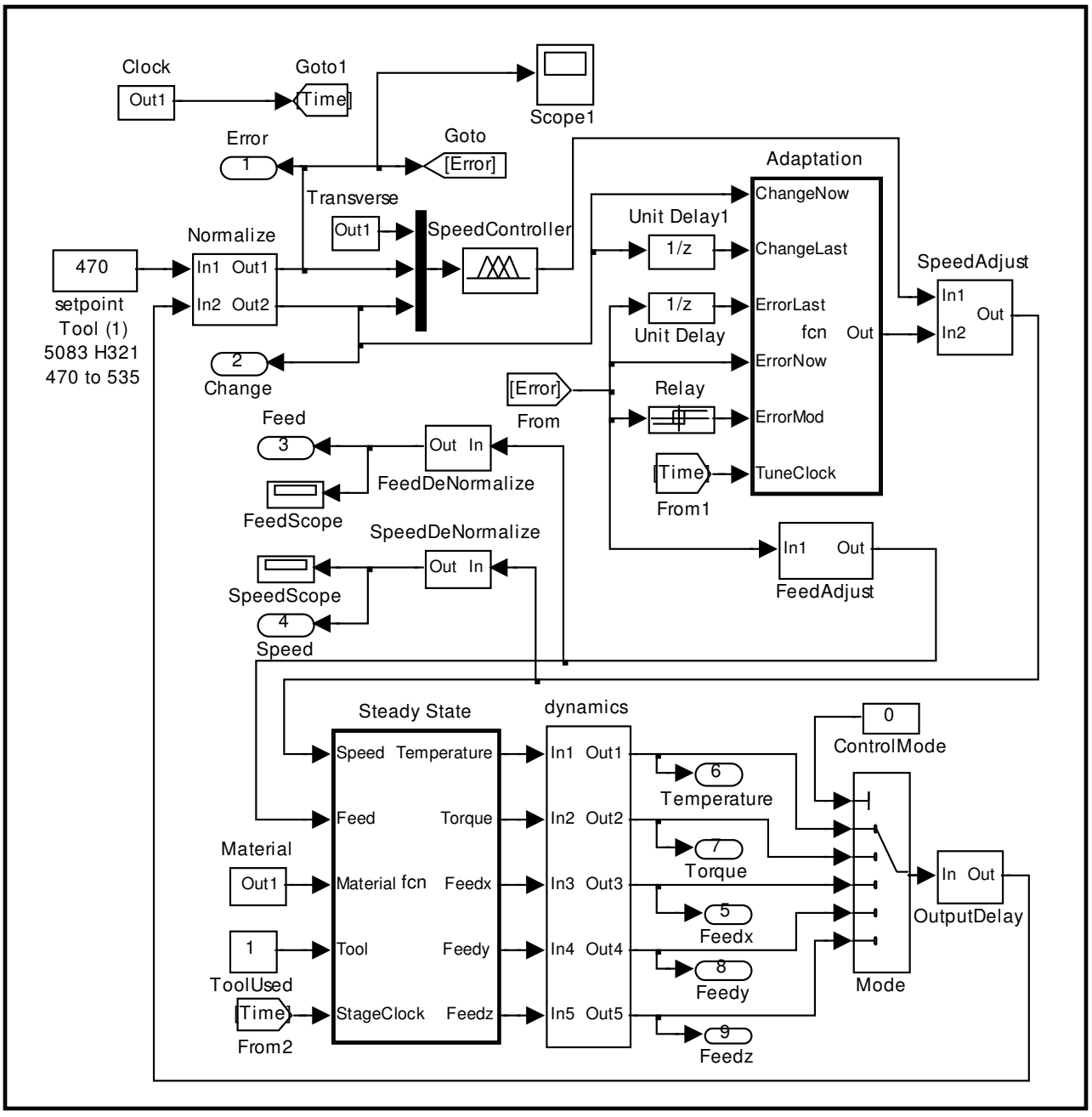

Figure 6.7: The FSW model for tool temperature regulation.

Figure 6.7 incorporates the adaptation mechanism to enable the adaptability of the FLC to the material and tool changes. Equation 3.19 presents this adaptation algorithm that utilises the error and rate of change of error to adjust the welding speed.

Figure 6.8 illustrates the transformation block for the tool temperature error and rate of change of the error. The constants 500 and 34 represent the experimental domain of the tool temperature and 1.4 represents the sensitivity of the controller to the tool temperature error around the zero error zone. Figure 6.9 illustrates the block use to “resolve” the feed rates to a certain value depending on the welding tool and material.

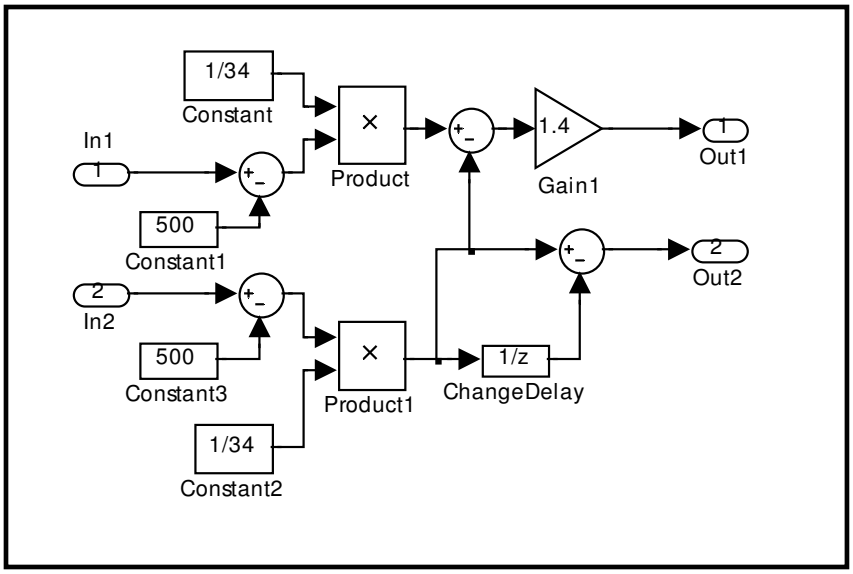

Figure 6.8: Normalization block for tool temperature control.

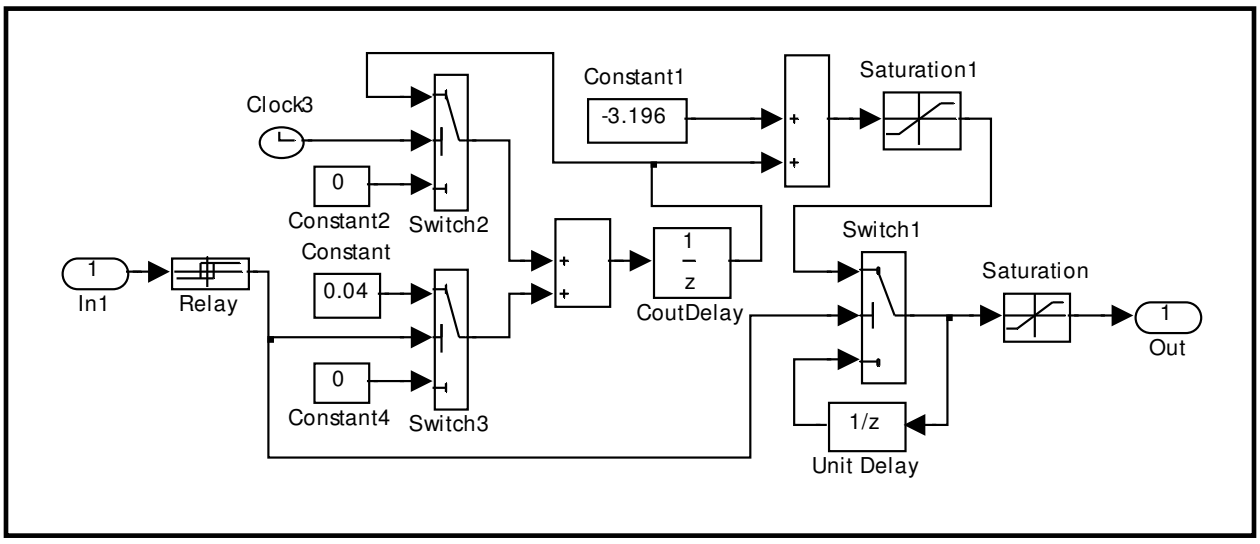

Figure 6.9: Feed rate adjustment block for tool temperature regulation.

6.4 Simulations for Tool Temperature Regulation

6.4.1 Tool Temperature Regulation on 5083 H321 Alloy

The tools and aluminium alloys have a large contribution to the magnitude of a tool temperature produced when compared to the welding speed and feed rate. The FSW tools have a major contribution to the tool temperature, over four times more than the influence of either the welding speed or feed rate.

The combination of the welding speed and feed rates, and the two alloys used produced a range of tool temperatures from 450 to 475 ^{0}C for the first tool. The same combination produces a range of tool temperatures between 370 to 400 ^{0}C when using the second tool.

The aim of this section is to evaluate the performance of the fuzzy control of welding speed to regulate the tool temperature when using different tool designs on the same aluminium alloy. Figure 6.10 illustrates the simulated response of the process using two FSW tools, one without a draft angle and the other with a draft angle of 30^0, when welding 5083 H321 alloy.

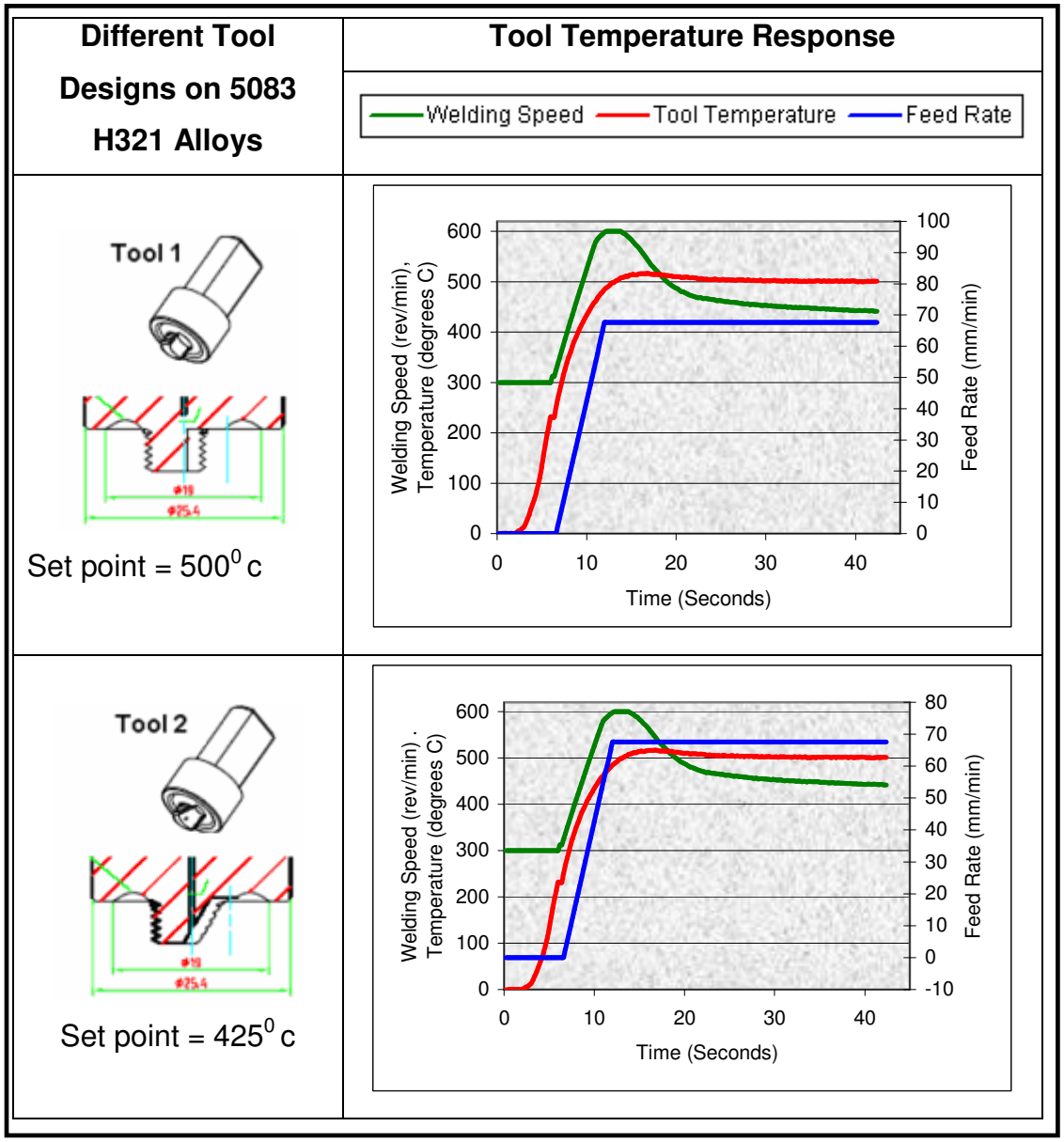

Figure 6.10: Effect of different alloys on the tool temperature regulation.

The simulation results indicate good performance of fuzzy control on the regulation of tool temperature when using the different tool designs. The welding speed was adjusted quickly and smoothly in response to the welding temperature dynamics introduced by the different profiles of the two tools.

The tool temperature was well regulated around the reference levels in the two cases. Each FSW tool produced different tool temperatures, at the same feed rate and welding speed, due to the different rates of material translation around the tool pin. The fuzzy control methodology was able to regulate the tool temperature set point, irrespective of the type of the tool design used.

6.5 Testing and Verification

The simulations indicated that fuzzy logic is a viable solution as a technology to be used to control the FSW process. The feed rate and welding speed were used to regulate the feed force and tool temperature, respectively, irrespective of the welding tool and material change during the welding cycle. These simulations need to be verified, by being compared to the actual response of the FSW process.

The current FSW process at NMMU does not enable the implementation of a closed-loop configuration. Therefore, it is not practical at this stage to implement the FLC online to the process. The comparative analysis between the simulations and the actual process was performed to relate the open loop dynamics of the FSW process.

6.5.1 Open Loop Feed Force Analysis

Figure 6.11 illustrates the comparison between the feed force response of the FSW process and the simulated case. This data was acquired when using tool 1 to weld 2024 T3 aluminium alloy. The feed rate and welding speed were preset at 100 mm per min and 600 RPM respectively. The two graphs are relatively the same while the FSW data also included the dynamics of the process that are not fully represented by the simulation data.

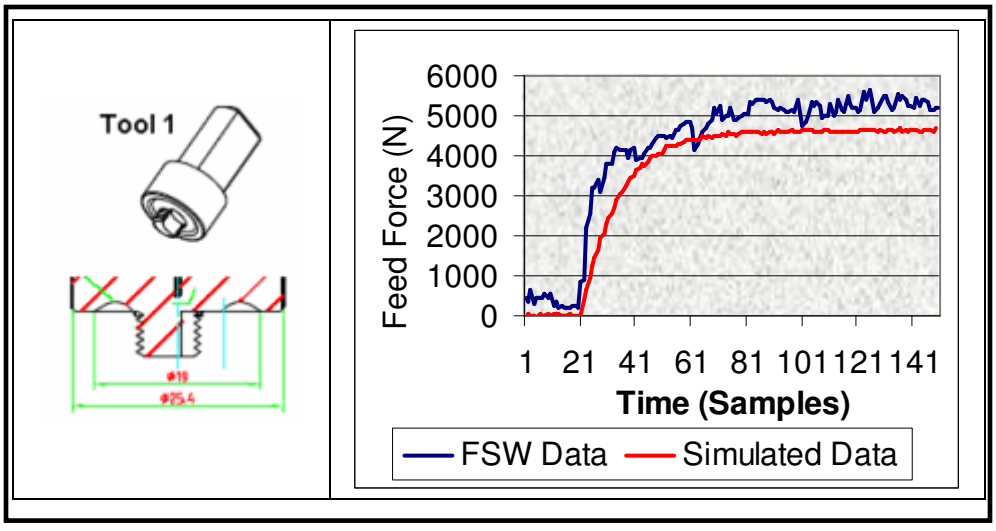

Figure 6.11: Actual and simulated feed force on 2024 T3 aluminium alloy.

Figure 6.12 illustrates the comparison between the feed force response of the FSW process and the simulated case when welding two aluminium alloys. This data was acquired when using tool 1 to weld 5083 H321 and 2024 T3 aluminium alloys. The feed rate and welding speed were preset at 50 mm per min and 300 RPM respectively.

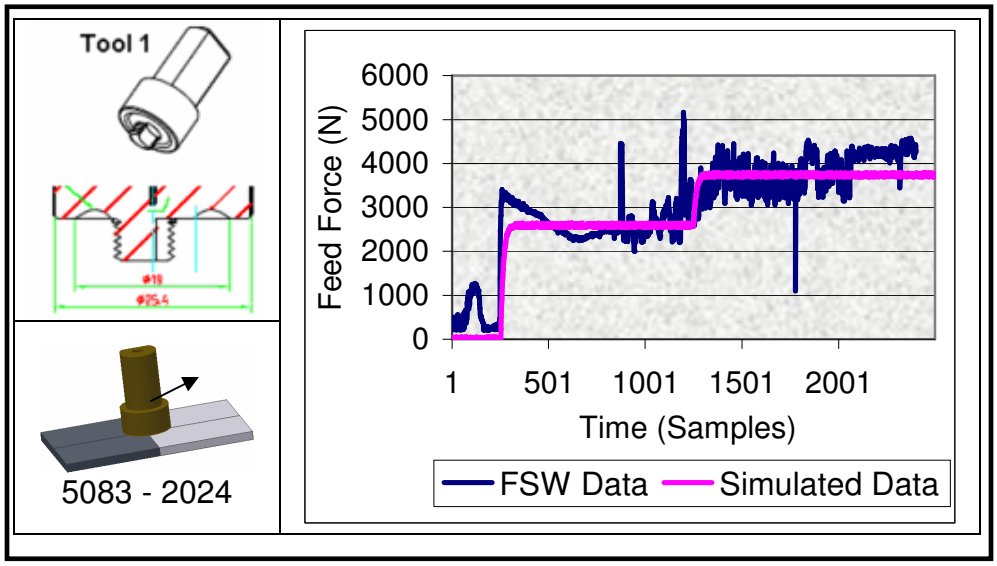

Figure 6.12: Actual and simulated feed force on 5083 H321 to 2024 T3 aluminium alloys.

Figure 6.13 illustrates the comparison between the feed force response of the FSW process and the simulated case. This data was acquired when using tool 2 to weld 5083 H321, 2024 T3 and 5083 H321 aluminium alloys. The feed rate and welding speed were preset at 50 mm per min and 600 RPM respectively.

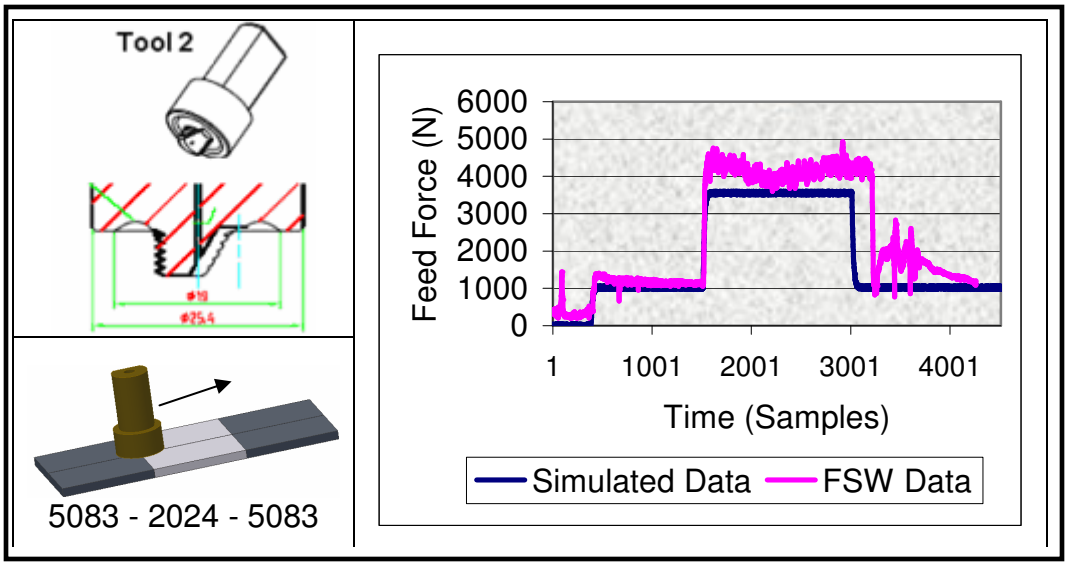

Figure 6.13: Actual and simulated feed force on 5083 H321 to 2024 T3 to 5083 aluminium alloys.

Figures 6.12 and 6.13 illustrate that the 2xxx series alloy produces higher feed than the 5xxx series alloy at the same feed rates and welding speeds. Similarly, Johnson had acquired the same responses when welding 2xxx and 5xxx series alloys using different tool designs [Johnson, 2001].

Therefore, the feed rate can be reduced with the 2xxx series alloy in a closed loop configuration, and increased when welding the 5xxx series alloy. This property enables the controller to adapt to the dynamics of the process. This process can be optimised by enabling faster feed rates when welding the 5xxxx series alloy while ensuring that a set point, such as the feed force, is not exceeded.

6.5.2 Open Loop Temperature Analysis

Figure 6.14 illustrates the comparison between the temperature response of the FSW process and the simulated case. This data was acquired when using tool 1 to weld 2024 T3 aluminium alloy. The feed rate and welding speed were preset at 50 mm per min and 600 RPM respectively. The simulated response had been able to track the actual response of the FSW process.

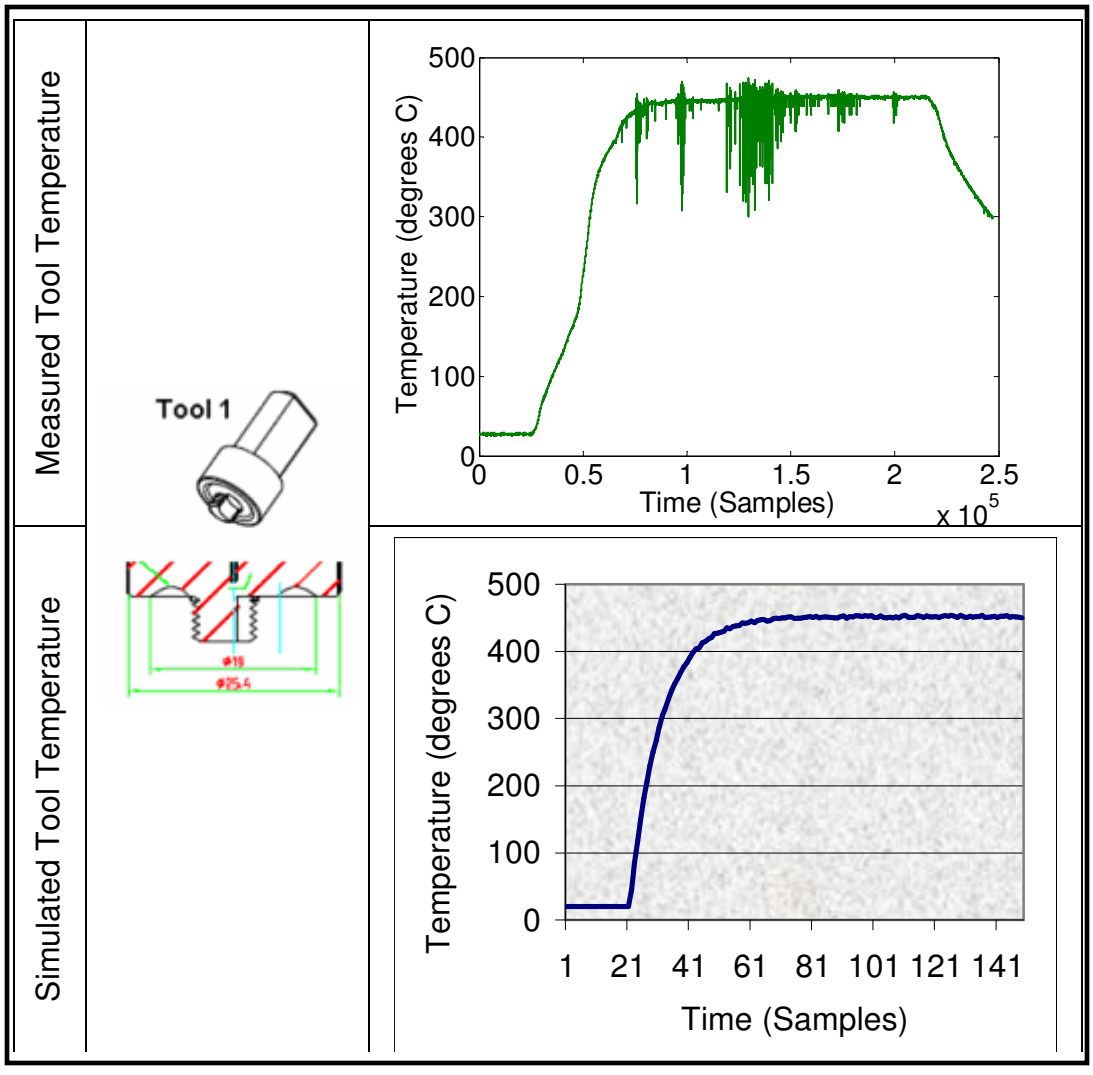

Figure 6.14: Comparing real and simulated tool temperature on 2024 T3 aluminium alloy.

Figure 6.15 illustrates the comparison between the tool temperature response of the FSW process and the simulated case. This data was acquired when using tool 1 to weld 5083 H321 and 2024 T3 aluminium alloys. The feed rate and welding speed were preset at 75 mm per min and 450 RPM respectively.

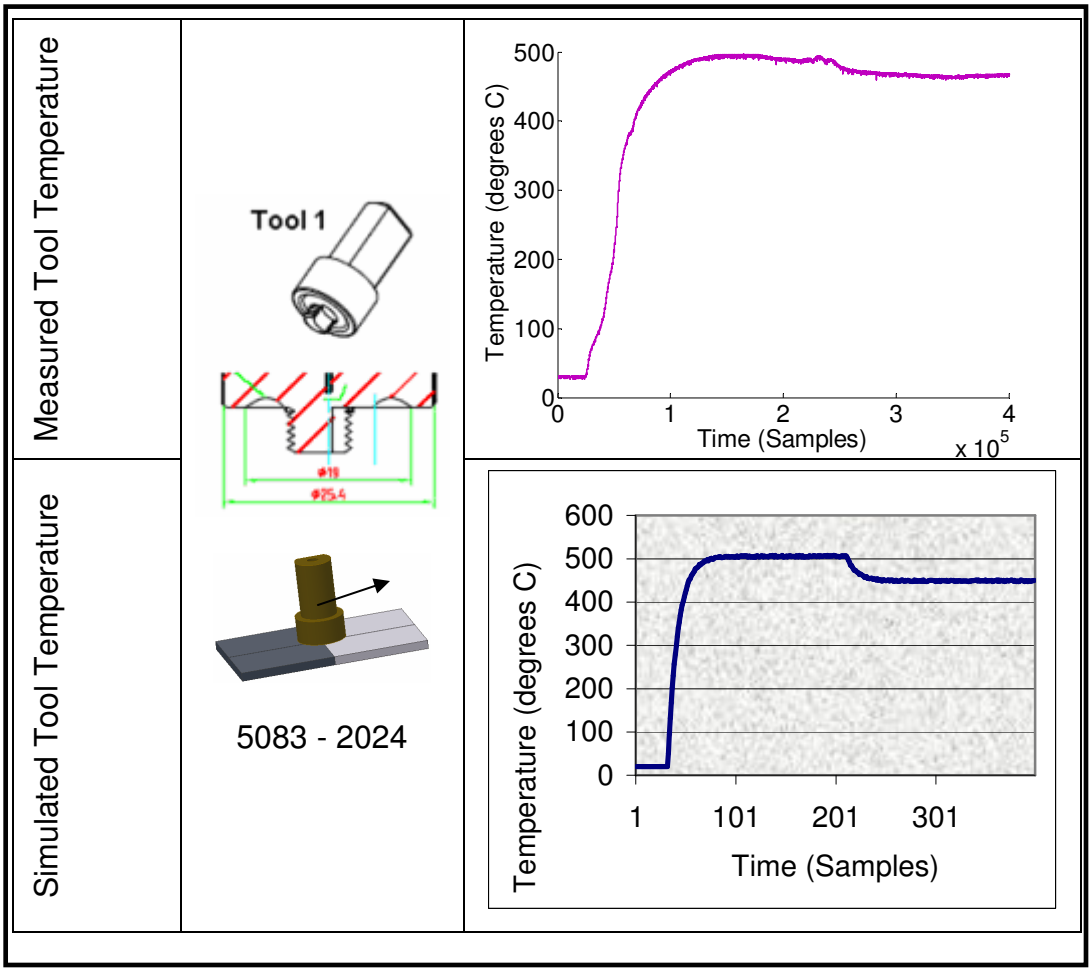

Figure 6.15: Comparing real and simulated tool temperature on 5083 H321 to 2024 T3 aluminium alloys.

Figure 6.16 illustrates the comparison between the feed force response of the FSW process and the simulated case. This data was acquired when using tool 2 to weld 5083 H321, 2024 T3 and 5083 H321 aluminium alloys. The feed rate and welding speed were preset at 50 mm per min and 450 RPM respectively.

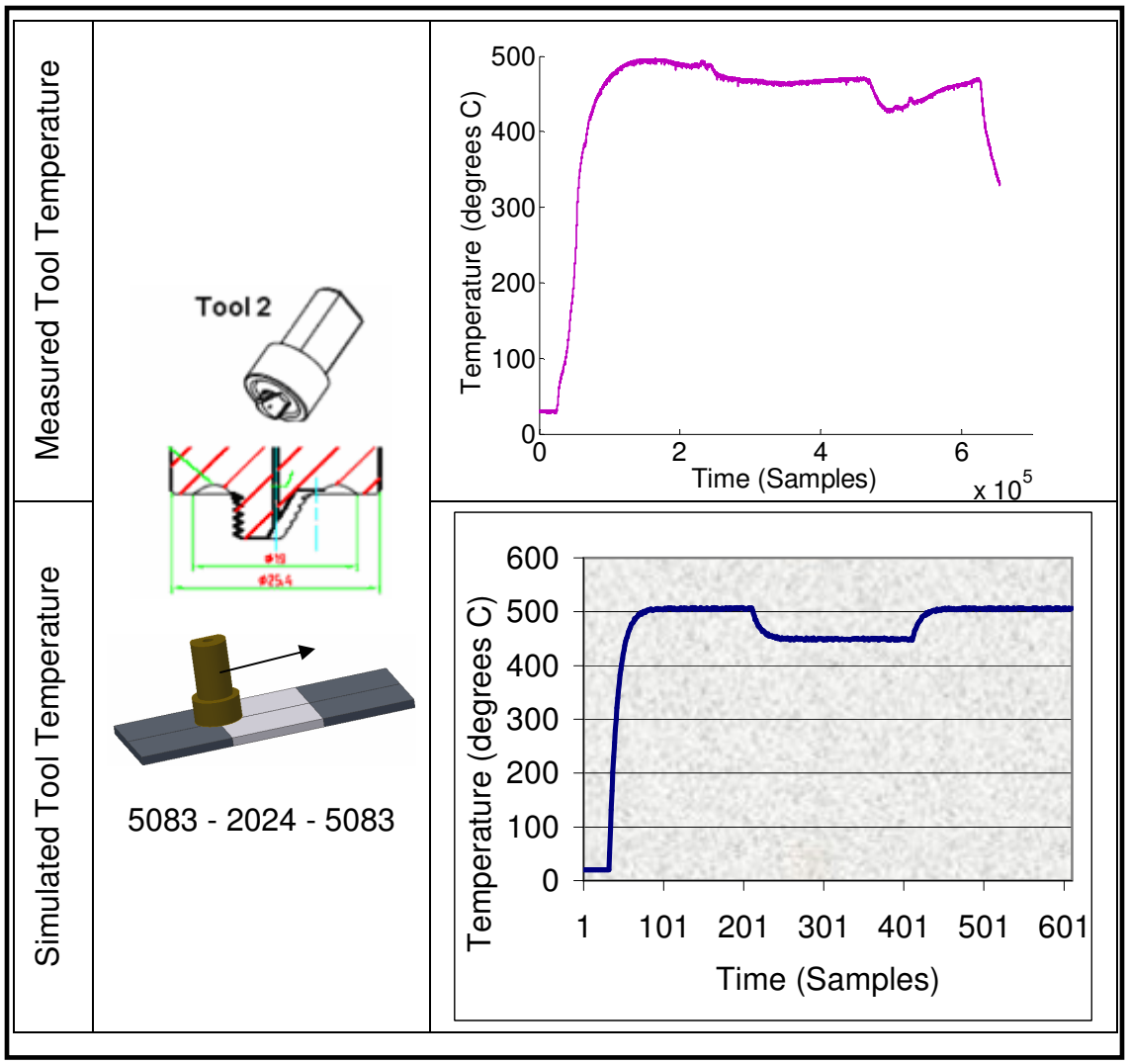

Figure 6.16: Comparing real and simulated tool temperature on 5083 H321 to 2024 T3 to 5083 H321 aluminium alloy.

6.6 Summary

The literature review in section 2.10 revealed that it is possible to design one FLC to regulate a process with all the expected dynamic responses that can be encountered. The FSW models were established and implemented in Simulink to evaluate the suitability of a FLC to regulate the variables of the FSW process.

The simulation results from sections 6.2 and 6.4 illustrated that a well designed fuzzy controller can successfully control FSW process in spite of material and tool changes. The feed rate and welding speed were adjusted to maintain the feed force and welding temperature respectively in a simulated closed-loop configuration.

It is not possible to implement the FLC online in the current experimental FSW machine at NMMU. The responses of the regression models were compared to the open-loop dynamics of the FSW process. The response of the models successfully resembled the actual performance of the FSW process.

It was demonstrated that the fuzzy control technology has the ability to control the dynamic processes. It is able to regulate the variables of the FSW process irrespective of the tool design and type of material to be welded. It is also possible to design a generic fuzzy controller to regulate a particular set point with the same weld run made up of different materials.

Chapter 7

Conclusions and Recommendations

The FSW is a complex problem with a lack of traditional dynamic modelling to describe the properties of friction and the plastic weld region. Therefore, it is a process difficult to model mathematically. The dynamics of the machine tool drives increases the complexity of the process.

The application of modern technology is used to deal with the complexity of the industrial processes. The current trend is the generalised application of new control strategies to improve controlled systems' responses.

Fuzzy logic technology, as one of the artificial intelligent strategies, is widely used because of its practical impact on dynamic plant control. This technology is robust and quick to implement as compared to traditional control strategies. It enables the application of casual models rather than using the accurate mathematical models which at times are not readily available.

Fuzzy logic technology enables quick and easy solutions to the industrial control problems. Furthermore, the productivity of the industrial processes is improved in the case where a plant reconfigures in multiple settings. It is also possible to develop a generic FLC to tolerate a range of dynamic conditions expected within a particular control process.

The statistical experimental design methodology was utilised to capture the characteristics of independent and dependent variables of the FSW process. The experimental design enabled the acquiring of the mathematical effects of one factor independently as well as the interactions between those factors.

The control rules of fuzzy rule bases were customised according to the specifications that define the mathematical modelling of the FSW process. The fuzzy controllers were trained using ANFIS methodology to adapt the parameters of the fuzzy controllers according to the provided matched sets of data representing the FSW inputs and outputs.

The customised fuzzy controllers were implemented in the Simulink environment and they were evaluated against the modelled FSW models. The simulation results had indicated the good performance of the fuzzy control of FSW process under varying material and tool changes.

Recommendations

I would recommend that the current FSW machine be upgraded to enable full automation of this welding process.

Welded Material

The market for FSW is growing strongly and also the introduction of other alloys, such as copper and magnesium alloys, are being introduced to the FSW process. There are also investigations to combine different alloys, such as aluminium and magnesium alloys, with a considerable interest for further research. I recommend that the FSW research at NMMU be extended to other alloys to expand the FSW process.

FSW Joint Design

Although the FSW process is suited to the manufacture of straight welds, it can also be used in a variety of welds. More research can be performed on the variety of different material geometries such as circular, lap and elbow, and T-shaped joints. I recommend that other welds of different shapes be considered as this technique is already applicable to the many shapes.

References

Anguilar L., Melin P. and Castillo O., 2003, Intelligent Control of a Stepping Motor Drive Using Neuro-fuzzy ANFIS Approach, Applied Soft Computing, Vol. 3, No.3, pp. 209 - 219.

Babuška R. and Verbruggen H., 2003, Review: Neuro-Fuzzy Methods for Nonlinear System Identification, Annual Reviews in Control, Vol. 27, No.1, pp. 73 - 85.

Berkan R.C. and Trubatch S.L., 1997, Fuzzy Logic Design Principles: Building Fuzzy IF-THEN Rule Bases, IEEE Press.

Blignault C., 2002, Design, Development and Analysis of the Friction Stir Welding Process, M.Tech Dissertation, PE Technikon.

Bolton, W., 1998, Control Engineering, Addison Wesley Longman Limited, 2nd Ed.

Bryan L.A. and Bryan E.A., 1997, Programmable Controllers - Theory and Implementation, Industrial Text Company.

Chao Y. J., Qi X. and Tang W., 2003, Heating in Friction Stir Welding - Experimental and Numerical Studies, ASME Journal of Manufacturing Science and Engineering, Vol. 125, pp. 138 -145.

Chen C.M. and Kovacevic R., 2003, Finite Element Modelling of Friction Stir Welding - Thermal and Thermomechanical Analysis, International Journal of Machine Tools & Manufacture, Vol. 43, No. 13, pp. 1319 - 1326.

Colegrove P. A. and Shercliff H.R., 2003, Experimental and Numerical Analysis of Aluminium Alloy 7075 - T351 Friction Stir Welds, Science and Technology of Welding and Joining, Vol. 8, No.5, pp. 360 - 368.

Colligan K., 1999, Material Flow During Friction Stir Welding of Aluminium, Welding Journal, Vol.78, No.7, pp. 229 – 237.

D'Errico G.E., 2001, Fuzzy Control Systems with Application to Machining Processes, Journal of Materials Processing Technology, Vol. 109, No. 1-2, pp. 38 - 43.

Deqing W., Shuhua L. and Zhaoxia C., 2004, Study of Friction Stir Welding of Aluminium, Journal of Material Science, Vol. 39, No. 5, pp. 1689 -1693.

Dweiri F., Al-Jarrah M. and Al-Wedyan H., 2003, Fuzzy Surface Modelling of CNC Down Milling of Alumic-79, Journal of Material Processing Technology, Vol. 133, No. 3, pp. 266 - 275.

Georgeou Z., 2004, Analysis of Material Flow Around a Retractable Pin in a Friction Stir Weld, M.Tech Dissertation, PE Technikon.

Goupy J., 1996, Unconventional Experimental Designs Theory and Application, Chemometrics and Intelligent Laboratory Systems, Vol. 33, No.1, pp. 3 -16.

Guerra M., Schmidt C., McClure J.C., Murr L.E. and Nunes A.C., 2003, Flow Patterns During Friction Stir Welding, Material Characterization, Vol. 49, No.2, pp. 95 - 101.

Haber R., Peres R., Alique A., Ros S., Gonzalec C. and Alique R., 1998, Toward Intelligent Machining: Hierarchical Fuzzy Control for the End Milling Process, IEEE Transactions on Control Systems Technology, Vol. 6, No. 2, pp.188 - 199.

Hattingh D.G., van Niekerk T.I, Blignault C., Kruger G. and James M.N., 2004, Analysis of the FSW Force Footprint and its Relationship with Process Parameters to Optimise Weld Performance and Tool Design, Journal of the International Institute of Welding - Welding in the World, Vol 28, No.1 - 2, pp. 50 - 58.

Isermann R., 1998, On Fuzzy Logic Applications for Automatic Control, Supervision, and Fault Diagnosis, IEEE Transaction on Systems, Man, and Cybernetics – Part A: Systems and Humans, Vol. 28, No.2, pp. 221 - 234.

Johnson R. and Kallee S., 1999, Friction Stir Welding, www.azom.com

Johnson R., 2001, Forces in Friction Stir Welding of Aluminium Alloys - Further Studies, The Welding Institute.

Johnson R. and Threadgill P., 2003, Friction Stir Welding of Magnesium Alloys, The Welding Institute.

Kallee S., Nicholas D., Powell H. and Lawrence J., 1998, Knowledge-Based Package for Friction Stir Welding, 7th International Conference on Joints in Aluminium, Abington, Cambridge, UK.

Kallee S., 1999, Application of the Friction Stir Welding Process in the Transport Industry, The Welding Institute.

Koivo H, 2004, Course Material, http://www.control.hut.fi/

Koren Y., 1997, Control of Machine Tools, Journal of Manufacturing Science and Engineering, Vol. 119, No. 4B, pp. 749 - 755.

Kruger G., 2003, Intelligent Monitoring and Control System for a Friction Stir Welding Process, M.Tech dissertation, PE Technikon.

Lee W., Yeon Y. and Jung S., 2003, The Joint Properties of Dissimilar Formed AL Alloy by Friction Stir Welding According to the Fixed Location of Materials, Scripta Materialia, Vol. 49, No. 5, pp. 423 - 428.

Liang M., Yeap T., Rahmati S. and Han Z., 2002, Fuzzy Control of Spindle Power in End Milling Processes, International Journal of Machine Tools & Manufacture, Vol. 42, No.14, pp. 1487 - 1496.

Liang M., Yeap T., Hermansyah A. and Rahmati S., 2003, Fuzzy Control of Spindle Torque for CNC Machining, International Journal of Machine Tools & Manufacture, Vol. 43, No.6, pp. 1497 - 1508.

Lin Z.C. and Liu C. Y., 2001, Application of an Adaptive Neuro-Fuzzy Inference System for the Optimal Analysis of Chemical-Mechanical Polishing Process Parameters, International Journal of Advanced Manufacturing Technology, Vol. 18, No.1, pp. 20 - 28.

Malan S.F., Paterson A.E., 1987, Introduction to Aluminium, Aluminium Federation of South Africa.

Nagarajan R. and Kumar R.N., 2001, A Predictive Fuzzy Logic Controller with an Adaptive Loop for the Manufacture of Resin Adhesives, Computers & Industrial Engineering, Vol. 38, No. 1 - 2, pp. 145 - 158.

Nicholas E.D., 1997, Friction Processing Technologies, The Welding Institute.

Shigematsu I., Kwon J., Suzuki K., Imai T. and Saito N., 2003, Joining of 5083 and 6061 Aluminium Alloys by Friction Stir Welding, Journal of Material Science Letters, Vol. 22, No.5, pp. 353 - 356.

Ship-Peng L., 2003, An Adaptive-Network Based Fuzzy Inference System for Prediction of Work-piece Surface Roughness in End Milling, Journal of Materials Processing Technology, Vol. 142, pp. 665 - 675.

Skinner M., 2003, Friction Stir Welding, www.mts.com.

The MathWorks, 2004, Fuzzy Logic Toolbox for Use with MatLab, The MathWorks Inc., Natick MA, USA.

Thomas W.N., Johnson K.I. and Wiesner C.S., 2003, Friction Stir Welding – Recent Developments in Tool and Process Technologies, Advanced Engineering Materials, Vol. 5, No. 7, pp. 485 - 490.

Thomas W. M., Nicholas E. D., Watts E. R. and Stainess D., 2002, Friction Based Welding Technology for Aluminium, The Welding Institute.

Threadgill P.L. and Nunn M.E., 2003, A Review of Friction Stir Welding: Part 1, Process Review, The Welding Institute.

Von Altrock C., 1995, Fuzzy Logic and Neurofuzzy Applications Explained, Prentice Hall.

Yang M. and Lee T., 2002, Hybrid Adaptive Control Based on the Characteristics of CNC End Milling, International Journal of Machine Tools and Manufacture, Vol. 42, No.4, pp. 489 - 499.

Yen J., Longari R. and Zadeh L., 1995, Industrial Applications of Fuzzy Logic and Intelligent Systems, IEEE Press.

Zeelie B., 2003, Experimental Design and Analysis for Scientists and Engineers, Department of Chemistry, PE Technikon.

Appendix A: Welded Material Properties

A1: Aluminium alloy (5083 H321)

Non Heat-Treatable **Al-Mg** **Wrought Alloy** **5083**

Chemical Composition Limits (in %)

Cu	Mg	Si	Fe	Mn	Zn	Ti	Cr	Other elements Each	Other elements Total
0,1	4,0 4,9	0,4	0,4	0,4 1,0	0,25	0,15	0,05 0,25	0,05	0,15

Outstanding Characteristics:

High strength after welding.
Very resistant to sea water and industrial atmosphere.

Standard Commodities:

Plate; sheet; extrusions.

Typical Uses:

Shipbuilding; car bodies, railway waggons.
Recommended for pressure vessels and low temperature applications. Structural plate for mine skips and cages. Tipper and dumper bodies.

Typical Physical Properties

Density	2,65	g/cm³
Modulus of Elasticity	72	GPa
Modulus of Rigidity	27	GPa
Melting Range	570—640	°C
Specific heat between 0—100°C (273—373 K)	0,97	J/g°C
Coefficient of linear expansion between 20—200°C (293—473 K)	25 x 10^{-6}	/°C
Thermal Conductivity at 25°C (298 K)	121—126	W/m°C
Resistivity at 20°C (293 K)	0,058 x 10^{-6}	Ωm

Other Characteristics

Corrosion Resistance	: Excellent
Weldability	: Good
Formability	: Good (in O temper)
Machinability	: Fair
Brazeability	: Not recommended

Mechanical Properties

Commodity and Temper U.K.	Gauge mm	0.2% Proof Stress MPa	Ultimate Tensile Strength MPa	Elongation A_5 %	Brinell Hardness HB	Ultimate Shear Strength MPa	Fatigue Strength MPa
Sheet							
M		(200)	(315)				
O		125 (170)	275 (300) 350	16 (20) *	(65)	160 (—)	
H2		235 (250)	310 (340) 375	8 (15) *			
Extrusions							
O	up to 75	125 (180)	275 (300)	13 (18)			
M	up to 75	130 (200)	280 (330)	11 (16)			

* 50 mm gauge length; Sheet: thickness 2,5—9,0 mm

Annealing

Temperature °C	Time h
350 ± 5	2—3 (to soften permanently)

Figure A -1: 5083 H321 aluminium specifications [Malan et al., 1987].

A2: Aluminium alloy (2024 T3)

Heat-Treatable **Al-Cu-Mg** **Wrought Alloy** **2024**

Chemical Composition Limits (in %)

Cu	Mf	Si	Fe	Mn	Zn	Ti	Zr + Ti	Cr	Other elements Each	Other elements Total
3,8 4,9	1,2 1,8	0,5	0,5	0,3 0,9	0,25	0,15	0,2	0,1	0,05	0,15

Outstanding Characteristics:

Strong alloy. Naturally ageing at room temperature after solution heat treatment.

Standard Commodities:

Plate; extrusions.

Typical Uses:

Stressed components in aircraft and other structures.

Typical Physical Properties

Density	2,77	g/cm³
Modulus of Elasticity	75	GPa
Modulus of Rigidity	28,5	GPa
Melting Range	500—640	°C
Specific heat between 0—100°C (273—373 K)	0,92	J/g°C
Coefficient of linear expansion between 20—200°C (293—473 K)	24 x 10^{-6}	/°C
Thermal Conductivity at 25°C (298 K)	113	W/m°C
Resistivity at 20°C (293 K)	0,057 x 10^{-6}	Ωm

Other Characteristics

Corrosion Resistance	Poor (when clad Excellent)
Weldability	Fair (resistance welding only)
Formability	Forming should be done immediately after quenching or in annealed temper
Machinability	Good
Anodizing	Good (for surface protection only)
Brazeability	Not done

Mechanical Properties

Commodity and Temper U.S.A.	Gauge mm	0,2% Proof Stress MPa	Ultimate Tensile Strength MPa	Elongation A_5 %	Brinell Hardness HB	Ultimate Shear Strength MPa	Fatigue Strength MPa
Plate							
T	12,5—25 25—40	280 310	430 430	10 12			
Extrusions							
T3	6,35—20	(380)	(510)	(14)	(120)		

Heat Treatment

Solution Heat Treatment			Ageing	
Temper	Temperature °C	Quenching	Temperature °C	Time h
T6	495 ± 3	In water	Room	5 days

Annealing

Temperature °C	Time h
425 ± 3	2—3 * to soften permanently

* Slow cool at less than 15°C per hour down to 250°C and remove from furnace.

Figure A -2: 2024 T3 aluminium specifications [Malan et al., 1987].

Appendix B: FSW Tools Designs

B1: FSW Tool With Small Profile (Tool 1)

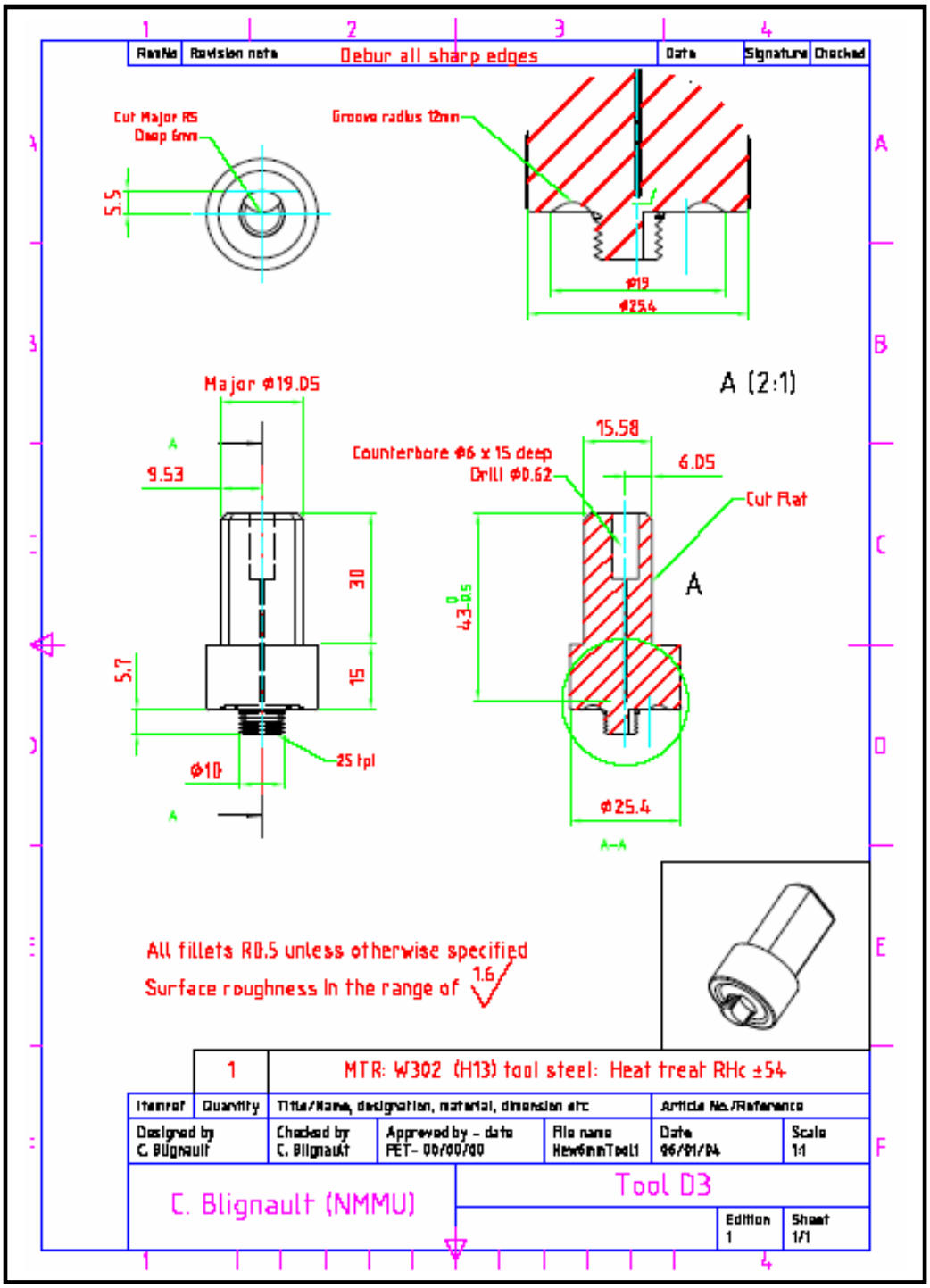

Figure B -1: FSW tool with small profile [Blignault, 2002].

B2: FSW Tool with big profile (Tool 2)

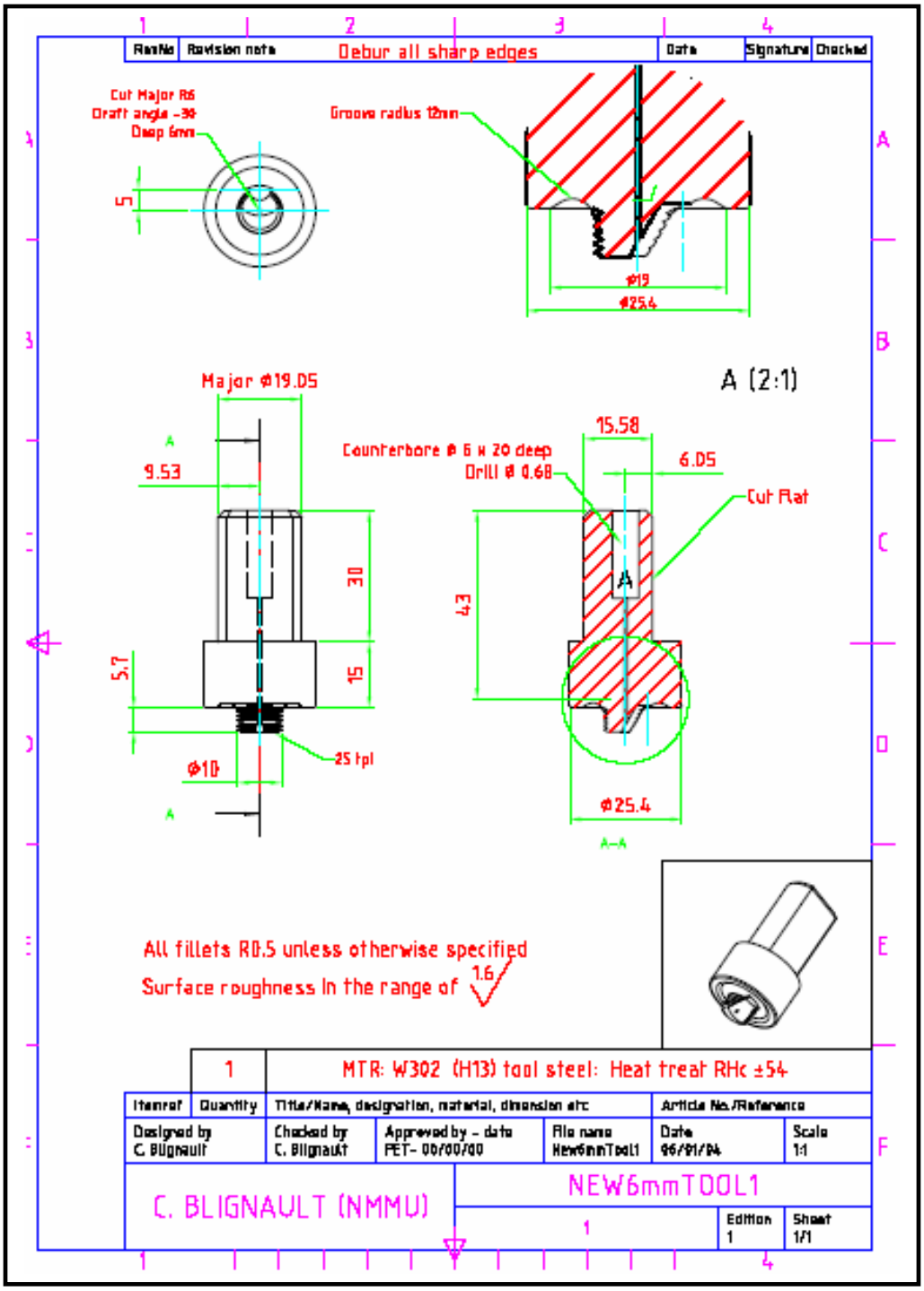

Figure B -2: FSW tool with big profile [Blignault, 2002].

Appendix C: FSW Experimental Data

C1: FSW machine data

Weld parameter	Variable Parameter Settings							
Weld	**1**	**2**	**3**	**4**	**5**	**6**	**7**	**8**
W_T	T1	T1	T2	T2	T2	T2	T1	T1
M	2024	2024	2024	2024	5083	5083	5083	5083
F_R (rev/min)	100	50	100	50	50	100	100	50
W_S (RPM)	300	600	600	300	600	300	600	300
F_X (N)	5558	3409	4629	3887	1022	5132	2534	2589
F_Y (N)	5553	3595	4227	3693	1521	5027	2765	2572
F_Z (KN)	11.663	7.61	8.524	8.429	6.177	10.363	11.166	10.718
T (^{0}C)	449	463	370	364	433	441	531	467
T_T (NM)	70.67	32.68	34	54.54	38.72	69.98	49.57	68.77

Table C - 1: FSW machine data

C2: Expanded View of FSW Welds

Figure C-1: FSW-weld (2024 alloy and Tool 1).

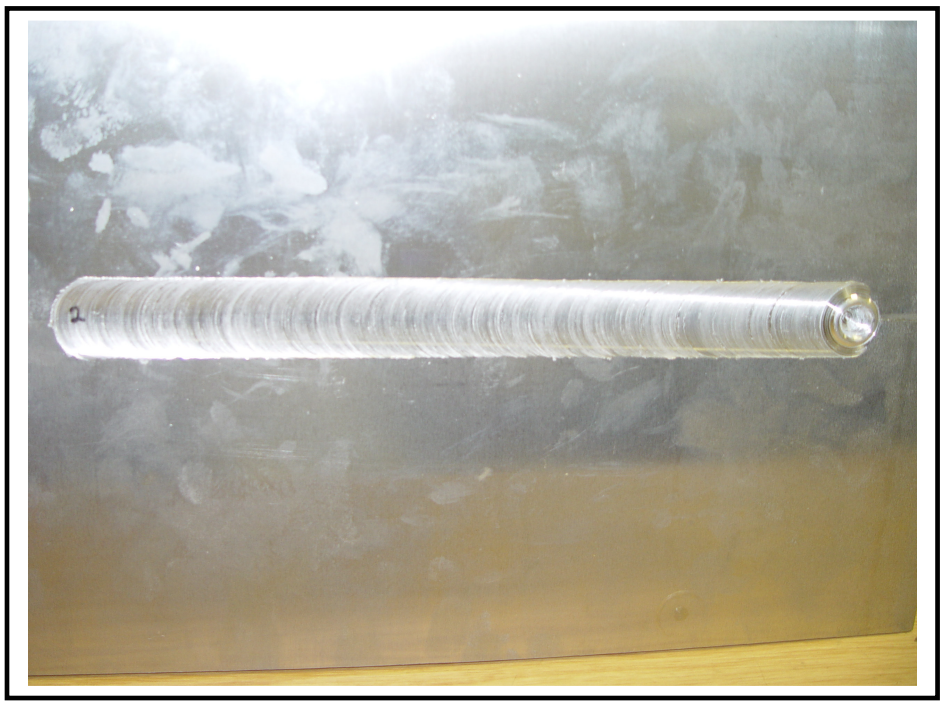

Figure C-2: FSW-weld (2024 alloy and Tool 1).

Figure C-3: FSW-weld (2024 alloy and Tool 2).

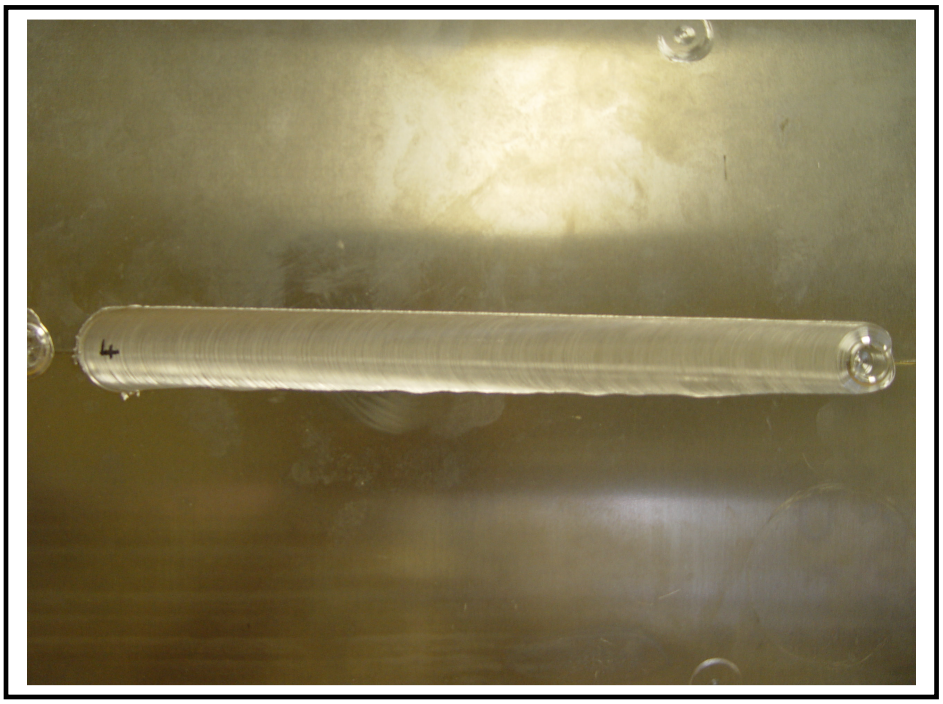

Figure C-4: FSW-weld (2024 alloy and Tool 2).

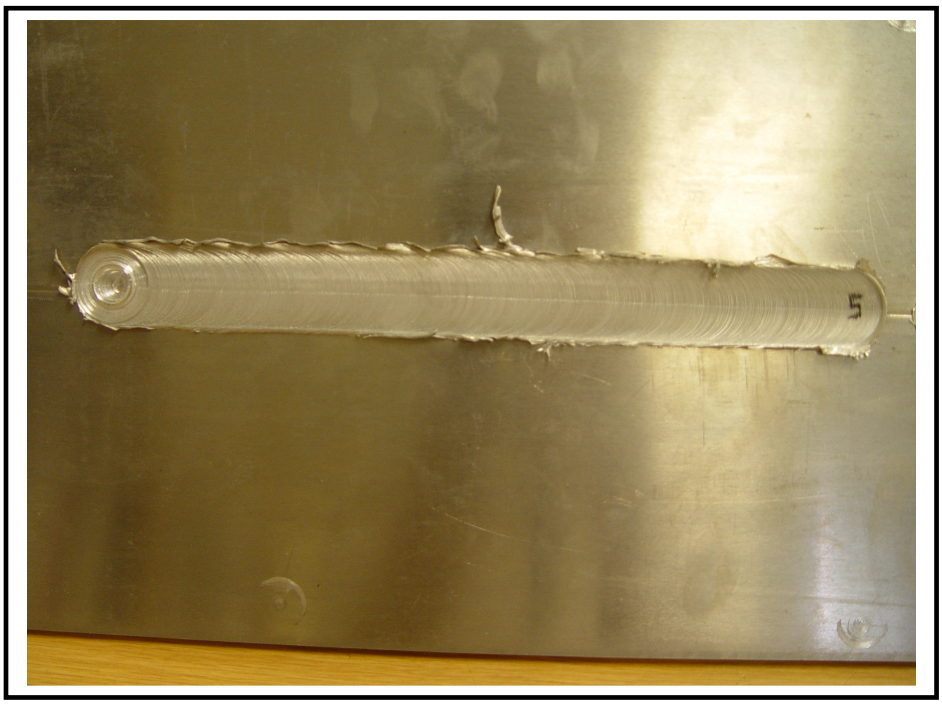

Figure C-5: FSW-weld (5083 alloy and Tool 2).

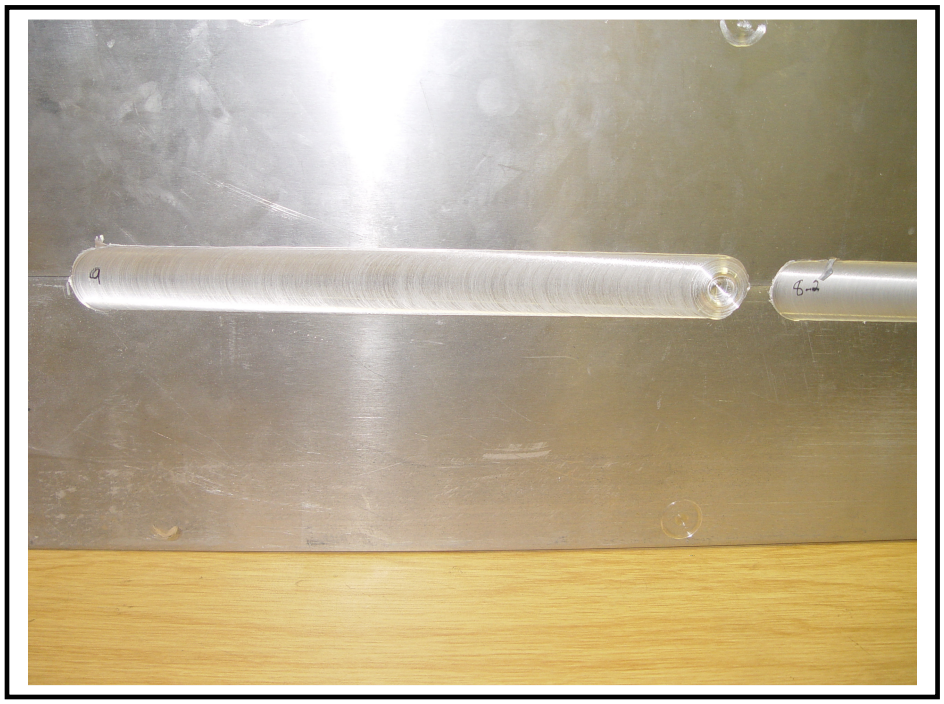

Figure C-6: FSW-weld (5083 alloy and Tool 2).

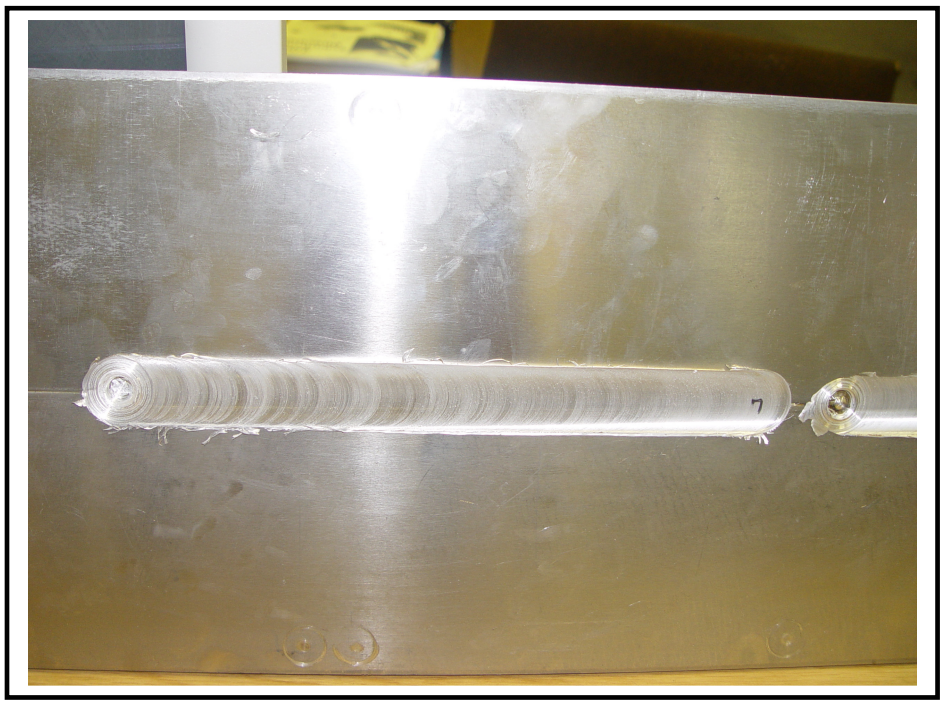

Figure C-7: FSW-weld (5083 alloy and Tool 1).

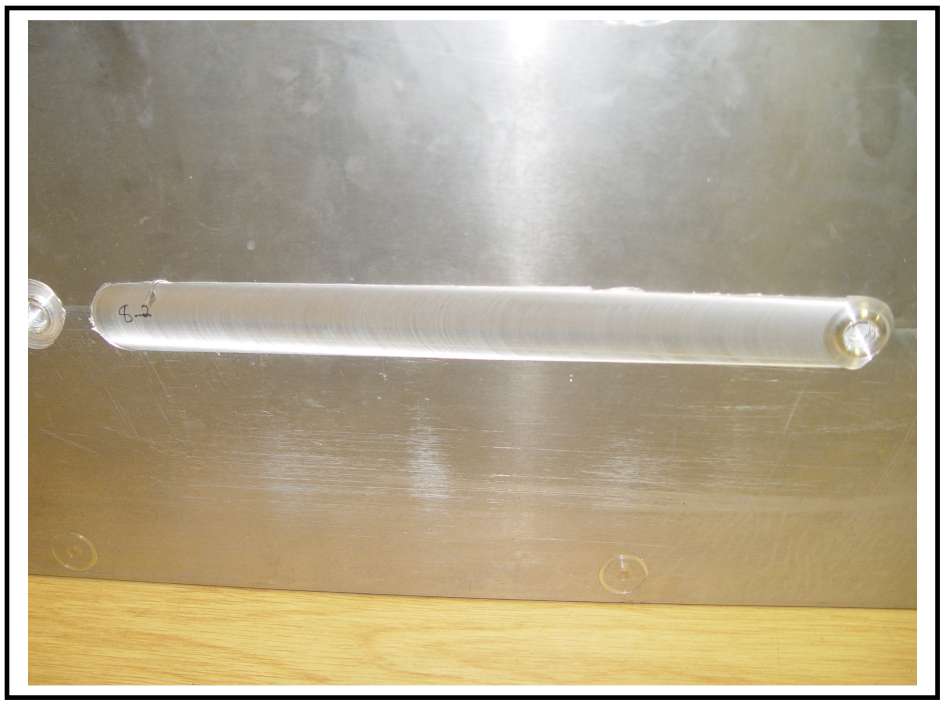

Figure C-8: FSW-weld (5083 alloy and Tool 1).

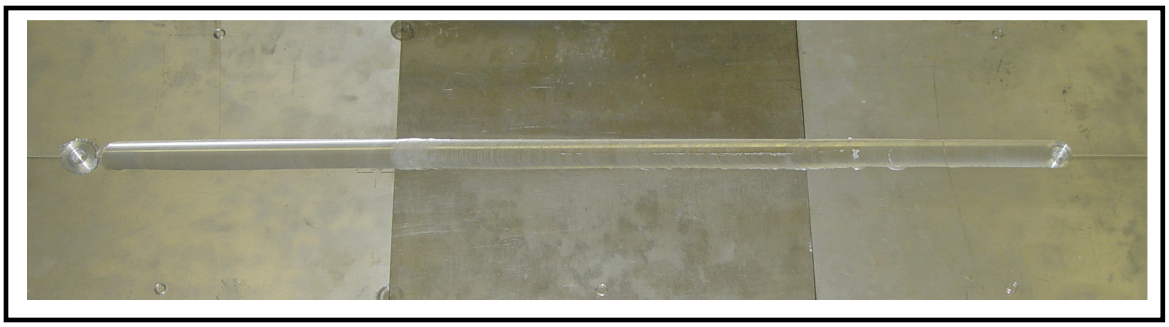

Figure C-9: FSW-weld (5083 – 2024 – 5083 alloy).

C3: FSW Machine Data Graphs

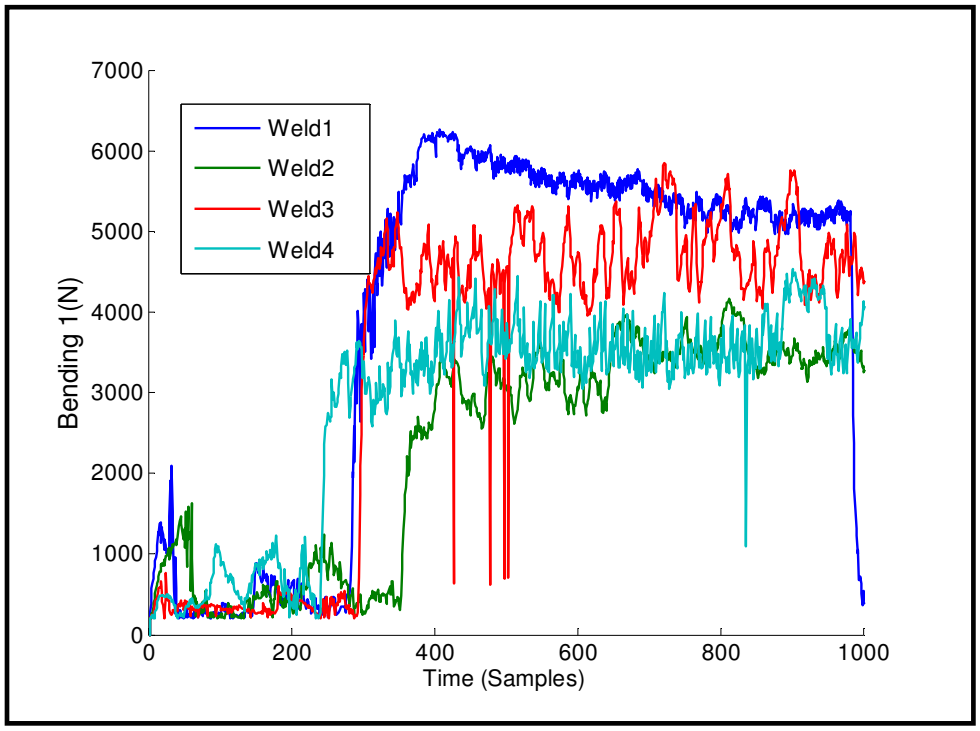

Figure C-10: Bending1 (F_X) vs time (samples) graphs for welds 1 to 4.

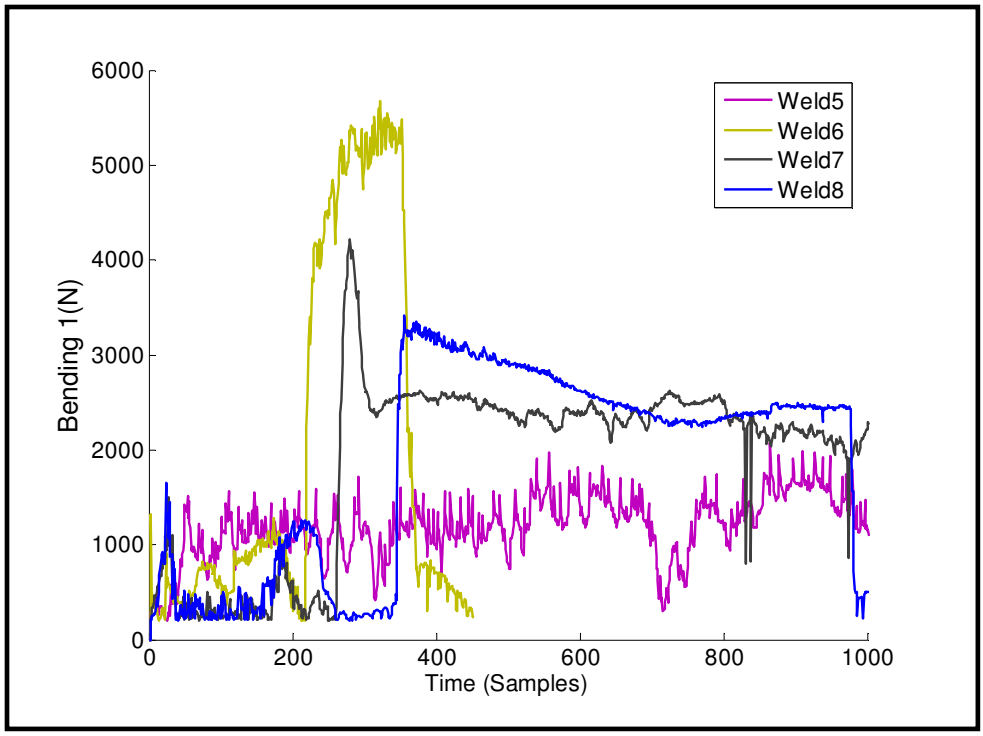

Figure C-11: Bending1 (F_X) vs time (samples) graphs for welds 5 to 8.

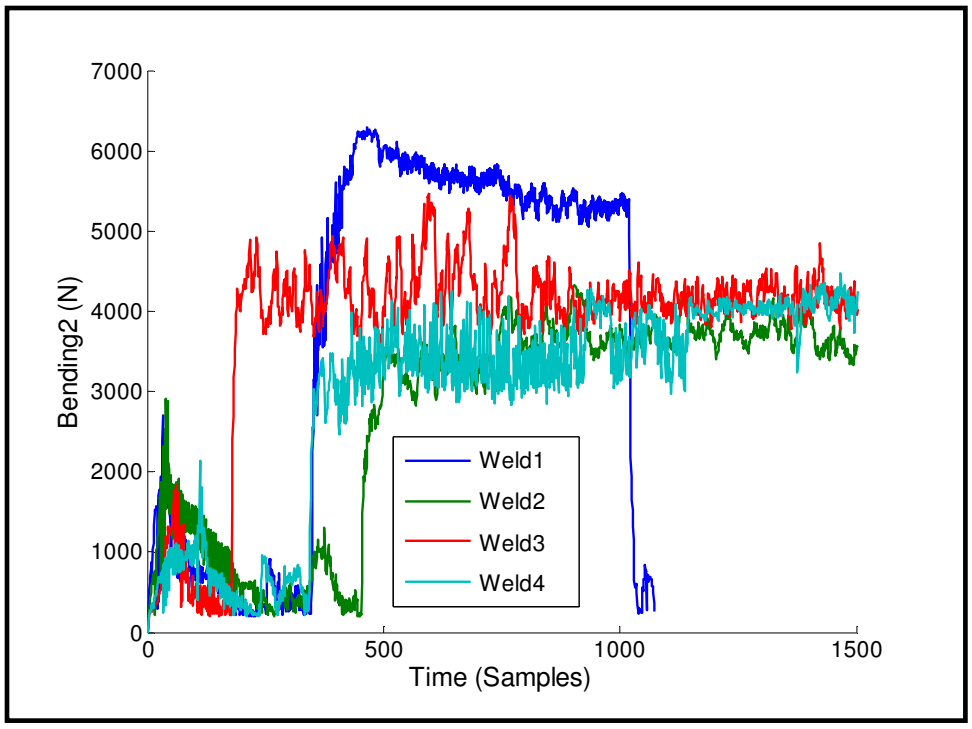

Figure C-12: Bending2 (F_Y) vs time (samples) graphs for welds 1 to 4.

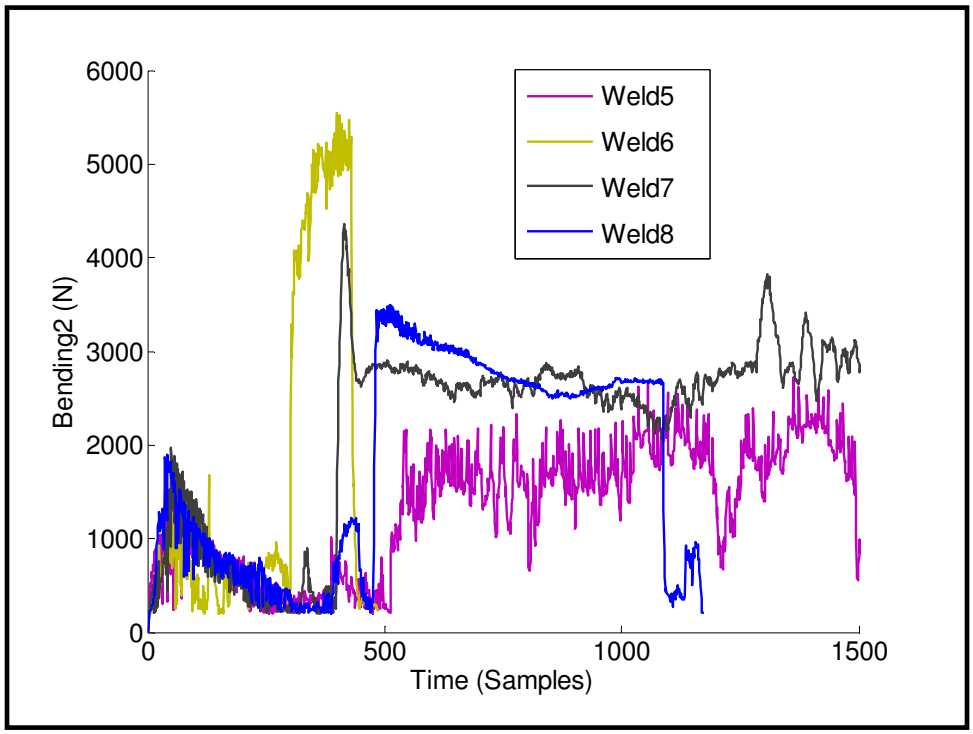

Figure C-13: Bending2 (F_Y) vs time (samples) graphs for welds 5 to 8.

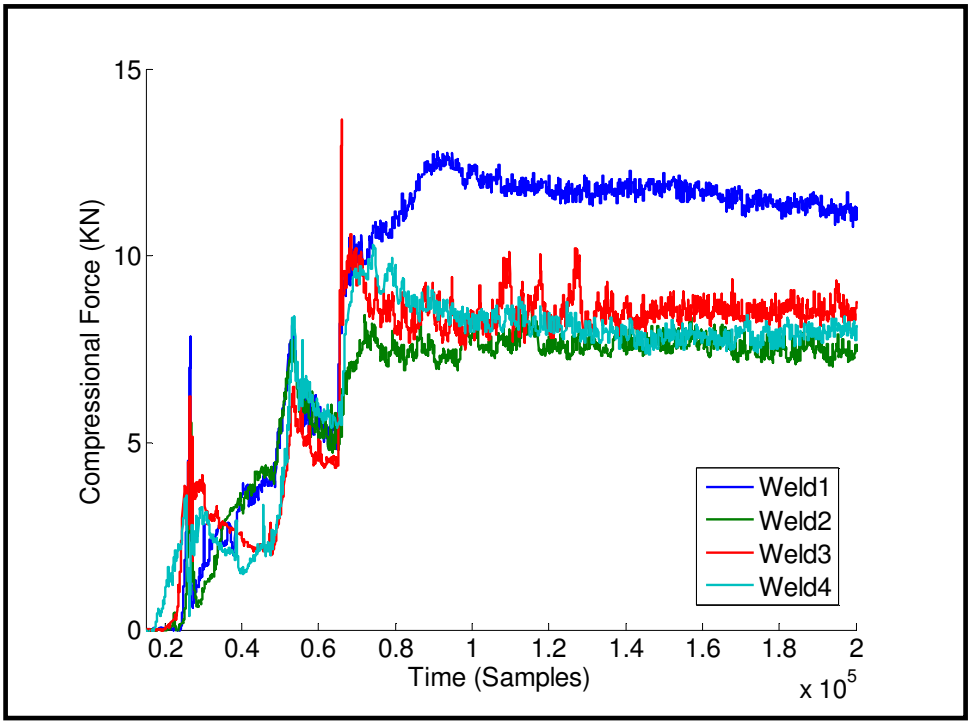

Figure C-14: Compression (F_Z) vs time (samples) graphs for welds 1 to 4.

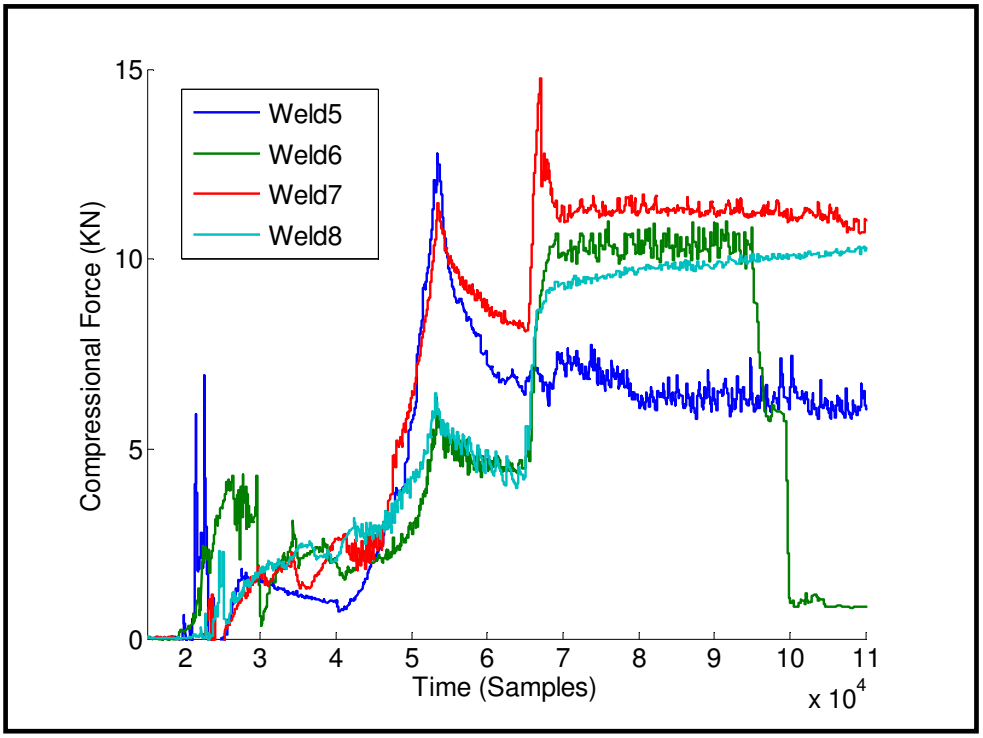

Figure C-15: Compression (F_Z) vs time (samples) graphs for welds 5 to 8.

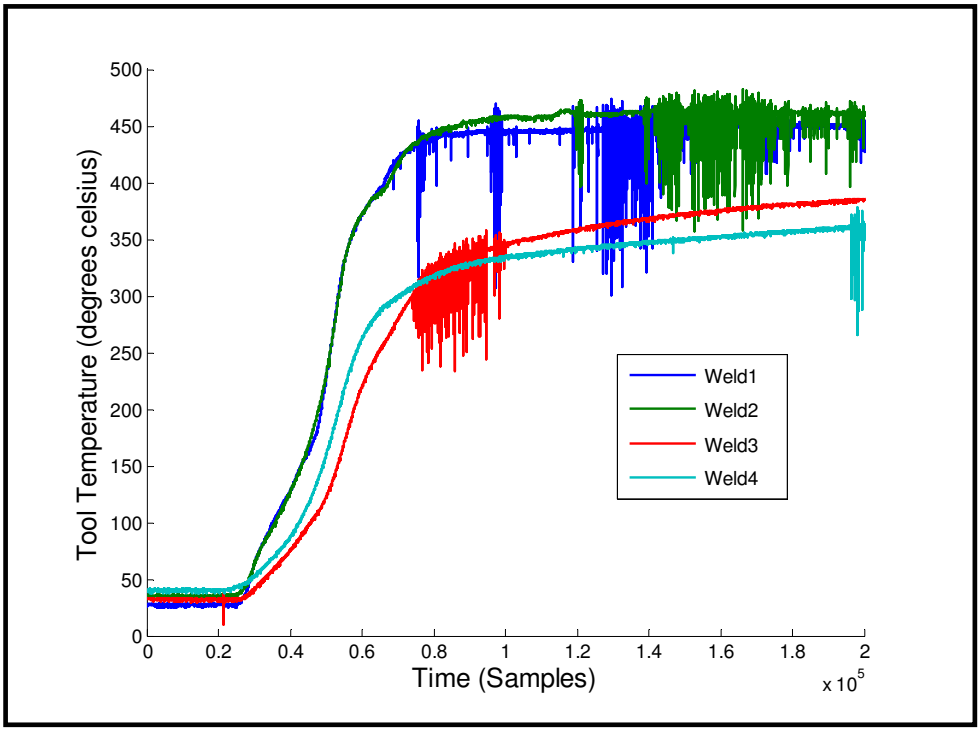

Figure C-16: Tool Temperature (T) vs time (samples) graphs for welds 1 to 4.

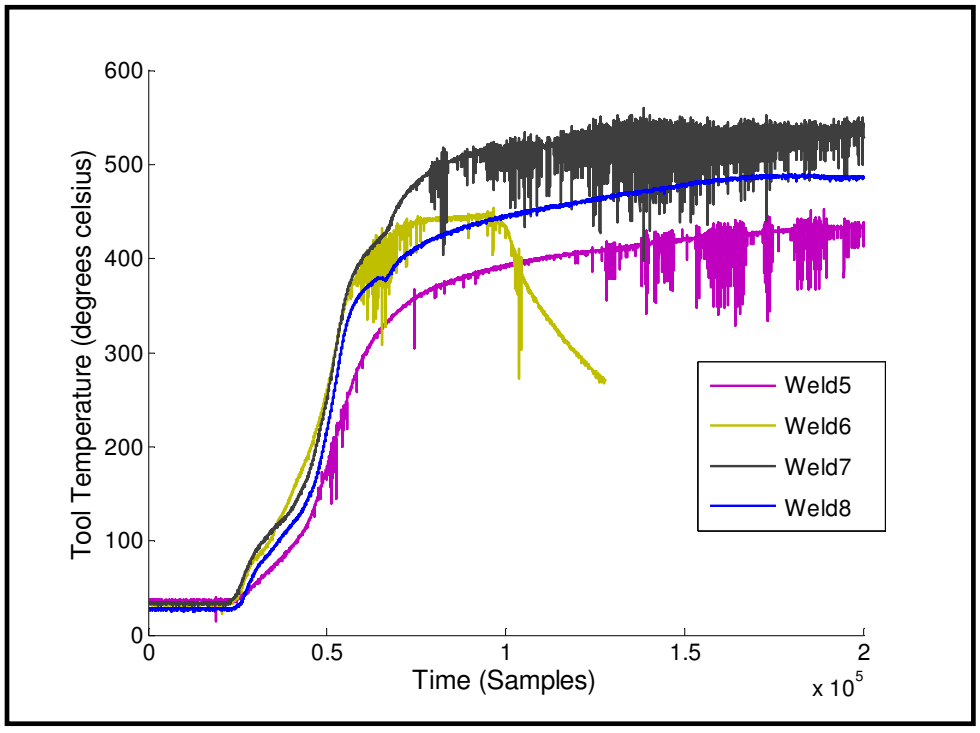

Figure C-17: Tool Temperature (T) vs time (samples) graphs for welds 5 to 8.

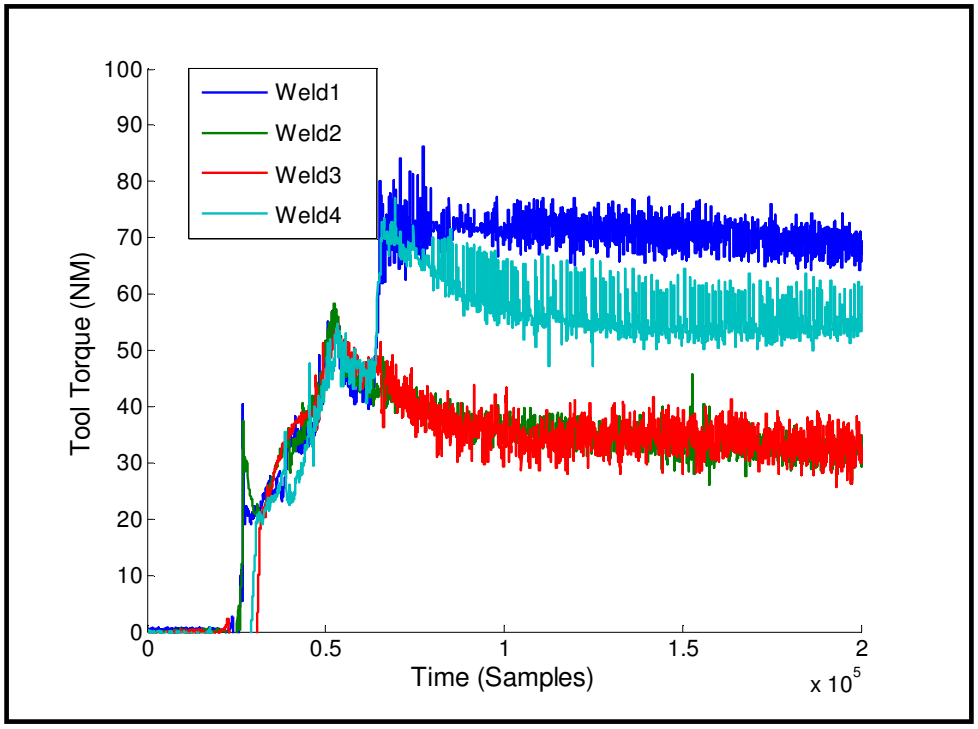

Figure C-18: Tool Torque (T_T) vs time (samples) graphs for welds 1 to 4.

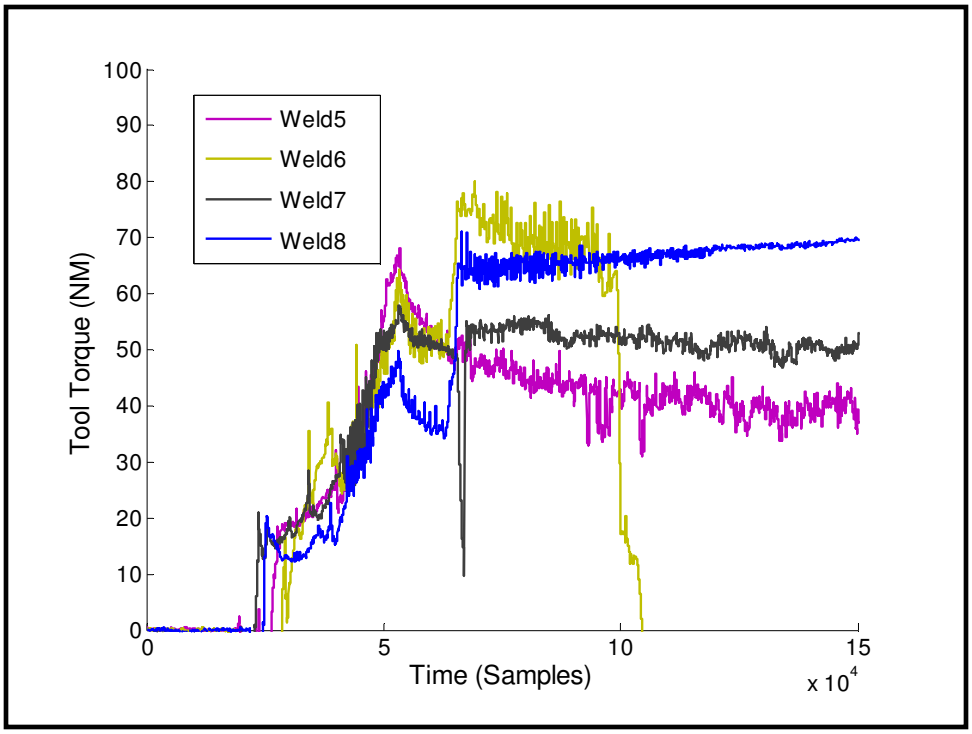

Figure C-19: Tool Torque (T_T) vs time (samples) graphs for welds 5 to 8.

C4: Summary of FSW Data

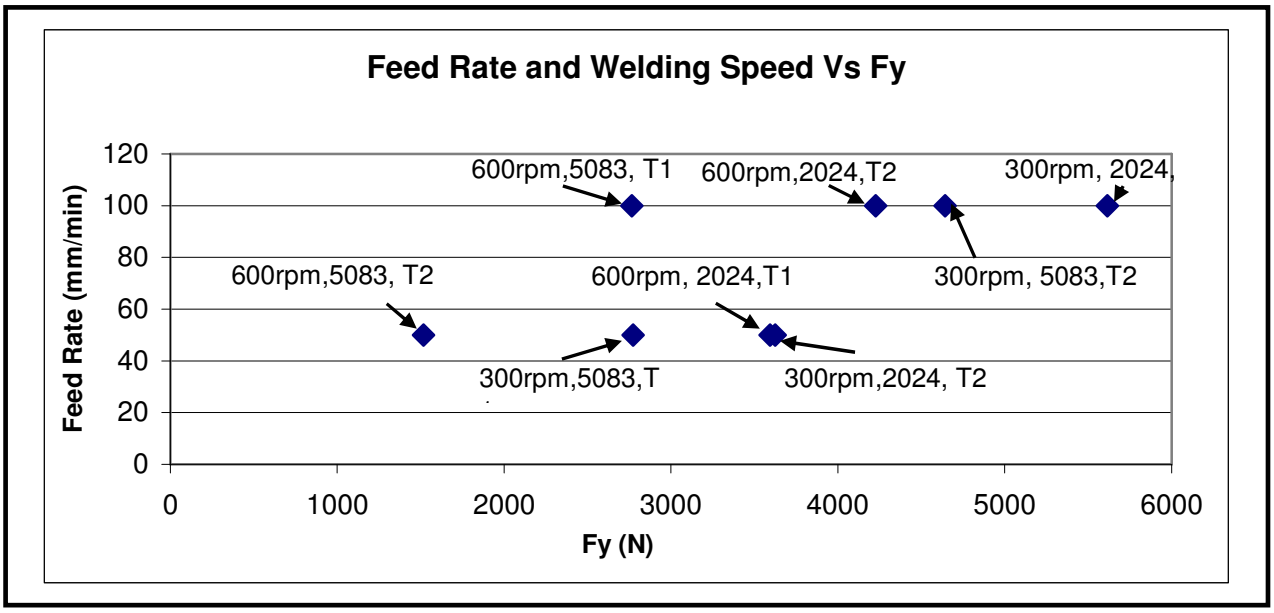

Figure C-20: Feed rate (F_R) and Welding speed (W_S) vs bending 2 (F_Y).

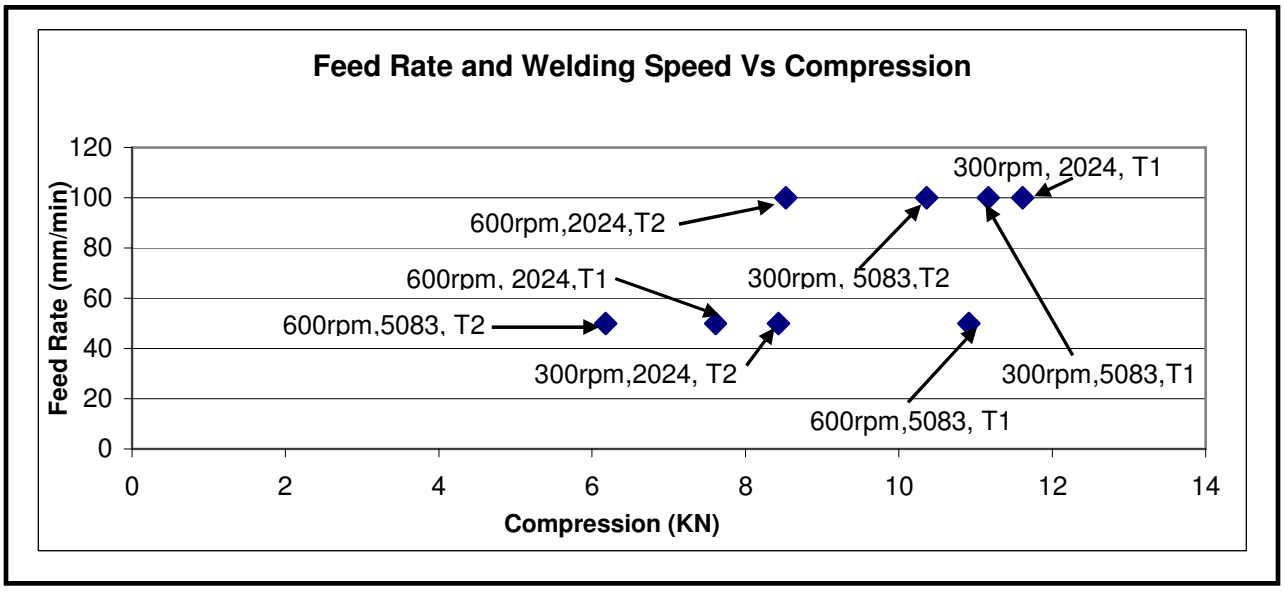

Figure C-21: Feed rate (F_R) and Welding speed (W_S) vs compression (F_Z).

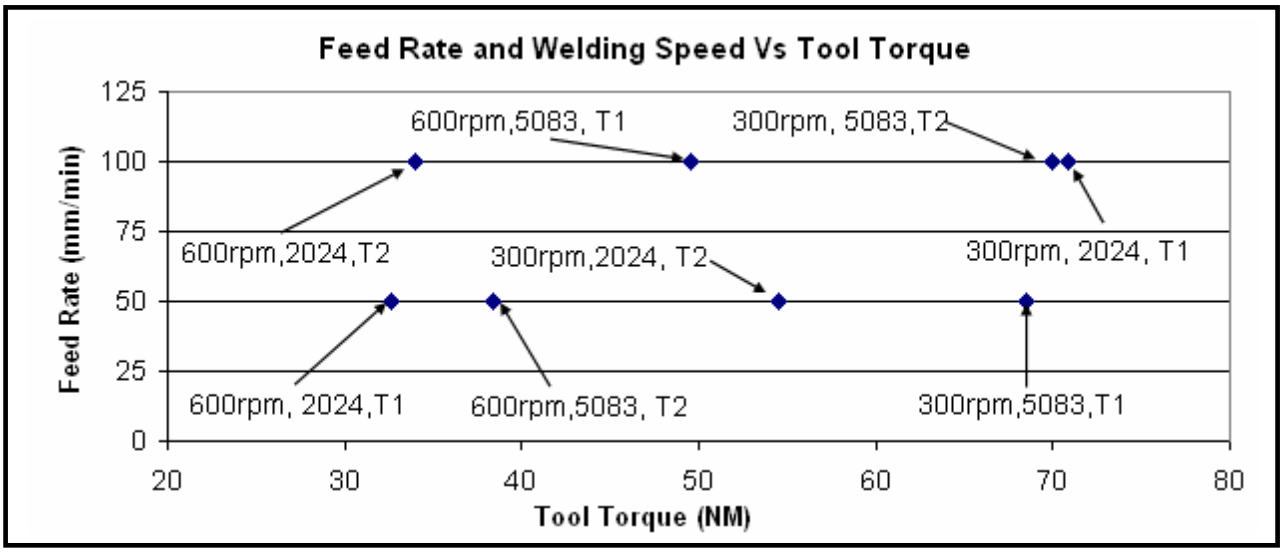

Figure C-22: Feed rate (F_R) and Welding speed (W_S) vs tool torque (T_T).